Development and functional regeneration of the zebrafish lateral line

Autor: Filipe Pinto Teixeira Sousa

TESI DOCTORAL UPF / L'any de la tesi: 2011

DIRECTOR DE LA TESI

Dr. Hernán Lopéz-Schier

DEPARTAMENT

Cell and Developmental Biology - CRG

The research in this PhD thesis was carried out at the laboratory of Sensory cell Biology and Organogenesis under the supervision of Dr. Hernán López-Schier at the Centre de Regulacío Genòmica (CRG), Research Programme of Cell and Developmental Biology, located at the Barcelona Biomedical Research Park (PRBB). This research was funded by Fundação para a Ciência e Tecnologia through the GABBA Phd Program by means of a fellowship (SFRH/BD/15906/2005) to the author of this thesis.

Mi relato será fiel a la realidad o, en todo caso, a mi recuerdo personal de la realidad, lo cual es lo mismo.

Jorge Luis Borges
El Libro de Arena

To my mother Camila, my grandfather António and my uncle Nuno for having shared with me the pleasure of studying.

Acknowledgements

This work would not have been possible without the help and support of many people and institutions that I would like to acknowledge.

I would like to start by thanking the GABBA PhD program and the Portuguese Foundation for Science and Technology that gave me the opportunity to be part of an outstanding scientific network and the total freedom to choose the laboratory that best suited my research interests.

I would like to thank Hernán López-Schier for giving me the opportunity to join his lab as one of his first Phd students, for his advices and for being available to provide his input to my work.

Special thanks to the people from my lab for their unlimited support and friendship. Foremost, Indra and Mariana for helping me in my first steps in the zebrafish world, for their continuous help and for their friendship. I could not have had better mates to start my PhD. To Adele I am enormously grateful for being always available, for her patience, for her good mood, for the restaurant tips and for proofreading my thesis. To Andrea for taking care of everything and for making the lab such a pleasant place to work. Your friendship is written in our kitchen's wall. To Jean Pierre for his friendship, good mood and valuable comments in the form of long emails after my lab meetings. To Jesus Pujol for his friendship and for sharing with me his love for research and for our long, always pleasant, conversations with the keywords "neural networks" and "behavior". To Alessandro for his bigness of heart and for helping me confirming some of my observations. To Jim for all his patience and for helping me to try to properly quantify the posterior lateral line morphogenesis. Thank you to all the members of Manuel Mendonça's lab, our close neighbors, for their friendship and outstanding work environment.

I would like to thank to my colleagues and friends who made my life in this city such an unforgettable and valuable experience. To Bernd Böhm for being a good friend. A special thanks to my Portuguese friends in town: Rita, Sónia and Lilia for your care over the years and for being always present. To Paulo, Elsa, André and Cátia for their friendship and for the good things they all have in their fridge. To Julien and Christophoros, for their love, friendship and invaluable moments together. To Pablo and Francois, for coping with my piano playing and for their friendship.

To my friends back home and around the globe who do not allow the distance to lessen our friendship. To my family, to my beloved grandmothers, to my aunt Nucha and my sister Camilinha, for their care and support. My deepest gratitude to my mom and dad, for their unconditional love and relentless support.

My last words are to Laura, whose love has shaped my last years. I am sure this would have been an easier journey if I had followed many of her advices.

Abstract

In this thesis I use the zebrafish lateral line as a model system to address two fundamental questions.

In a first line of investigation I explore the relation between an organ function and its architecture. The regeneration of hair cells in the zebrafish lateral line occurs trough the division of hair-cell progenitors at specific locations in the dorsal and ventral aspects of the neuromasts. As hair cells regenerate a vertical midline that bisects the neuromast epithelium into perfect mirror-symmetric plane-polarized halves is formed. Each half contains hair cells of identical planar orientation but opposite to that of the confronting half. How hair cell regeneration anisotropy is controlled and how this process is integrated in the establishment of this organ bilateral symmetry is poorly understood. Here I show that the neuromast bilateral symmetry is sustained by compartmentalized Notch activity, which governs regeneration anisotropy by permitting the stabilization of hair cell progenitors in specific polar compartments.

In a second line of research I report the role of the chromatin remodeling complex ATPase *brg1* during mechanosensory organ formation in the zebrafish. I show that *brg1* mutants develop a truncated lateral line system as *brg1* is needed in the regulation of multiple cellular events in the lateral line primordium.

Resumen

Per a aquesta tesi, utilitzo la línia lateral del peix zebra com a sistema model per adreçar dues qüestions fonamentals:

En una primera línia d'investigació exploro la relació entre la funció d'un òrgan i la seva arquitectura. La regeneració de cèl.lules ciliades a la línia lateral del peix zebra ocorre mitjançant la divisió dels seus progenitors en determinades posicions dins les zones ventral i dorsal del neuromast. Durant la regeneració de les cèl.lules ciliades, es forma una línia de simetria vertical, que bisecciona l'epiteli del neuromast en dues meitats de polaritats planars oposades. La qüestió de com es controla l'anisotropia de la regeneració de les cèl.lules ciliades i com integrar aquest procés en l'establiment de la simetria bilateral d'aquest organ, roman encara per esclarir. En aquest estudi mostro que la simetria bilateral del neuromast es sosté degut a l'activitat compartimentalitzada de Notch qui, permetent l'estabilització dels progenitors de cèl.lules ciliades en compartiments polars específics, organitza l'anisotropia de la regeneració.

En una segona línia d'investigació, descric el rol del complex de remodelació de cromatina ATPasa *brg1* durant la formació d'organs mecanosensorials al peix zebra. Així mostro que els mutants de *brg1* desenvolupen un sistema de linia lateral truncat, donat que *brg1* es necessari per a la regulació de múltiples events cel.lulars al primordi de la línia lateral.

Preface

The zebrafish lateral line is a collection of external sensory organs called neuromasts, populated with polarized mechanotransductive hair cells on which the animal relies to detect hydro-mechanical variations around its body. During embryogenesis, on each side of the embryo, a cephalic neurogenic placode gives rise to a motile primordium that will migrate collectively along the horizontal myoseptum, periodically depositing the neuromasts that will constitute the lateral line.

In a first line of research, we explore the relationship between organ architecture and its function. To properly execute its function, an organ has to maintain its three-dimensional structure. In the zebrafish, the loss of hair cells upon damage triggers a precise regeneration process by which cell fate and epithelial planar polarity are fully restored. Hair cells are born in pairs from a common immediate progenitor on the dorsal or ventral aspects of the neuromast, with sibling hair cells adopting opposite polarities. As hair cells regenerate, a vertical midline is formed, bisecting the neuromast sensorial epithelium into two mirror-symmetric plane-polarized halves, so that each half contains hair cells of identical orientation, and opposite to the confronting half. Also, it was not known how the anisotropic hair cell regeneration is controlled and how the neuromast sensory epithelium functional polarity is properly restored. We address these questions and we show that hair-cell regeneration is a strictly mitotic dependent process. We demonstrate that the neuromast bilateral symmetry is sustained by compartmentalized Notch signaling, which regulates the anisotropic regeneration process through the dynamic stabilization of hair cell progenitor identity, in permissive polar compartments in the dorsal and ventral areas of the neuromast with low Notch activity. Additionally, we show that hair cell regeneration is strongly directional along an axis perpendicular to the epithelial planar polarity. Despite this invariably

directional hair cell regeneration, the planar polarization of the epithelium eventually propagates symmetrically, when mature hair cells move centrifugally towards the periphery of the neuromast, as new hair cells are produced in the polar compartments. Furthermore, we show that oriented progenitor cell division is not necessary for regeneration anisotropy. We conclude that the neuromast sensorial epithelium bilateral symmetry is sustained by a strongly anisotropic regeneration process that relies on the stabilization of hair cell progenitor identity in permissive polar compartments.

In a second line of investigation we study the role of the chromatin remodeling complex ATPase Brg1 in the zebrafish lateral line morphogenesis.

The collective migration of cells is a fundamental process during embryonic development and throughout life. Its deregulation can lead to developmental abnormalities and several pathologic, even life-threatening consequences. Collective cell migration is the product of numerous cellular processes, therefore, a major challenge of a migrating cohort is the coordination of these multiple activities among its cells. This requires a broad coordination of gene expression, which can be achieved by genome-wide chromatin remodeling. Previous observations showed that the chromatin remodeling complex ATPase *brg1* is expressed in the neuromasts of the zebrafish lateral line system. We further extend this observation and find that, in the lack of Brg1 activity, a truncated lateral line is formed, suggesting a role for *brg1* during lateral line morphogenesis. In this study we use the zebrafish deficient in ***b****rg1* (*yng*) to address the role of Brg1 during the posterior lateral line primordium (pLLp) migration. The lateral line primordium is a polarized entity. While primordial cells display a mesenchymal behavior at the primordium leading edge, rear cells become epithelialized into two to three epithelial rosettes corresponding to the proneuromasts that will periodically

be deposited at the trailing edge. We show that, in the lack of *brg1*, primordial cells are unable to coordinate their migratory behavior and the pLLp migrates aberrantly. Additionally, Brg1 activity is necessary to maintain the pLLp homeostasis by regulating the maintenance of progenitor cells in the leading edge and the proliferative capacity of the primordium. As a consequence, rosette renewal fails and the primordium becomes progressively smaller, eventually running out of cells. Furthermore we show that, at later stages, *brg1* plays a fundamental role in the functional homeostasis of the lateral line, being necessary for the production and proper polarization of a full complement of hair cells in neuromasts. These findings reveal a role for *brg1* during mechanosensory organ formation in the zebrafish.

Contents

Table of Contents

Introduction

1.1 Hallmarks of collective cell migration

Cell migration is a crucial event in a wide variety of biological processes. During embryogenesis, cells, either individually or collectively, migrate to their final destination were they differentiate to form tissues and organs. Cell migration is also present during the adult life. As in morphogenesis, both tissue homeostasis and wounding repair rely in cell migration for processes such as skin renewal, where new epithelial cells migrate from the basal layer, or fibroblast migration and vessel sprouting in the regeneration of a damaged organ. Cell migration is also a fundamental component of immune surveillance, as in the inflammation response, where leukocytes migrate towards infection sites to destroy infected cells and pathogens and to clear debris.

Single cell migration has been the subject of an extensive study for the last decades (Mogilner and Keren, 2009; Ridley et al., 2003; Van Haastert and Devreotes, 2004) and is known to contribute to several processes during development and immune surveillance, and also in disease, such as in cancer metastasis (Deisboeck and Couzin, 2009; Friedl et al., 2004; Friedl and Weigelin, 2008; Ridley et al., 2003). Leukocytes, primordial germ cells and hematopoietic stem cells are examples of individual migratory cells.

Collective cell migration in the form of cellular clusters, sheets and chains is a common, multiphylletic and crucial phenomenon during morphogenesis, regeneration and disease (Aman and Piotrowski, 2009a; Friedl and Gilmour, 2009; Rorth, 2009) (Figure 1). In *Drosophila*, this mode of migration is the basis for border cell migration, tracheal development and dorsal closure. In vertebrates, collective cell migration is employed in a variety of morphogenetic events such as neural crest migration, mammary gland development and lateral line formation (Gompel et al., 2001; Huang and Saint-Jeannet, 2004; Lu et al., 2006; Ma and Raible, 2009), as well as in regenerative processes such as vascular sprouting and epidermal wound closure (Friedl and Gilmour, 2009). Independently of the function and shape

of the collective group of cells, it is compulsory the coordination of the migratory behavior among its cells to guarantee the proper movement of the group. Collective cell migration is therefore a highly regulated phenomenon and its deregulation underlies several pathologic conditions such as developmental abnormalities, inflammatory diseases, vascular diseases, tumor formation and metastasis.

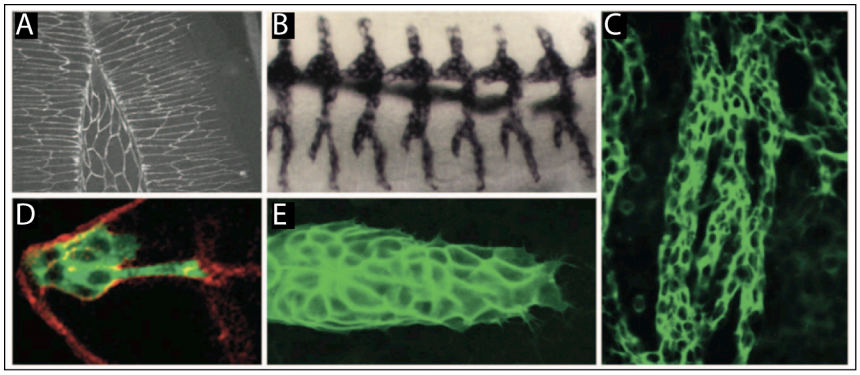

Figure.1 Different types of collective cell migration
(A) Dorsal closure in the Drosophila embryo, an example of epithelial sheet migration, a common feature of morphogenesis. **(B)** The Drosophila branched tubular networks that forms the tracheal system develops by tracheal or vascular-type branch outgrowth. **(C)** Chain migration of neuronal precursors in the sub ventricular zone of the adult rodent brain. **(D,E)** the pLLp of the zebrafish and the Drosophila border cells are two examples of migrating cohorts. Adapted from (Lecaudey and Gilmour, 2006).

1.1.1 Organization of a migratory collective group of cells

In order to reach their final target destination, migrating cells must, in general, be able to interpret an instructive external gradient of negative or positive guiding molecules and translate it into a chemotactic behavior, as in the absence of external cues cells may exhibit random locomotion (Van Haastert and Devreotes, 2004). Such gradients can be as shallow as no more than a 10% concentration difference across the length of the cell (Devreotes and Janetopoulos, 2003; Ridley et al., 2003), therefore, a keystone in cell migration is the capacity to amplify a subtle extracellular gradient into a steeper intracellular signaling gradient in order to generate the chemotactic response. For this purpose, migratory cells possess a "chemical compass", which is activated upon guidance receptor activation, that works as a

directional sensing system, by which "compass molecules" are recruited to the cell's leading edge while their degradation rate is increased at the trailing part, thereby reflecting the chemoattractant gradient steepness (Bourne and Weiner, 2002; Weiner, 2002) (Figure 2).

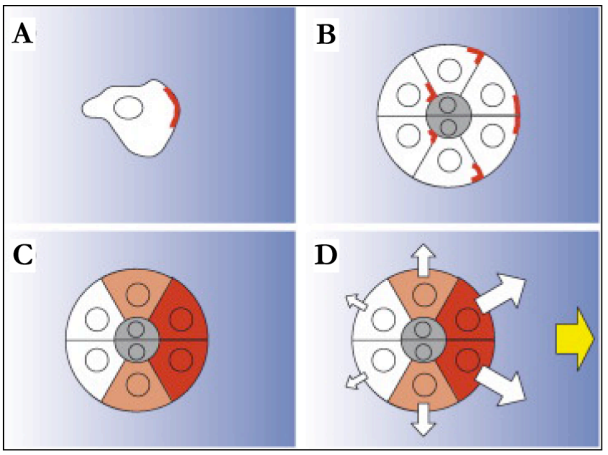

Figure 2. Guidance signaling: solitary and collective guidance
In all panels the graded blue shade represents the guidance cue concentration and the correspondent intracellular directional response is in red (intensity indicating strength). (**A**) localized classical guidance signaling in a solitary cell. The higher level of attractant is perceived at the front of the cell where it induces a local response promoting movement in the direction of increased attractant concentration. (**B**) localized classical guidance signaling response by all the migratory cells of the border cell cluster. Each cell reaction is independent of its neighbor cells reaction. (**C-D**) collective guidance signaling model. (**C**) The gradient of attractant is locally read out by each cell whose reaction is proportional to the local concentration of attractant. (**D**) white arrows indicate the preferential migratory direction of each cell of the cluster in (**C**). The size of the arrows indicate the strength of each individual cell action that sum in the net direction of the cluster indicated by the yellow arrow. Adapted from (Rorth, 2007).

However, while both single and collective migratory groups of cells usually rely on the same chemical cues to guide directional migration it is often the case that in collective cell migration only a subset of peripheral leader cells respond to the signaling guiding molecules thereby being responsible for the directional migration of the group. A migrating cohort of cells is then polarized into "leaders" and "followers" who are distinct both at the morphological and gene expression levels (Friedl and Gilmour, 2009; Vitorino and Meyer, 2008). Leading edge cells are usually less ordered and

have a mesemchymal-like shape, often displaying more evident morphological features of migratory cells, such as filipodia and pseudopodia, and generate greater traction force than their follower cells (Rorth, 2003), which tend to be tightly packed and assembled in cellular collectives, such as rosettes or tubular networks (Friedl and Gilmour, 2009). Experimental evidence supporting the role of leading cells in coordinating the migration of the cohort comes from *Dyctyostelium* slugs that migrate as a collective of thousands of cells. Here, a group of leading cells, known as prestalk cells, is responsible for the establishment of migratory waves that spread through the cohort, so that if the leading group is separated from the remaining cells it continues its migration while the remaining followers are left behind halted (Dormann and Weijer, 2001). The observation that *Drosophila* mutants where border cell clusters are immotile and whose migration can be rescued by a few wild-type cells further demonstrates that guidance of a migrating cohort can be non cell autonomous and dependent on a small subset of cells from the group. Additionally, guidance information can also be signaled at the level of the collective group (Figure 2C,D). In this case, different levels of receptor activation are established across the migrating group, with the highest activation levels at the leading edge cells (Valentin et al., 2007). This is known as collective guidance since individual cells do not have directional information but the group does (Rorth, 2007). An example of such regulation as been proposed in the migration of the zebrafish lateral-line primordium (pLLp) (Valentin et al., 2007) and in *Drosophila* border cells (Bianco et al., 2007).

1.1.2 Cell cohesion and mechanotaxis

A hallmark of collective cell migration is that cells remain attached via cell-cell junctions as they migrate. Migrating clusters often derive from epithelia, therefore displaying cadherin mediated adhesion in the form of adherens junctions, which, due to their structures, provide a dynamic mechanically

robust cohesion allowing for the rapid remodeling of the group (Kametani and Takeichi, 2007; Yamada and Nelson, 2007). An immediate consequence of cell cohesion is that the behavior of each cell affects the entire group. The maintenance of cell-cell junctions is fundamental for the transfer of directional migration information among cells, so that leading cell extension, force generation and rear cell retraction are properly coordinated among the cohort (Friedl and Gilmour, 2009). Supporting evidence comes again from *Dictyostelium*, where mutants lacking myosin II migrate as individual cells but not as a collective (Parent, 2004), suggesting that the actin-myosin network must be organized at a supracellular level for the proper spatiotemporal coordination of multicellular chemotaxis (Friedl and Gilmour, 2009; Rorth, 2009). It remains unknown how this organization is established and how mechanical tension is communicated among cells but most probably resides in paracrine signaling and the combined activity of cell-cell coupling by the action of cadherins and gap junctions (Friedl and Gilmour, 2009).

The zebrafish posterior lateral line primordium (pLLp), due to its structural simplicity and amiability for genetic manipulation and suitability for live imaging, has emerged in the last years as a powerful *in vivo* vertebrate model to study the molecular genetic mechanisms underlying the regulation of collective cell migration (Aman and Piotrowski, 2009b; Ghysen and Dambly-Chaudiere, 2004; Ghysen and Dambly-Chaudiere, 2007; Ma and Raible, 2009).

In the next subchapter I will focus on the development of the posterior lateral line system, as this is the model system that I used for the work presented in this thesis.

1.2 The zebrafish posterior lateral-line sensory system

The organs of the auditory and vestibular system in vertebrates develop near the embryonic rhombencephalon from an ectodermal thickening called neurogenic placode. In the case of the inner ear, the placode gives rise to the

otic vesicle and the neuroblast precursors of the VIIIth cranial nerve (Torres and Giraldez, 1998). The octavolateralis sensory system of some aquatic vertebrates, such as fishes and some amphibians, includes both the internal ear and the lateral line, an additional mechanosensory system that was lost in terrestrial tetrapods (Ghysen and Dambly-Chaudiere, 2004) (Figure 3A).

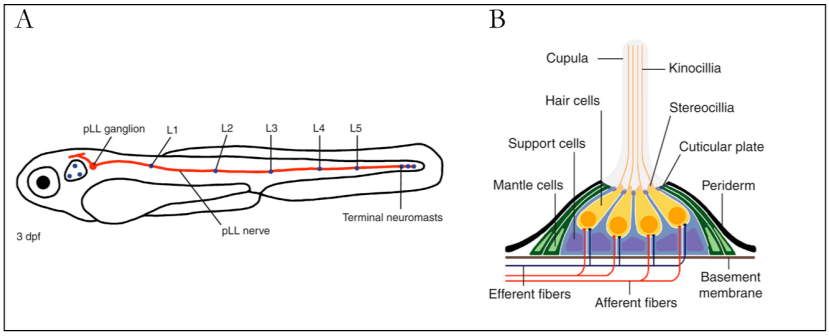

Figure 3. Posterior lateral line of the Zebrafish
(**A**) Schematics showing the posterior lateral line at 3 days post fertilization. At this stage the posterior lateral line consists of five neuromasts (L1–L5) and 2–3 terminal neuromasts. The posterior lateral line ganglion is located caudal to the developing ear and neuromasts are invervated by the posterior lateral line nerve. (**B**) Schematic diagram of a neuromast cross-section showing different structures, cell types, and innervation. Adapted from (Ma and Raible, 2009).

This sensorial system allows the animal to detect mechanical movements and flow in the surrounding water (Montgomery, 1997) mediating a touch-at-a-distance sense (Dijkgraaf, 1963). It is involved in a large variety of behaviors, from prey detection, predator avoidance and swimming to sexual courtship (Ghysen and Dambly-Chaudiere, 2004). The functional units of the lateral line are the neuromasts (Lowenstein, 1967; Metcalfe et al., 1985; Winklbauer, 1989), arranged on the body surface in a species-specific pattern and whose activity relies on a core of mechanotransductive hair-cells that share physiological, cellular and molecular properties with those in the inner ear (Nicolson, 2005) (Figure 3B).

1.2.1 Embryonic development of zebrafish posterior lateral line

The development of the lateral-line system is distinctive among sensory organs in that its individual functional units derive from cephalic placodes that undergo a stereotyped migration during which clusters of 20 to 30 cells are deposited, the proneuromasts. The lateral-line system comprises two major branches, an anterior lateral line (aLL) that extends to the head, and a posterior part that extends on the trunk and tail and forms the posterior lateral line (pLL) (Ghysen and Dambly-Chaudiere, 2007). The pLL system arises form a cranial placode that first appears caudal to the otic vesicle by 18 hours postfertilization (hpf) (Kimmel et al., 1995) (Figure 4). This placode splits in a small anterior group of around 20 cells, which will become the posterior lateral-line ganglion, and a posterior group of around 100 cells, the pLL primordium (Metcalfe et al., 1985) (Figure 4A). The pLLp is compartmentalized along its axis of migration, with cells in the leading edge adopting a mesemchimal like shape, followed by two or three garlic bulb-shaped rosettes, each with 20 to 30 epithelial cells, corresponding to a proneuromast (Haas and Gilmour, 2006) (Figure 4A,B).

The pLLp is first recognized at 18 hpf as a group of cells with a single rosette. At this stage, the premigratory primordium shows non directional protrusion extension and a tumbling motility (Aman and Piotrowski, 2010). Additional rosettes are sequentially added towards the future leading edge of the primordium during the next hours, and by 22 hpf protrusions become oriented and migration towards the tail begins (Nechiporuk and Raible, 2008). Following the pLLp are the sensory neuron growth cones from the lateral-line ganglion that will innervate the deposited neuromasts and comigrate with the pLLp till it reaches the tail, its final destination, by 44 hpf (Metcalfe, 1985). At the end of migration five to six neuromasts (named L1 to L6) have been produced and deposited along the trunk of the fish plus a terminal cluster of two to three neuromasts at the end of the tail (Kimmel et al., 1995), forming a prominent line of discrete neuromasts connected by

interneuromast cells that extends from head to tail along the flanks of the fish, giving the system its name.

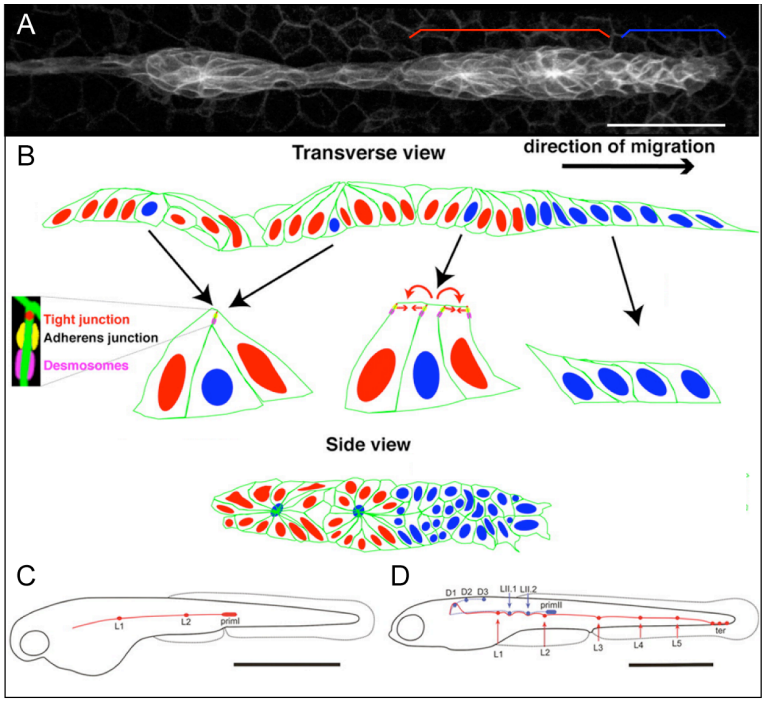

Figure 4. Development of the posterior lateral-line system
(**A**) Migrating primordium at 30 hpf. (**B**) Schematic representation of the pLLp. Leading cells adopt a mesemchimal like shape (blue) followed by two or three garlic bulb-shaped rosettes, composed by 20 to 25 epithelial cells (red), each corresponding to a proneuromast. (**C**) Development of the posterior lateral-line system periodic neuromast deposition as the primordium migrates from its origin, just posterior to the otic vesicle, to the tip of the tail. Primordium migration starts at ~20hpf and lasts ~20 hours. At 32 hpf, the migrating primordium is about halfway. having deposited two proneuromasts conected by a stream of interneuromastic cells. (**D**) As the pLLp (primI) reaches the tail, a second primordium is formed ~38hpf and splits to form PrimD, that gives rise to the dorsal lateral line (blue) and PrimII , which during the next two days will follow the path of PrimI depositing additional neuromasts. Scale bars, 50um in (**A**) and 1 mm in (**C**) and (**D**). Adapted from (Ghysen and Dambly-Chaudiere, 2007; Lecaudey et al., 2008)

Soon thereafter, a second and smaller primordium (primII), originating from a pre-somitic post-otic region will migrate along the same path and deposit two to three additional neuromasts interspersed between the primary neuromasts L1 and L3 (Sapede et al., 2002) (Figure 4C,D). The whole population of posterior neuromast will then drift ventrally, starting with the

more rostral neuromasts to its final location, below the horizontal myoseptum (Ledent, 2002; Nunez et al., 2009; Sapede et al., 2002).

1.2.2 Chemokine signaling mediates primordium migration

As in the zebrafish progenitor germ cells, *sdf1a* (*cxcl12a*) functions as a chemoattractant for the migrating primordium (David et al., 2002; Li et al., 2004). The migrating primordium expresses the chemokine receptor *cxcr4b*, which is strongly expressed in the leading edge of the primordium and down regulated in the cells that are about to be deposited in the trailing edge (David et al., 2002). Cxcr4b activity allows the primordium to follow a path laid down by the chemokine Sdf1a (David et al., 2002) along the horizontal myoseptum, between the dorsal and ventral myotomes (Figure 5A). Knocking down either gene causes a severe impairment of the pLLp migration (David et al., 2002). The onset of *cxcr4b* expression in the pLLp is between 18 and 20 hpf (David et al., 2002), coinciding with the beginning of the tumble behavior that precedes directional migration, suggesting that chemokine activity can trigger protrusion activity. However, mutants for *odysseus*, the *cxcr4b* receptor or for *medusa*, the *sdf1a* gidding chemokine, still show random protrusion formation and tumbling (Haas and Gilmour, 2006). A second *sdf1a* receptor, *cxcr7b*, is expressed in the migrating primordium in an almost complementary domain of *cxcr4b*, being expressed in deposited neuromast, interneuromast cells and in the trailing edge of the primordium, (Dambly-Chaudiere et al., 2007; Valentin et al., 2007) (Figure 5A). The presence of both chemokine receptors is essential for directional migration as loss of either receptor leads to stalling of the primordium (Dambly-Chaudiere et al., 2007; Valentin et al., 2007).

Very elegant genetic mosaic analysis demonstrated the requirement for the spatial restriction of *cxcr4b* and *cxcr7b* during pLLp migration (Haas and Gilmour, 2006; Valentin et al., 2007).

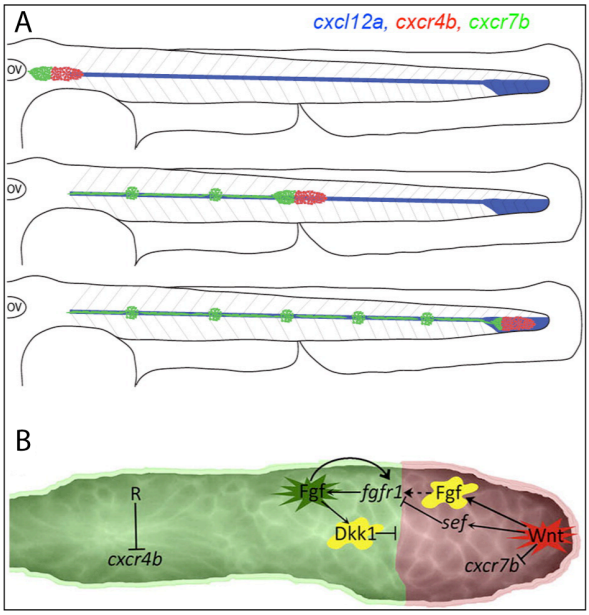

Figure 5. Schematic representation of pLLp compartimentalization.
The pLLp is a polarised structure with domains of gene expression whose compartmentalization is essential for directional migration and lateral line morphogenesis. (**A**) The pLLp migrates along a stripe of the *sdf1a* attractant (blue). The migrating primordium expresses two Sdf1a binding receptors: *cxcr4b* (red) in the leading two thirds of the primordium, and *cxcr7b* (green), expressed in the trailing part of the primordium, deposited proneuromast and interneuromast cells. As the primordium migrates, proneuromast are cyclically deposited at its trailing end (green rosettes). (**B**) Cell signaling interaction within the primordium responsible for maintenance of chemokine receptor asymmetry. Solid lines denote genetic interactions and dashed lined denote protein diffusion. A crosstalk of Fgf and Wnt/β-catenin signaling regulates the spatiotemporal patterning of the pLL and additionally pLLp directional migration, by maintaining chemokine receptor asymmetry. By mutually restricting each other, Wnt/β-catenin pathway activation is restricted to the leading zone (red) while Fgf signaling activation is confined to the trailing zone (green). Exclusivity of these domains is maintained by the induction of Wnt inhibitor *dkk1* through Fgf signaling in trailing cells and induction of *sef* by Wnt/β-catenin signaling in leading cells. *cxcr7b* expression in leading cells is inhibited by Wnt/β-catenin signaling, and *cxcr4b* expression is restricted from the trailing zone via the activity of the estrogen receptor *esr1* whose expression, or a putative cofactor might be inhibited by Wnt signaling, as ectopic expression of Wnt signaling results in the concomitant expansion of *cxcr4b*. Adapted from (Aman and Piotrowski, 2010)

This observation demonstrates that even though *cxcr4b* has a broad expression in the primordium it is only required in a few tip cells to direct primordium migration. The same approach was used to show the spatial requirement of *cxcr7b* in the trailing cells of the pLLp. *sdf1a* is a chemotactic cytokine, a family of molecules that usually directs cell chemotaxis via the expression of a gradient of the ligand (Luster, 1998). *sdf1a* is homogeneously expressed along the myoseptum (David et al., 2002; Haas and Gilmour, 2006; Li et al., 2004). It has thus been proposed that the asymmetric expression of the chemokine receptors *cxcr4b* and *cxcr7b* directs migration. In *fused somites* mutants, the expression of *sdf1a* is truncated, not reaching the tail tip. In these mutants, the migrating primordium stalls once it has reached the end of the *sdf1a* stripe, after which it migrates ventrally towards the pronephros that express *sdf1b*. In some cases, the primordium turns dorsally over itself, describing a "U-turn" and resumes migration, this time towards the head (Haas and Gilmour, 2006). This observation reveals the intrinsic polarity of the primordium but does not entirely rule out the presence of a Sdf1a gradient whose hypothesis must not be discarded, as chemokines are known to be post-transcription regulated in other contexts (Boldajipour et al., 2008; Nakayama et al., 2007).

Two non-mutually exclusive models have been proposed to explain the need of chemokine receptors polarity for primordium migration. Dambly-Chaudière *et al* proposed a model in which Cxcr7b works as a sink of Sdf1a. According to the authors, both chemokine receptors mutually repress each other expression and, in this model, Cxcr7b would not signal but rather sequesters the Sdf1a chemokine establishing a local gradient of Sdf1a over which Cxcr4b would signal and drive migration. In this case, primordium migration could be independent of an external gradient of Sdf1a since the gradient could be generated or amplified by the primordium itself (Dambly-Chaudiere et al., 2007). Supporting this model is the biochemical analysis of the mammalian Cxcr7 protein that was shown to have a higher affinity to

Sdf1a than Cxcr4 (Balabanian et al., 2005). Furthermore, in zebrafish germ cell migration, it was shown that *cxcr7b* is expressed in the somatic cells where it acts as a sink of Sdf1a, regulating the signaling levels of Cxcr4b by reducing the amount of Sdf1a in the extracellular environment (Boldajipour et al., 2008). Valentin *et al* proposed a distinct model. The authors could not find evidence for a mutual antagonism of expression between the two chemokine receptors. Additionally, the observation that the leading cells of *cxcr7b* morphants preferentially extend protusions in the direction of migration, while the trailing cells move randomly and project extensions in all directions indicates that the pLLp overall directionality is maintained in the absence of Cxcr7b activity. These observations lead the authors to propose a model where Cxcr7b activity is required in the trailing cells to detect and extend along the *sdf1a* stripe (Valentin et al., 2007).

1.2.3 Wnt/β-Catenin and Fgf signaling maintain primordium polarity coupling morphogenesis and migration in the lateral line primordium.

The relevance of primordium polarity for directed migration raises the question of how it is established and maintained. This is indeed a very interesting question since, as the primordium migrates, it must maintain its polarity while at the same time it loses its most trailing cells, as proneuromast deposition occurs. During the last years several studies have shed light onto the complex signaling network that governs primordium migration and how this relates with neuromast formation and deposition (Aman and Piotrowski, 2008; Lecaudey et al., 2008; Lopez-Schier, 2010; Matsuda and Chitnis; Nechiporuk and Raible, 2008). These studies have shown that a crosstalk of Fgf and Wnt/β-catenin signaling regulates the spatiotemporal patterning of the pLLp and directional migration by mutually restricting the activity of these two signaling pathways to opposite poles of the primordium (Figure 5B).

1.2.4 Wnt/b-catenin signaling regulates Fgf signaling in the migrating primordium

Wnt/β-catenin signaling is active in the leading zone of the primordium, as revealed by the expression of its components *lef1* and *axin2*, where it induces the expression of the secreted ligands *fgf3* and *fgf10*, whose expression is limited to the leading zone being down regulated in the trailing edge, with single foci of expression of *fgf10* in the center of the rosettes. Simultaneously, Wnt/β-catenin signaling upregulates the expression of the Fgf membrane bound inhibitor *sef,* supporting the hypothesis that Wnt signaling inhibits Fgf activity in this region. As Fgf ligands diffuse out of this inhibitory domain they stimulate the expression of target genes in the trailing region, as revealed by the expression of the Fgf signaling downstream target *pea3*, whose expression is complementary to that of the Fgf ligands, being limited to the rear part of the primordium, where *fgf10* is strongly expressed. Fgf signaling in the trailing region in turn promotes the expression of the diffusible Wnt inhibitor *dkk1*, whose activity restricts Wnt/β-catenin activation to the leading portion of the primordium (Aman and Piotrowski, 2008) establishing a coupled mutually inhibitory relation between the Wnt/β-catenin and Fgf signaling pathways (Figure 5B).

1.2.5 Wnt/β-catenin signaling regulates the asymmetric expression of chemokine receptors

Alterations in Wnt/β-catenin signaling affect primordium migration and, indirectly, proneuromast patterning and deposition through the regulation of Fgf signaling. In zebrafish mutants for *apc*, an essential component of the β-catenin destruction complex, the Wnt/β-catenin pathway is constitutively active and independent of Wnt signaling (Aman and Piotrowski, 2008). In this mutant condition the primordium migrates for 8-10 hours, after which the tip cells attempt to migrate while held back by the trailing cells that tumble randomly, with the primordium eventually stalling. When Wnt/β-

catenin is inhibited, and as a consequence Fgf signaling as well, the primordium continues to migrate in the absence of rosette formation. Therefore, Wnt/β-catenin is not required for primordium migration although its ectopic expression blocks migration (Aman and Piotrowski, 2008). These observations suggest that a Wnt/β-catening Fgf network regulates the asymmetric expression of the chemokine receptors *cxcr4b* and *cxcr7b*. Indeed, Fgf inhibition, or constitutive Wnt/β-catenin signaling, lead to ectopic *cxcr4b* expression in the primordium trailing cells and a reduction of the *cxcr7b* domain (Aman and Piotrowski, 2008; Lecaudey et al., 2008). Surprisingly, abrogation of Wnt/β-catenin signaling by heat shock induced *dkk1* expression has no effect on *cxcr4b* expression but leads to an expansion of *cxcr7b* into the leading zone. These observations suggest that Wnt/β-catening activity inhibits *cxcr7b* expression in the leading zone, maintaining its polarized expression. Additionally, the lack of *sdf1a* signaling, by the downregulation of either the ligand or its *cxcr4b* receptor, leads to a reduction of the expression of *cxcr4b*, and the concomitant expansion of the *cxcr7b* domain. This observation shows that not only Cxcr4b activity is required to suppress *cxcr7b* expression in the leading edge (Dambly-Chaudiere et al., 2007; Gamba et al., 2010), but also that *cxcr4b* can autoregulate itself and maintain its expression independent of Wnt signaling, explaining why inhibition of Wnt signaling does not effect *cxcr4b* expression. As for the definition of the *cxcr4b* expression pattern, it was shown to be dependent on Estrogen Receptor 1 (*esr1*) whose activity inhibits *cxcr4b* expression in the trailing part of the primordium (Gamba et al., 2010). As *esr1* transcripts can be found throughout the pLLp, the specific downregulation of *cxcr4b* by Esr1 in the trailing domain must depend either on the presence of an Esr1 cofactor in the trailing part of the primordium, or Esr1 activity is downregulated in the leading region of the primordium (Gamba et al., 2010).

1.2.6 Wnt signaling dependent neuromast deposition and pattern formation

Over the course of migration the primordium exhibits a cyclical behavior with the deposition of proneuromasts at its trailing edge at a regular interval (five to seven somites), and the generation of new proneuromasts near the leading edge of the primordium, that remains unpatterned (Ghysen and Dambly-Chaudiere, 2007; Lecaudey et al., 2008; Nechiporuk and Raible, 2008). The leading edge has thus been proposed as a progenitor zone for proneuromast production, which was confirmed by following the cell fate of small clusters of labeled cells in the leading region (Nechiporuk and Raible, 2008). At the end of migration all the primordium and the most posterior neuromasts were originated from the labeled cells, demonstrating that a small number of cells in the leading edge represent a progenitor zone. Additionally, the pLLp shows higher levels of proliferation towards the leading edge and reduced proliferation in the trailing edge (Laguerre et al., 2009; Laguerre et al., 2005), further supporting its role as a regenerative zone.

The periodic deposition of proneuromasts can be a consequence of the internal dynamics of the primordium or determined by external cues. If initial studies suggested that the periodic organization of the somites could instruct neuromast deposition (Haines et al., 2004), Aman *et al* showed that, by analyzing the *trilobite* mutant, where somite patterning is compromised without affecting the pattern or neuromasts deposition, this is unlikely to happen (Aman et al., 2011). The authors observation that primordium length increases during the deposition cycle and that decreased cell proliferation leads to the deposition of fewer proneuromasts lead Aman *et al* to propose a model by which the proliferation rate regulates proneuromast deposition (Aman et al., 2011). As cells are produced in the regenerative leading edge and proliferate along the leading two thirds of the primordium, this one increases in length, maintaining a constant *cxcr7b*-free zone while cells in the most trailing edge start to express *cxcr7b*. As more cells are added at the

leading edge, additional cells at the trailing edge are being included in the *cxcr7b* domain that will then expand, eventually incorporating all cells in the most rostral rossete. At this point, the proneuromast starts to slow down until deposition occurs. Additionally, Aman *et al* showed that the general abrogation of Wnt signaling in the transgenic line *Tg(hs:dkk1)* reduces the rate of proliferation in the pLLp, suggesting that Wnt-dependent proliferation activity regulates the rate of neuromast deposition.

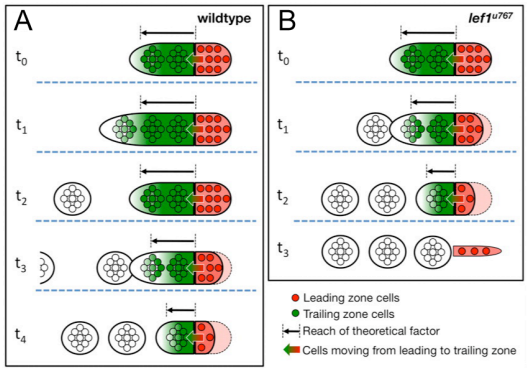

Figure 6. Model describing proneuromast deposition regulation of wild-type and *lef1* mutants. (**A**) In the wild-type siblings the high proliferation in the leading zone (red) continuously feeds cells to the primordium as proneuromast are deposited in the trailing zone (green) (t0-t2). In this way the proportions of the primordium remain constant as it migrates. At the end of migration (t3-t4), the leading zone and the rate of proliferation decrease and as a consequence the putative leading zone secreated factors have a smaller area of action which promotes neuromast deposition at the trailing edge (**B**). In *lef1* mutants the loss of leading cells to the trailing zone results in a reduced proliferation in the leading zone, which results in premature neuromast deposition and termination of migration (t0 to t3). Adapted from (Valdivia et al., 2011).

This was further confirmed by two independent studies that showed that Wnt signaling via Lef1 activity is necessary to maintain the identity of the regenerative leading edge cells and the proliferation pattern in the pLLp (McGraw et al., 2011; Valdivia et al., 2011). In the absence of *lef1*, progenitor cells are not retained in the leading edge and become incorporated in the developing rosettes, being eventually deposited in the formed proneuromasts. As a consequence, as proneuromast are deposited, the pLLp becomes progressively smaller eventually running out of cells until it stalls. Additionally, proneuromasts are progressively deposited at shorter intervals in the absence of Lef1 activity. These observations lead Valdivia *et al* to

extend the model proposed by Aman *et al*, advancing the hypothesis that unidentified factors in the leading edge control the size of the pLLp (Figure 6). In the absence of Lef1 activity, the progenitor leading zone becomes progressively smaller, resulting in a deficit of these factors, which would explain the shorter rate of proneuromast deposition as the pLLp shrinks in size (Valdivia et al., 2011).

1.2.7 Fgf signaling regulates rosette morphogenesis and sensory hair cell precursor specification

Cells within the rosettes have a distinct morphology from the leading cells, being radially arranged and apically constricted with their nuclei basally positioned. As the primordium migrates, cells behind the leading edge adopt a heightened columnar epithelial shape, after which their actin membranes become constricted and focal points are formed, shaping the rosettes (Hava et al., 2009; Lecaudey et al., 2008). In the absence of Fgf signaling rosettes disassemble and cells lose their epithelial columnar morphology while increasing their filopodial projections dynamics, revealing their regain of mesenchyme like characteristics (Lecaudey et al., 2008; Nechiporuk and Raible, 2008). Additionally, ectopic expression of Fgf ligands results in supernumerary rosette formation (Lecaudey et al., 2008), which, together with the observation that inhibition of Fgf signaling with Su5402 does not affect the epithelial morphology of deposited neuromasts, further supports a major role of Fgf signaling in the spatiotemporal regulation of the mesemchymal to epithelial transition and rosette morphogenesis.

As rosettes are assembled, differentiation of hair cells and supporting cells is already taking place in the migrating primordium (Gompel et al., 2001; Hernandez et al., 2007; Itoh and Chitnis, 2001). The early hair cell marker bHLH transcription factor *atoh1a* is specifically expressed in hair cell precursors in the center of the rosettes, while *notch3* is expressed in the prospective supporting cells that surround the *atoh1a* positive cell. *atoh1a*

expression is absent upon depletion of Fgf signaling (Nechiporuk and Raible, 2008), suggesting that this pathway has two key functions in the pLL primordium: it regulates the spatiotemporal epithelialization of proneuromasts and determines hair cell progenitor fate.

1.2.8 Hair cell precursor specification must be restricted for proper morphogenesis of the pLL

As proneuromasts start to be formed Fgf signaling initiates the expression of *atoh1a* and *deltaA* in a central cell of the newly formed rosette (Matsuda and Chitnis, 2010) (Figure 7). DeltaA activates Notch in adjacent cells that, by lateral inhibition, down regulate *atoh1a* expression. As the proneuromast matures, Atoh1a upregulates the expression of an additional Notch ligand, *deltaD*, which together with *deltaA* will reinforce Notch activity in the surrounding cells. As a consequence, *Atoh1a* expression, and therefore hair-cell fate, is restricted to a central cell in the rosettes while the surrounding *notch* expressing cells are specified as supporting cells (Matsuda and Chitnis, 2010). At this stage, the hair cell progenitor in the center of the rosette becomes a source of Fgf signaling as Atoh1a promotes the expression of *fgf10*, while at the same time inhibits the expression of its receptor, *fgfr1* (Lecaudey et al., 2008; Matsuda and Chitnis, 2010) (Figure 7A). As Notch activation downregulates *atoh1a* expression in the surrounding cells, these continue to express *fgfr*, and so, remain competent to respond to the Fgf and Delta signals from the central hair cell progenitor. If initially *atoh1a* expression was dependent on Fgf signaling, the downregulation of *fgfr* in the central hair-cell progenitor makes it less responsive to Fgf signaling and, as a consequence, *atoh1a* expression becomes less dependent on Fgf signaling. At this late stage, hair cell progenitor identity is maintained by Atoh1a auto-regulation as it promotes the expression of *atoh1b* which, by cross activation, will maintain *atoh1a* expression (Matsuda and Chitnis, 2010).

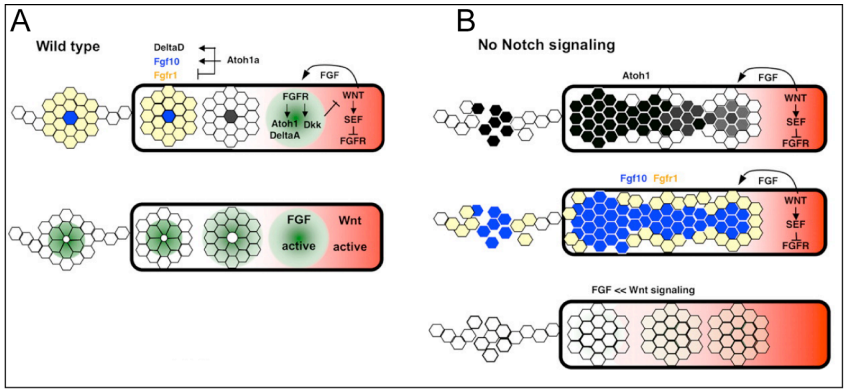

Figure 7. Atoh1 establishes a focal Fgf signaling center in maturing proneuromasts. (**A**) Fgf activation drives the expression of *atoh1a* and *deltaA*. DeltaA activates Notch in neighboring cells restricting *Atoh1a* expression to a central cell (black). Atoh1a establishes a focal Fgf signaling system in maturing proneuromasts by driving the expression of *fgf10* (blue) and inhibiting *fgfr1* expression(yellow). (**B**) In the absence of Notch signaling, additional cells express *atoh1a* and *fgf10*, shutting off *fgfr1* expression, which results in decreased Fgf signaling and the concomitant loss of *dkk1* and expansion of Wnt signaling domain. Adapted from (Matsuda and Chitnis, 2011).

Supporting the role of Notch signaling in pLL morphogenesis comes from the characterization of the pLLp migration in the *mind bomb* mutant, where Notch signaling is severely impaired and *atoh1a* expression is not longer restricted by lateral inhibition to the center of the rosettes (Itoh and Chitnis, 2001) (Figure 7B). This expansion of *atoh1a* expression is accompanied by the downregulation of *fgfr* leading to a failure of Fgf dependent processes, such as rosette morphogenesis and maintenance of the coupled mutually inhibitory network between the Wnt/β-catening and Fgf signaling systems.

1.3 SWI/SNF chromatin remodeling complexes

Chromatin remodeling complexes are large macromolecular protein complexes of ~2MDa that use the energy of ATP to change nucleosomal structure and position, thereby playing a crucial role in transcription regulation, being involved in processes such as cell proliferation, differentiation, embryonic patterning and tumor formation (Becker and Horz, 2002). Chromatin remodeling complexes are grouped in 4 different families: SWI/SNF, ISWI, NuRD and INO80, defined by the identity of

their respective ATPase subunits Brg1 or hBrm, ISWI, MIA-2 and Ino80 (Trotter and Archer, 2008)

The SWI/SNF complexes were the first of the chromatin remodeling complexes to be identified, and since their first description in yeast (Winston and Carlson, 1992) they have been extensively characterized (Kadonaga, 1998; Martens and Winston, 2003). Briefly, SWI/SNF complexes consist of 7-13 highly conserved multi-subunit complex (Cairns et al., 1994; Peterson and Tamkun, 1995) whose specific identity is defined by their subunit composition (Lemon et al., 2001; Nie et al., 2000; Trotter and Archer, 2008; Yan et al., 2005).

In mammals, SWI/SNF complexes contain one of the two mutually exclusive paralogous catalytic subunits hBrm (Brahma) or Brg1 (Brahma-related gene1) (Martens and Winston, 2003). Even though *brg1* and *hbrm* share a high degree of sequence identity and similar *in vitro* activity (Khavari et al., 1993) the two ATPases play different roles *in vivo* by having distinct target gene specificity (Bultman et al., 2000; Kadam and Emerson, 2003; Strobeck et al., 2002).

1.4.1 *brg1* in transcription regulation

By opening chromatin and through its interaction with DNA-binding motifs, transcription factors and the general transcription machinery, SWI/SNF complexes play a crucial role in gene transcription regulation. *brg1* is generally associated with transcription activation, however there is evidence that chromatin remodeling complexes can interact with transcription co-repressors, therefore promoting gene silencing (Trotter and Archer, 2008) .

1.4.2 *brg1* in the zebrafish, the *young* mutant

In the zebrafish, *brg1* is expressed during early embryonic development. *In situ* mRNA expression pattern reveals the presence of *brg1* transcripts at one cell stage, showing that it is a maternally expressed gene (Eroglu et al., 2006; Gregg et al., 2003). *brg1* expression is ubiquitous until 24 hpf, after which it

becomes restricted to the anterior part of the embryo, with stronger expression in the telenchephalon, cerebellum and hindbrain regions. Interestingly, *brg1* expression is maintained in deposited neuromasts of the lateral line system (Eroglu et al., 2006; Gregg et al., 2003) (Figure 8A).

In the zebrafish, *brg1* has been shown to have a critical role during development, affecting neurogenesis and neural crest induction (Eroglu et al., 2006), consistent with its predominantly anterior expression, but also cardiac development (Takeuchi et al., 2010) and the establishment of left/right asymmetry (Takeuchi et al., 2007). A zebrafish recessive mutant for *brg1*, *Young* (*yng*) has been particularly well characterized for its need in mediating retinal cell differentiation, with *yng* mutants showing specification of all major retinal cell types but failing to accomplish cellular differentiation (Gregg et al., 2003; Link et al., 2000).

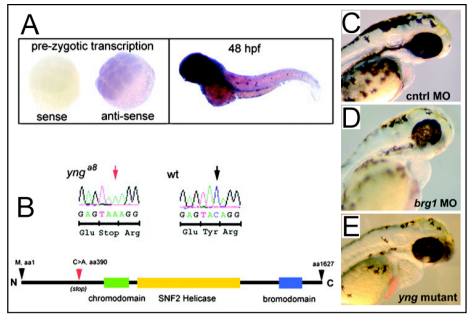

Figure 8. ***brg1*** **expression in the zebrafish and the** ***yng*** **mutant**.
(**A**) *in situ* mRNA analysis of *brg1*. *brg1* is maternally expressed as transcripts are detected at the sixteen-cell stage embryo, before zygotic transcription begins. At 48 hpf *brg1* is strongly expressed in the anterior part of the fish and in the lateral line neuromast (**B**) The *yng* mutant lacks a functional Brg1 protein. Sequence analysis and predicted protein structure. A C to A transversion creates a premature stop codon deleting all the identified functional domains. (**C**-**E**) Standard control oligo in (**C**); *brg1* morpholino injected in (**D**) and *yng* mutant in (**E**) at 3 dpf. *brg1* morphants and *yng* mutants show similar disrupted morphogenesis of the heart, ear and fin and pigment cell development. *yng* mutants show a strong curved body axis and die by 6-7 dpf most probably due to cardiac failure. Adapted from (Eroglu et al., 2006; Gregg et al., 2003).

1.4 Sensory regeneration and functional architecture

The capacity to maintain the functional architecture of an organ is essential for its proper function throughout the entire life of the individual. This is of particular relevance in sensorial organs, whose function is essential for the correct interaction of the individual with the environment and that, due to their nature, are particularly exposed to a number of environmental insults that can damage them.

1.4.1 Hair cell regeneration

In the inner ear, hair cells are the sensorial receptors of both the auditory and vestibular system. Through them, a mechanical stimulus, caused either by head motions or sound vibrations, is converted into an action potential in the auditory and vestibular neurons (Hudspeth, 1989). A fundamental characteristic of hair cells is their striking planar polarity: a single kinocilium if positioned on one side of the cell with a bundle of stereocilia at its side disposed in a staircase fashion with the longest stereocilia closer to the kinocilium. This morphological polarity is critical for its function: pushing the bundle in the direction of the kinocilium depolarizes the hair cell while the movement in the opposite direction hyperpolarizes, which results in either an increase or decrease in the hair cell afferent neurons firing frequency (Figure 9). Cilia movement in an orthogonal direction does not elicit hair cell activity. The presence of a population of functional and properly oriented hair cells is, therefore, *condicio sine qua non* for normal hearing and posture equilibrium.

Sensory cell turnover occurs in both mammalian olfactory and gustatory epithelia (Beites et al., 2005; Miura et al., 2006). However, this is not the case in the inner ear, where cochlear hair cell loss is irreversible, leading to hearing deficits (Chardin and Romand, 1995; Davis et al., 1989), while vestibular hair cell replacement occurs at very a low rate, discarding any functional significance (Forge et al., 1998; Rubel et al., 1995).

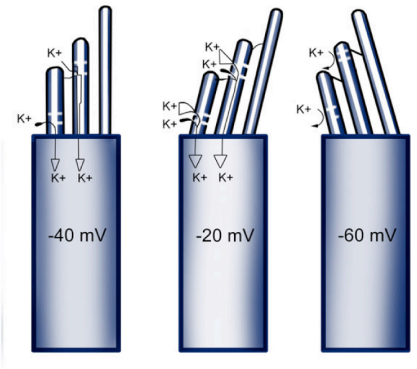

Figure 9. The hair cell functions as a variable resistor.
Bending toward the tallest row of stereocilia causes an opening of channels in the stereocilia, providing a route for influx of K+ ions, causing depolarization of the hair cell. Stereocilia bending in the opposite direction creates a hyperpolarization by closing those channels that are constantly open, even in the resting state, thus further obstructing K+ flow down the electrochemical gradient. Adapted from (www. emedicine.medscape.com).

Unlike mammals, non-mammalian vertebrates are able to regenerate hair cells upon damage through their adult lives. The first evidence came from studies of the lateral line of both amphibians and cartilaginous fishes where hair cells are continuously produced throughout the animal's life as part of its normal growth (Balak et al., 1990; Corwin, 1981; Corwin, 1985). In newts, and later in the zebrafish, it was shown that upon amputation of the tip of the tail, new neuromasts are produced from the supporting cells of the last neuromast adjacent to the amputation plane, that eventually divides and migrate to colonize the blastema in order to form the new neuromasts as the tail regenerates (Dufourcq et al., 2006; Jones and Corwin, 1993). Additionally, upon specific hair cell ablation, it has been observed the increase of hair cell production, in a process dependent on supporting cell proliferation (Jones and Corwin, 1993; Jones and Corwin, 1996). Similar observations have been done in the zebrafish where a similar increase in supporting cell proliferation and subsequent hair cell production occurs upon ototoxic damage (Hernandez et al., 2007; Ma et al., 2008; Williams and Holder, 2000). Hair cell regeneration has been studied as well in the vestibular organs, where ongoing regeneration of hair cells has also been

observed in the fishes, bullfrogs, newts, and also in birds, that also show, functional regeneration of the auditory system (Cotanche et al., 1987).

In all cases the loss of hair cells triggers an unknown mechanism that promotes hair cell regeneration either by division of supporting cells (Baird et al., 1993; Corwin and Cotanche, 1988; Jones and Corwin, 1993; Ryals BM, 1988; Stone and Cotanche, 1994), or by direct transdifferentiation of supporting cells (Adler and Raphael, 1996; Roberson et al., 2004), or both (Baird et al., 1996; Brigande and Heller, 2009; Duncan et al., 2006).

1.4.2 Notch signaling regulates hair cell specification during development and regeneration

During cochlea development the first sign of hair cell differentiation is the expression of the bLHL transcription factor *atoh1* (Bermingham et al., 1999; Chen et al., 2002; Woods et al., 2004). As hair cells mature, *atoh1* is down regulated, revealing its major role as a hair-cell fate determinant (Bermingham et al., 1999). While it is not known what triggers *atoh1* expression during development, it is well established that as hair cells mature they express the Notch ligand Delta, inhibiting surrounding supporting cells to differentiate into hair cells by Notch lateral inhibition (Brooker et al., 2006; Haddon et al., 1998; Kelley, 2006; Kelley, 2007; Kiernan et al., 2005a) (Figure 10).

In the adult avian basilar papila there is no expression of *atoh1*. However, upon damage, the supporting cell population soon starts to express *atoh1a* and activates the Notch pathway anticipating hair cell production (Cafaro et al., 2007; Daudet et al., 2009). Similar results have been obtained in the zebrafish lateral line where upon hair cell ablation, *atoh1* and the *delta* ligands are upregulated in hair cell precursors, while *notch* expression is induced in the supporting cell population (Ma et al., 2008).

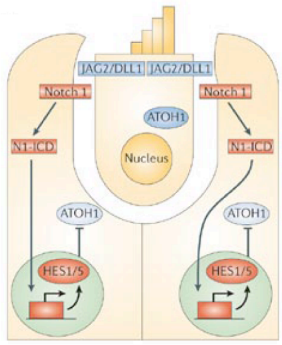

Figure 10. Model for Notch signaling in hair cell and supporting cell specification. Hair cells express the hair cell-specific transcription factor *atoh1* and the Notch *delta* and *jagged* ligands that signal to neighbor cells via Notch receptors. Notch activation in these cells will promote the transcription of Notch target genes such as members of the *hes* and *hey* gene families that will repress the expression of hair cell-specific genes such as *atoh1*, thereby promoting a supporting cell fate. Adapted from (Kelley, 2006)

Additionally, blocking Notch activity both during hair cell development and regeneration results in the overproduction of hair cells, revealing that Notch mediated lateral inhibition regulates hair cells specification during regeneration like it does during development (Ma et al., 2008) (Haddon et al., 1998; Haddon et al., 1999). Interestingly, the farmacological inhibition of Notch activity in the differentiated undamaged avian basilar papilla or in the zebrafish lateral line does not result in the upregulation of *atoh1* expression in the supporting cells, therefore no additional hair cells are produced (Daudet et al., 2009; Ma et al., 2008). This observation shows that both hair and supporting cell fate specification by Notch lateral inhibition only takes place during development or upon damage, therefore, cell fate maintenance seems independent of Notch activity in the undamaged epithelium. All together these observations suggest that, independently of the particular contribution of cell proliferation and transdifferentiation in hair cell regeneration, the interactions between hair cells and supporting cells must regulate the proliferation and differentiation of new cells.

1.3.3 Establishment of hair cell polarity and organ functional architecture

To have functional significance, regenerated hair-cell must be properly incorporated in the sensory epithelium, preserving the organ's architecture.

Hair-cell planar polarity along the sensory epithelium can assume distinct functional patterns. For instance, hair cells in the organ of Corti orient all in the same direction, away from the neural side of the organ, while in the zebrafish lateral line, the neuromast is bilaterally divided in two halves, each one preferentially populated by hair cells of identical orientation but opposite to that of the confronting half (Lopez-Schier et al., 2004; Rouse and Pickles, 1991), and even more complex patterns are observed in the vestibular system macula, where each hair cell is aligned with its immediate neighbors with polarity reversal occurring in the striolar regions (Denman-Johnson and Forge, 1999; Platt, 1977). Regardless of the differences in complexity two general properties emerge: first, individual hair cells have a well-defined planar polarity, with the kinocillium and the staircase stereocillialy located asymmetrically in the cell, independently of its relative position in the macula, and second, neighboring hair cells show strongly correlated orientations. From these observations one can then infer three levels at which hair cell polarity is regulated: at the level of the individual hair cell asymmetry, dependent on its own internal cytoskeleton symmetry breaking, at the level of neighbour cells where hair cell orientation must be coupled to that of its surrounding cells, and at a global level where the orientation the group must be specifically controlled dependent on its position in the sensory organ.

1.3.4 The neuromast, a "bonsai ear"

The neuromast is the functional unit of the zebrafish lateral line. It is found at the surface of the skin allowing the animal to perceive differential water movements (Montgomery et al., 2000). Each individual neuromast contains a

core of hair cells in its center, innervated by both afferent and efferent neurons that project to the central nervous system, surrounded by an internal population of nonsensory internal sustentacular supporting cells and an outer population of supporting mantle cells, that wrap the neuromast in its volcano shape and secrete a gelatinous cupola that embeds the hair cells processes (Alexandre and Ghysen, 1999; Gompel et al., 2001; Metcalfe et al., 1985; Raible and Kruse, 2000) (Figure 11A-C). Similar to the inner ear hair cells, lateral line hair cells bear a "hair bundle" composed of approximately 100 actin based stereocilia and an additional single microtubule-based kinocilium (absent in the mature mammalian cochlear hair cells), whose asymmetric localization defines the hair cell polarity axis.

During development, hair cells populate the neuromast in two groups containing an equal number of hair cells with opposite hair bundle polarity arranged across a plane of mirror symmetry, suggesting that hair cell orientation is tightly controlled (Figure 11D-L). Whereas hair cells of neuromasts deposited by PrimI are oriented antero-posteriorly, hence named parallel neuromasts, PrimII deposited neuromasts have their hair cells polarized along the dorso-ventral axis, and therefore are named perpendicular neuromasts.

Hair cells are continuously produced during the zebrafish lifetime, assuring the maintenance of a functional epithelium, however this is a relatively slow process, therefore making it difficult to follow with high temporal resolution. Hair cells have been shown to be susceptible to aminoglycosides (Harris et al., 2003; Owens et al., 2007; Song et al., 1995; Williams and Holder, 2000) as well as copper (Hernandez et al., 2006; Hernandez et al., 2007), which can be used to eliminate the hair cell population and accelerate the regeneration process.

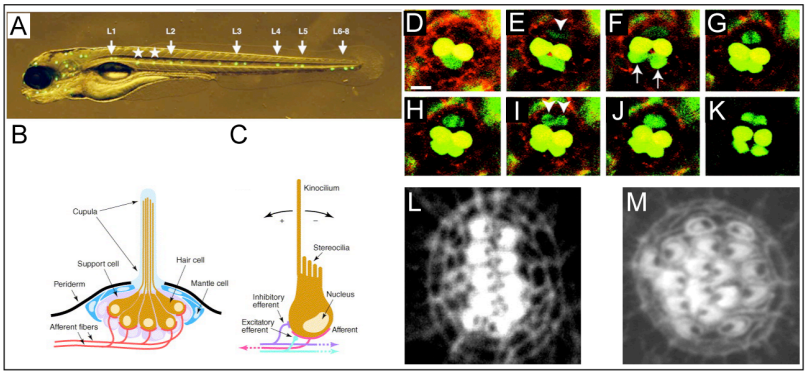

Figure 11. The zebrafish lateral line.

(**A**) Superimposition of a bright field and fluorescent image of a zebrafish larva at 5 dpf with neuromasts labelled with Yo-Pro-1. Arrows point to neuromasts (L1 to L8) deposited by PrimI on the left side of the embryo. Secondary neuromasts (*) and a few neuromasts from the right side of the embryo and from the anterior lateral line (not labelled) are also visible. (**B**) Scheme of a neuromast, illustrating its different cell types. Hairs cells are surrounded by a protruding jelly-like cupula secreted by the supporting cells. (**C**) Scheme of a hair cell, illustrating its functional asymmetry, as well as its afferent and efferent innervation. (**D-K**) 12-h-long time-course analysis of hair-cell production at 2 dpf. Labeling of an SqEt4 larva with Texas red-ceramide (red) reveals two GFP-positive mature hair cells (yellow). At the lower edge of the neuromast, a pair of immature hair cells (green; arrows in **F**), separate over the course of 3 hours (**E** and **F**) and mature (**G**–**K**). A hair-cell precursor develops at the upper edge of the neuromast (arrowhead in **E**) and eventually divides (**H**) giving rise to two sister cells (**I**). (**L**) At early stages of development and upon hair cell ablation new pairs of sister hair cells are produced with their hair bundles with opposite polarity demarcating a line of symmetry dividing the neuromast into two halves along the dorsoventral midline. At this stage all of the hair bundles on each side of the line of symmetry have the same orientation. (**M**) The continuous expansion of the macula along the axis of symmetry reaches a limit imposed by the size of the neuromast and the macula evolves from its initial oval shape to a circular shape as the hair-cell population expands in a direction perpendicular to that of regeneration. A single line of symmetry is at this stage less evident, as both halves are now populated with hair cells of both polarities. Scale bars are 10μm. Adapted from (Chitnis et al., 2011; Ghysen and Dambly-Chaudiere, 2004; Lopez-Schier and Hudspeth, 2006).

Taking advantage of the accessibility of the lateral line to acquire time-lapse sequences, López-Schier and Hudspeth showed that upon hair-cell ablation in neuromasts, some cells start to express a hair-cell marker (SqET4) and eventually divide in a plane perpendicular to the neuromast's axis of planar polarity, giving rise to two sister cells with opposite polarities (Lopez-Schier and Hudspeth, 2006) (Figure 11D-K). Importantly, hair cell progenitors are first identified and divide at the dorsal and ventral aspects of a parallel neuromast, whose hair cells are oriented anteroposteriorly, while in perpendicular neuromasts, which show a dorsoventral polarity, hair cell progenitors position is also shifted, being first identified at the anterior and posterior extremes of the neuromast. As a consequence, as new progenitors sequentially divide along a single axis, producing sister hair-cells with opposite polarities, a line of mirror symmetry is created, dividing the organ in two halves with an equal number of hair cells polarized in opposite directions (Figure 11L). Eventually the continuous expansion of the macula along the axis of symmetry reaches a limit imposed by the size of the neuromast and the macula evolves from its initial oval shape to a circular one (Figure 11M). At this mature stage, a single line of symmetry is less evident as both halves are now populated with hair cells of both polarities. The generation of sister hair cells with opposite polarity that align along each side of the line of mirror symmetry suggests that cell polarity depends on the position of its sibling (Lopez-Schier and Hudspeth, 2006). Insights on the molecular basis of hair cell polarization come from the authors characterization of the *trilobite* mutant, which lacks the *vangl2* gene. *vangl2* is a component of the Planar Polarity System, which is involved in the polarization of different epithelia such as the *Drosophila* ommatidia, the alignment of mammalian body hair along the anterior-posterior axis and more importantly in the polarization of stereociliary bundles in the inner ear. (Devenport and Fuchs, 2008; Montcouquiol et al., 2003). Additionally, it has been shown that during zebrafish gastrulation, the orientation of cell division

is *vangl2*-dependent (Gong et al., 2004). Not surprisingly, *trilobite* mutants show aberrant hair cell polarity. However, time lapse analyses of hair cell regeneration revealed that mitoses are normal and sibling hair cells align along the neuromast's axis, which lead the authors to propose a two step mechanism underlying the establishment of hair cell planar polarity. In a first step, localized hair cell progenitors divide producing sibling cells along the neuromast axis of symmetry while in a second step, the *vangl2*-dependent movement of the kinocilium assures that sibling cells adopt opposite polarities (Lopez-Schier and Hudspeth, 2006).

It remains unknown what determines and maintains the neuromast axis of symmetry, however, the observation that the direction of migration of the pLLp strongly correlates with the axis of symmetry of the deposited neuromasts suggests that the axis of hair cell progenitor division, and therefore the polarity of the epithelium, is defined by the direction of migration of the primordium. Supporting this hypothesis is the observation that PrimII derived neuromasts show a dorso ventral polarity, consistent with their ventral migration as they are being deposited. Additional evidence comes from the analysis of the *fused somites* mutant where primI follows an aberrant migration, which results in the mislocalization of the neuromasts along the trunk and whose polarity becomes randomized relatively to the A-P axis of the fish but remains aligned with the migrating trajectory of the primordium (Lopez-Schier et al., 2004).

An additional standing question concerns the origin of hair cell progenitors and the regulation of their specific location along the axis of polarity of the neuromast and the origin of these cells. A recent study suggests that the source of hair cell progenitors is the *sox2* positive population of supporting cells that reside under the hair cell population (Hernandez et al., 2007). *sox2* is essential for the establishment of sensory domains in the mammalian inner ear where it acts upstream of *math1* (the mammalian homolog of the zebrafish *atoh1*) being expressed in the supporting cell and hair cell

population at early stages of the organ development and downregulated in mature hair cells. (Kiernan et al., 2005b). Upon hair cell ablation the neuromast supporting cell population shows increased mitotic activity, as revealed by the incorporation of BrdU. The majority of the BrdU positive cells correspond to internal sustentacular supporting cells, suggesting them as the source of the newly regenerated hair cells (Ma et al., 2008). The observation that the *sox2* positive cells coincide topologically with the internal sustentacular cells and that newly formed hair cells show weak levels of *sox2* expression supports a role for *sox2* in hair-cell specification in the lateral line neuromasts (Hernandez et al., 2007). Additionally, Hernandez *et al* showed evidence for hair-cell regeneration trough supporting cell transdifferentiation, therefore without the intervention of a mitotic precursor, contrasting with the observations by other groups (Hernandez et al., 2007; Lopez-Schier and Hudspeth, 2006; Ma et al., 2008). In particular, the authors showed that upon exposing 76 hpf larvae to 1μM CuSo4, regenerated hair cells differentiate from a post mitotic cell, while those regenerating after exposure to 10μM CuSo4 arise from a mitotic precursor. Whether all the supporting cell population is *sox2* positive and share the potential to produce new hair cells, either by transdifferentiation or cell division, remains unknown.

Aims

This thesis was aimed at studying two fundamental biological problems.

First Aim

Previous studies in the host laboratory have characterized the postembryonic regeneration of hair cells, during which hair cell fate and epithelial planar polarity are recovered. These results revealed two important characteristics of the regenerative process:

1) hair-cells are always born in pairs from a common immediate progenitor;

2) pairs of hair-cells are produced sequentially on the dorsal or ventral aspects of the neuromast, along a single axis with hair cells at each side of the midline orienting identically.

These results were further extended using the *Tg(SqEt20)*. This line expresses GFP in the supporting cell population, with low or no expression in a putative regenerative zone where the new hair cells immediate progenitors are first identified.

It is not know how regeneration anisotropy is controlled and how this process is integrated to generate the neuromast bilateral symmetry. Understand these processes constitutes the first aim of this thesis.

Second Aim

The pLLp is an example of a migrating cohort where multiple biological processes must be finely maintained to allow the coordinated multicellular movement in a tissue that is under constant remodeling. This requires a precise coordination of gene expression among the migrating cells, which can be achieved by genome-wide chromatin remodeling.

The chromatin remodeling complex ATPase *brg1* is expressed in the neuromasts of the posterior lateral line. Previous observations in the host laboratory suggested that the zebrafish deficient in *brg1* (*yng*) lack a full complement of neuromasts in the posterior lateral.

These observations prompted us to analyze the role of *brg1* in the development of a functional lateral-line system, which constitute the second aim of this thesis.

Chapter 1

Compartmentalized Notch signaling sustains epithelial mirror symmetry

Indra Wibowo[1†], Filipe Pinto-Teixeira[1†], Chie Satou[2], Shin-ichi Higashijima[2] and Hernán López-Schier[1]

1 Laboratory of Sensory Cell Biology & Organogenesis, Centre de Regulació Genòmica - CRG, c/Dr Aiguader 88, (08003) Barcelona, Spain

2 National Institutes of Natural Sciences, Okazaki Institute for Integrative Bioscience, Higashiyama 5-1, Myodaiji, Okazaki, Aichi 444-8787, Japan

† *These authors contributed equally to this work*

Development 2011 (138), 1143-1152

1.1 Abstract

Bilateral symmetric tissues must interpret axial references to maintain their global architecture during growth or repair. The regeneration of hair cells in the zebrafish lateral line, for example, forms a vertical midline that bisects the neuromast epithelium into perfect mirror-symmetric plane-polarized halves. Each half contains hair cells of identical planar orientation but opposite to that of the confronting half. The establishment of bilateral symmetry in this organ is poorly understood. Here we show that hair-cell regeneration is strongly directional along an axis perpendicular to that of epithelial planar polarity. We demonstrate compartmentalized Notch signaling in neuromasts, and show that directional regeneration depends on the development of hair-cell progenitors in polar compartments that have low Notch activity. High-resolution live cell tracking reveals a novel process of planar cell inversions whereby sibling hair cells invert positions immediately after progenitor cytokinesis, demonstrating that oriented progenitor divisions are dispensable for bilateral symmetry. Notwithstanding the invariably directional regeneration, the planar polarization of the epithelium eventually propagates symmetrically because mature hair cells move away from the midline towards the periphery of the neuromast. We conclude that a strongly anisotropic regeneration process that relies on the dynamic stabilization of progenitor identity in permissive polar compartments sustains bilateral symmetry in the lateral line.

1.2 Introduction

The three-dimensional organization of tissues is essential for the efficient function of organs. It must also be maintained during the entire life of the individual and recovered during organ repair because its loss can generate devastating pathologies (Wodarz and Nathke, 2007; Zallen, 2007). The pervasive planar cell polarity has emerged as an architectural property of tissues that allows investigations of the link between form and function

(Axelrod, 2009; Strutt and Strutt, 2009). One group of organs that relies on planar cell polarity for coherent sensory function is the acusticolateralis system that comprises the inner ear and lateral line, whose shared plane-polarized elements are the mechanosensory hair cells (Lewis and Davies, 2002; Rida and Chen, 2009). The planar polarization of the hair cells allows animals to detect and interpret the direction of propagation of a sound (Hudspeth, 1985). Hair cells are substantially similar in their development and physiology across species. However, while their loss in mammals is irreversible leading to permanent deafness, other vertebrates are endowed with a hair-cell regenerative capacity during their entire lives (Collado et al., 2008; Corwin and Cotanche, 1988; Lopez-Schier, 2004; Ryals and Rubel, 1988). During organ repair, cell fate and tissue architecture are often acquired concurrently to allow functional recovery before full anatomical repair, which may be essential for organs on which animals depend for survival. In the sensory organs of the zebrafish lateral line, called neuromasts, the complete loss of hair cells triggers a rapid and precise regeneration process (Brignull et al., 2009; Lopez-Schier and Hudspeth, 2006; Williams and Holder, 2000), during which cell fate and epithelial planar polarity are recovered progressively along three phases (Figure 1A). Phase I commences when hair cells begin to regenerate. During this phase the central part of the neuromast epithelium (the macula) becomes increasingly oval because it elongates along a single axis (Figure 1C,D) (Lopez-Schier and Hudspeth, 2006). Phase II begins when the neuromast macula expands symmetrically to regain its circular shape. During this phase epithelial planar polarity propagates laterally (Figure 1A,E). Phases I and II last circa 30 hours each. A Phase III of homeostasis begins after around 60 hours from the onset of regeneration. During Phase I the neuromast becomes bilaterally symmetric because a vertical midline separates the epithelium in two halves. Each half contains hair cells of identical orientation but opposite to that of the confronting half (Figure 1D). This occurs because three processes integrate

with remarkable spatiotemporal precision. First, hair cells regenerate in pairs and their soma localize adjacent to each other along the direction of epithelial planar polarity. Second, each hair cell of the pair orients opposite to its sibling within the plane of the macula. Third, all the hair cells at each side of the midline orient identically. It is not known how these processes integrate to generate bilateral symmetry. In the present study we use high-resolution live imaging in transgenic zebrafish, genetic and pharmacological perturbations of regeneration, and fluorescent sensors to address this question.

1.3 Results

1.3.1 Cellular heterogeneity and compartmentalization of neuromasts

Previous work has revealed that the mature neuromast is formed by the mechanosensory hair cells and by two types of supporting cells: peripheral mantle cells and central sustentacular cells (Chezar, 1930; Ghysen and Dambly-Chaudiere, 2007). Lateralis hair-cells regenerate in pairs and sequentially on the dorsal or ventral aspect of parallel neuromasts (Fig. 1B) (Lopez-Schier and Hudspeth, 2006). The spatiotemporal precision of the regenerative process suggested further heterogeneity in the neuromast. We decided to interrogate cellular identity in mature organs at 7 days post fertilization (7dpf) by characterizing transgenic lines that express the green-fluorescent protein (GFP) in the lateral line (Lopez-Schier and Hudspeth, 2006; Parinov et al., 2004). The *Tg(SqET20)* line expresses the GFP in supporting cells (Hernandez et al., 2007). The staining of *Tg(SqET20)* animals with an antibody to the pan-supporting cell marker ClaudinB revealed that GFP expression was heterogeneous, showing areas with low levels of green fluorescence located at both poles of a line perpendicular to

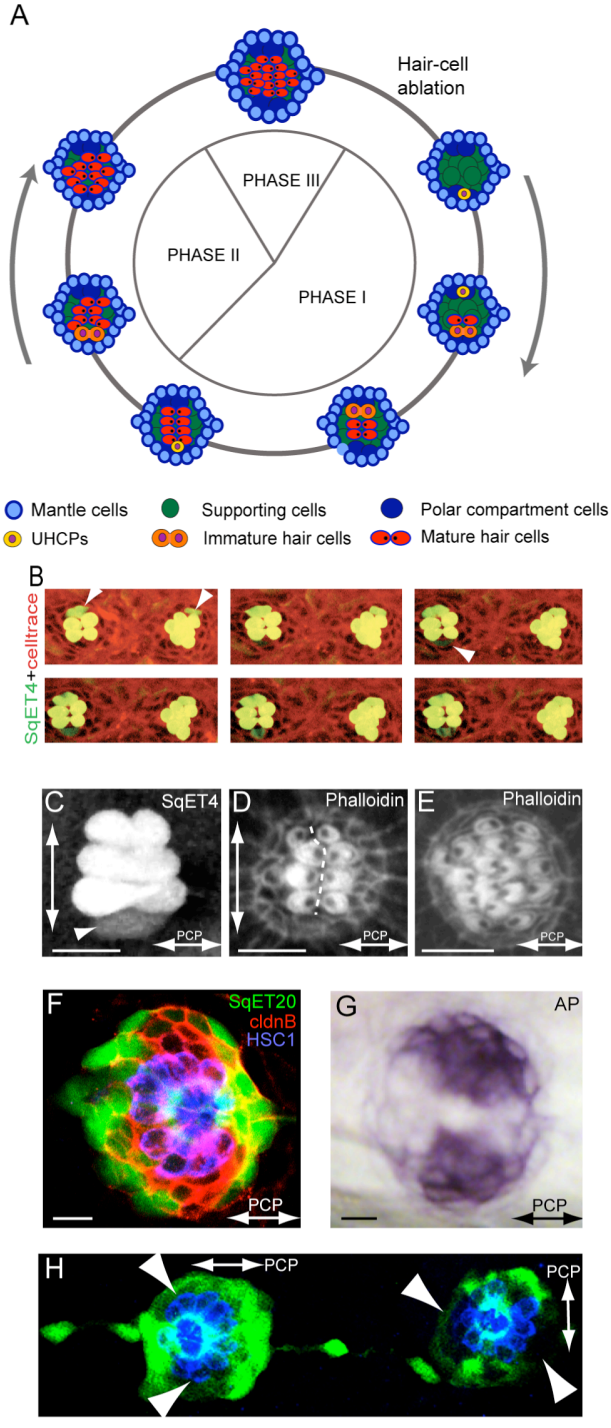
A
Hair-cell ablation
PHASE III
PHASE II
PHASE I
Mantle cells
Supporting cells
Polar compartment cells
UHCPs
Immature hair cells
Mature hair cells
B
SqET4+celltrace
C
SqET4
D
Phalloidin
E
Phalloidin
PCP
F
SqET20
cldnB
HSC1
PCP
G
AP
PCP
H
PCP
PCP

Figure 1. Epithelial planar polarization of neuromasts
(**A**) Schematic description of the three phases of regeneration and homeostasis and the planar polarization of the neuromast epithelium (macula). Cell types are color-coded: most peripheral mantle cells (light blue), central supporting (sustentacular) cells (green), polar compartment resident cells (dark blue), UHCPs (yellow), immature hair cells (orange), and mature hair cells (red). The axis of planar polarity is evidenced by the position of the kinocilium within the mature hair cells (black dot). (**B**) Time-lapse of two adjacent parallel SqET4 neuromasts showing hair cells and their progenitors (green) and stained with Celltrace to reveal cellular boudaries (red). White arrowheads on the first panel point to a pair of newly developed hair cells on the dorsum of both neuromasts. The white arrowhead on the third panel points to a new ventral UHCP, which divides into two hair cells on the last panel. Hair cells develop in pairs, sequentially, and on the dorsal or ventral aspect of the neuromasts. (**C**) A regenerating SqET4 neuromast revealing six GFP-positive hair cells. A UHCP develops at the lower edge of the neuromast (arrowhead). The orthogonal axes of planar polarization (horizontal) and direction of regeneration (vertical) are indicated by double-headed arrows. (**D**) Actin staining of a regenerating neuromast, showing the orientation of four pairs of hair bundles and revealing the vertical line of bilateral symmetry (dotted white line). (**E**) Actin staining of neuromast in phase III of regeneration showing the lateral expansion of the macula. A double-headed arrow indicates the axis of planar polarity. (**F**) A SqET20 neuromast expressing GFP (green), and stained with antibodies to Claudin-b (red), which marks all the suporting cells, and to HCS1 (blue), which highlights the hair cells. GFP^{low} compartments are located at the poles of the vertical axis of bilateral symmetry. (**G**) The GFP^{low} compartments coincide with the endogenous expression of alkaline phosphatase. In all figures, anterior is left and dorsal is up. (**H**) A SqET20 larva expressing GFP (green), and stained with the antibody HCS1 (blue). The neuromast to the left of the image is L1 (a parallel neuromast), whereas the one of the right is L2 (a perpendicular neuromast). This image shows that the GFP^{low} compartments rotate through 90° in parallel versus perpendicular neuromasts. Scale bars: 10 μm.

the neuromast's axis of planar cell polarity (Figure 1F). Strikingly, this line shifts through 90º in perpendicular neuromasts to remain perpendicular to the direction of epithelial planar polarity (Figure 1H). The GFP^{low} areas in *Tg(SqET20)* also coincide with those expressing high levels of alkaline phosphatase (Figure 1G) (Ghysen and Dambly-Chaudiere, 2007; Villablanca et al., 2006). These $SqET20^{GFP\text{-}low}/AP^{+}$ areas demonstrate previously unknown compartments located at the poles of the midline of bilateral symmetry. We call them "polar compartments". We have previously shown that the SqET4 transgenic line expresses high levels of GFP in postmitotic hair cells, as revealed by their incorporation of the fluorescent dye DiAsp, which permeates through the mechanotransduction channels (Lopez-Schier and Hudspeth, 2006). Every DiAsp(+) cell was also GFP(+), excluding the possibility that *Tg(SqET4)* reveals only a subset of the hair cells in the neuromast. In addition to hair cells, live imaging of *Tg(SqET4)* animals also

identified individual cells expressing lower levels of GFP (Figure 1B,C) (Lopez-Schier and Hudspeth, 2006). Live imaging showed that SqET4$^{GFP\text{-}low}$ cells invariably undergo a single mitosis to produce a pair of hair cells (Figure 1B) (Lopez-Schier and Hudspeth, 2006). SqET4$^{GFP\text{-}low}$ cells never generated cell types other than hair cells, suggesting that they are "unipotent hair-cell progenitors" (UHCPs). From these results we conclude that the neuromast is compartmentalized and that it contains at least five distinct cell populations: mantle cells, sustentacular cells, polar-compartment cells, transient UHCPs, and the hair cells.

1.3.2 The mitotic division of UHCPs is essential for regeneration

It has been previously reported that mitotically active supporting cells are the main contributors to hair-cell regeneration in the zebrafish lateral line (Ma et al., 2008). However, other data suggested a role of supporting-cell transdifferentiation for the regeneration of hair cells (Hernandez et al., 2007). Therefore, the relative contribution of supporting-cell proliferation versus transdifferentiation remains unknown. We decided to use the SqET4 line to resolve this question. We started by treating 5 dpf SqET4 animals with 250 μM of neomycin for 1 hour. We have previously demonstrated that this regime eliminates the hair cells of the lateral line (Lopez-Schier and Hudspeth, 2006). Neuromasts achieve near complete regeneration 48 hours after hair-cell ablation. Upon neomycin treatment, regenerating animals were left to recover in water containing the DNA synthesis marker Bromo-deoxy-Uridine (BrdU) (Figure 2A). We found that 59% of the hair cells were BrdU(+) at 48 hpt (Figure 2B,C), suggesting that proliferation and transdifferentiation could contribute to hair-cell regeneration. However, neomycin cannot kill young, non-mechanoreceptive hair cells because this aminoglycoside antibiotic permeates through the mechanotranduction channels. Thus, the presence of immature, neomycin-resistant hair cells in the neuromast could explain why just over half of the hair cells were

BrdU(+) at 48 hpt. Another explanation for this result is that hair-cell precursors remain arrested in a stage of the cell cycle beyond the S-phase, and would progress to mitosis upon hair-cell loss without incorporating BrdU. To discriminate between these possibilities, we exposed fish to BrdU for 8 hours during their fourth day of age before neomycin treatment at 5 dpf, in order to incorporate the BrdU in UHCPs and non-mechanoreceptive hair cells that may be present in the neuromast (Figure 2D). These animals were also left to recover for 48 hours, again in the presence of BrdU. Under this condition, almost 100% of the hair cells were BrdU(+) at 48hpt (Figure 2E-F). This result strongly suggests that cell division is the main or the obligatory process underlying hair-cell regeneration. To further test the extent to which mitotic activity is essential for hair-cell regeneration, we ablated hair cells in SqET4 animals with neomycin, and let them to recover in the presence of several inhibitors of the cell cycle (Figure. 2 G-J). Treatments with nocodazole, aphidicolin, genistein and colchicine revealed that genistein and colchicine were the most effective suppressors of regeneration (Figure 2H). However, control animals showed that genistein and colchicine were toxic to hair cells (Figure. 2G). Aphidicolin and nocodazole, by contrast, did not affect the viability of hair cells over a 48-hour period (Figure 2G-J). Therefore, the nearly complete lack of hair-cell regeneration in genistein- and colchicine-treated animals may represent a compound effect of these drugs on UHCPs mitoses and hair-cell viability. This assertion is further supported by the progressive reduction of the number of hair cells at 48 hpt compared to 24 hpt in animals not treated with neomycin (Figure 2G). Aphidicolin and nocodazole strongly suppressed hair-cell regeneration but did not completely prevent the production of GFP(+) cells.

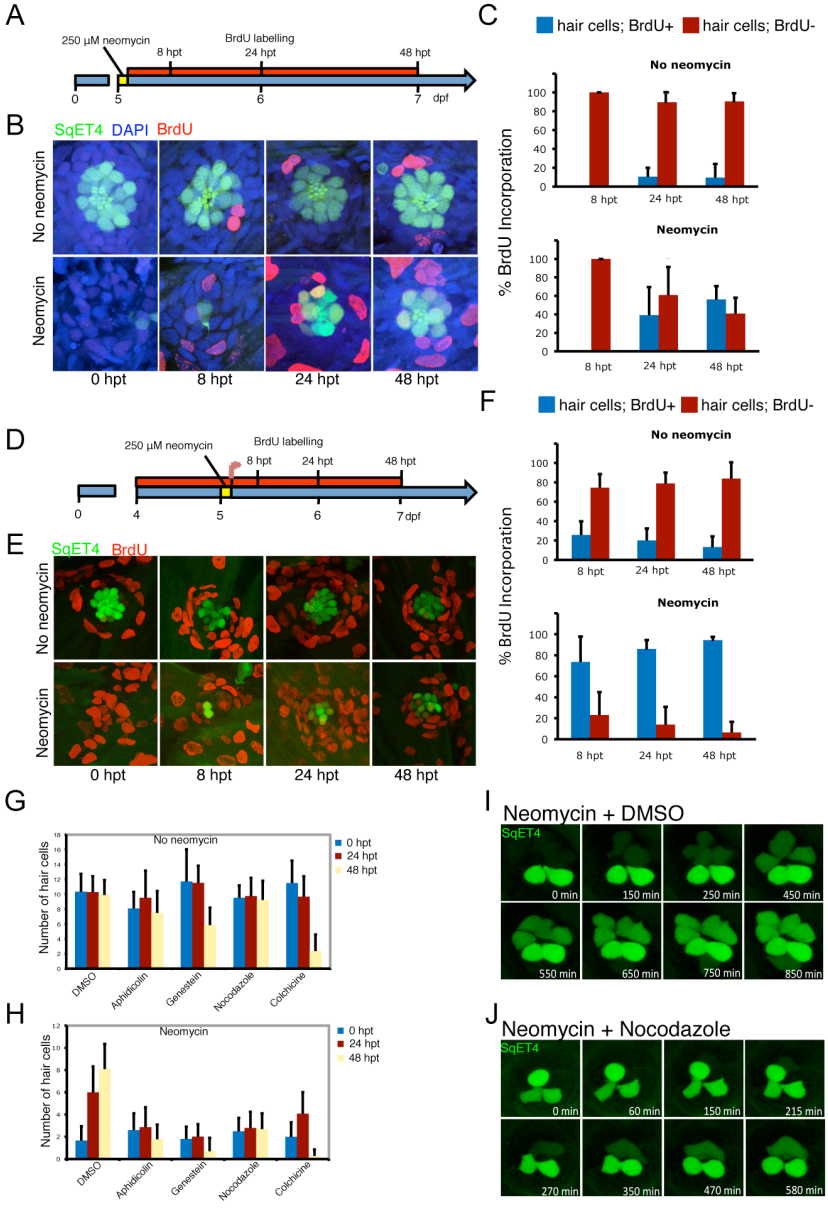
A
250 µM neomycin
8 hpt
BrdU labelling
24 hpt
48 hpt
0
5
6
7 dpf
B
SqET4 DAPI BrdU
No neomycin
Neomycin
0 hpt
8 hpt
24 hpt
48 hpt
C
hair cells; BrdU+
hair cells; BrdU-
No neomycin
Neomycin
% BrdU Incorporation
8 hpt
24 hpt
48 hpt
D
250 µM neomycin
BrdU labelling
8 hpt
24 hpt
48 hpt
0
4
5
6
7 dpf
E
SqET4 BrdU
No neomycin
Neomycin
0 hpt
8 hpt
24 hpt
48 hpt
F
hair cells; BrdU+
hair cells; BrdU-
No neomycin
Neomycin
% BrdU Incorporation
8 hpt
24 hpt
48 hpt
G
No neomycin
Number of hair cells
0 hpt
24 hpt
48 hpt
DMSO
Aphidicolin
Genestein
Nocodazole
Colchicine
H
Neomycin
Number of hair cells
0 hpt
24 hpt
48 hpt
DMSO
Aphidicolin
Genestein
Nocodazole
Colchicine
I
Neomycin + DMSO
SqET4
0 min
150 min
250 min
450 min
550 min
650 min
750 min
850 min
J
Neomycin + Nocodazole
SqET4
0 min
60 min
150 min
215 min
270 min
350 min
470 min
580 min

Figure 2. Mitotic activity is essential for hair-cell regeneration in neuromasts
(**A**) Scheme representing the experiments in which hair cells were ablated with neomycin in SqET4 transgenic zebrafish larvæ at 5 dpf, and subsequently incubated continuously in BrdU for 8, 24 and 48 hrs after neomycin treatment (hpt). (**B**) Confocal images of neuromasts showing hair cells in green, and BrdU in red. All cell nuclei were labelled with DAPI (blue). (**C**) Bar graphics showing the quantification of the number of GFP(+) hair cells that were BrdU(+) *versus* BrdU(-) in control and treated larvæ at 8, 24 and 48 hpt (n = 70 for each timepoint). In control samples not treated with neomycin, few hair cells were labeled with BrdU at 48 hpt, whereas 59% of regenerated hair cells were BrdU(+) in neomycin-treated fish at 48 hpt. (**D**) Scheme representing the experiments in which SqET4 transgenic zebrafish at 4 dpf were incubated continuously in BrdU, treated with neomycin to ablate hair cells at 5 dpf, and subsequently incubated continuously in BrdU for 8, 24 and 48 hpt, shown in (**E**,**F**). (**E**) Confocal images of neuromasts showing hair cells in green, and BrdU in red. (**F**) In control samples not treated with neomycin, 74% of regenerated hair cells at 8 hpt are BrdU positive (n = 70), compared with only 26% BrdU-positive hair cells in untreated larvæ (n = 70). By 48 hpt, 94% of regenerated hair cells are BrdU(+), compared to only 13% in untreated specimens. This finding indicates that virtually all regenerated hair cells develop from progenitors that have undergone cell division following neomycin-induced hair-cell ablation and that progenitors enter the cell cycle less than 8 hours after hair-cell death. (**G**) SqET4 transgenic larvæ were incubated in several inhibitors of the cell cycle for 24 and 48 hours following neomycin treatment. The quantifications showed that the number of hair cells remained relatively constant upon treatments with the cell-cycle blockers aphidicolin, genistein and nocodazole in control samples (not treated with neomycin). All cell-cycle inhibitors blocked hair-cell regeneration in samples treated with neomycin. (**I**-**J**) These results were confirmed by time-lapse videomicroscopy in regenerating SqET4 control (**I**) and nocodazole-treated (**J**) larvæ. Controls regenerated normally, whereas nocodazole blocked regeneration and the division of a UHCP that appears at the top of the neuromast in (**J**).

In control animals not treated with neomycin, the number of GFP(+) cells in neuromasts did not vary between 0, 24 and 48 hpt under aphidicolin and nocodazole (Figure 2G). Thus, the few GFP(+) cells present in inhibitor-treated neuromasts are likely to be hair cells that were immature at the time of neomycin treatment. Alternatively, under cell-cycle inhibition, the UHCPs that may have been already present by the time of neomycin treatment could transdifferentiate into hair cells without undergoing mitosis. To address this question we directly visualized regeneration using SqET4 fish, and compared hair-cell production between control animals and those under nocodazole. Live imaging revealed that over a period of 10 hours, control animals developed 6 hair cells (Figure 2I), whereas nocodazole-treated animals developed 2 hair cells and sometimes a single UHCP that could never divide or produce hair cells (Figure 2J) and Supplementary Movie 1), with the consequent arrest of regeneration. The pair of hair cells that frequently developed in nocodazole-treated fish could have been immature at the time

of neomycin treatments, which may also explain why we did not achieved 100% of BrdU(+) hair cells after regeneration. We interpret these results as an indication that supporting-cell transdifferentiation does not contribute to hair-cell regeneration in the lateral line.

1.3.3 The orientation of UHCPs divisions is dispensable for bilateral symmetry

Regeneration in neuromasts is always progressive. Live imaging of SqET4 fish showed that UHCPs develop within or in close proximity of the dorsal and ventral polar compartments (Figure 1B). Consequently, hair-cell regeneration is strongly directional along an axis perpendicular to that of the eventual planar polarity of the epithelium. Hair-cell siblings develop opposite planar orientation and remain adjacent to each other during Phase I. Thus, regeneration anisotropy defines the midline of bilateral planar-polarity symmetry (Figure 1C-D). These observations led us to ask how regeneration anisotropy is controlled. Oriented cell divisions can direct growth anisotropy in epithelia (Baena-Lopez et al., 2005; Lecuit and Le Goff, 2007). Therefore, the orientation of UHCP divisions could underlie hair-cell regeneration anisotropy and the formation of the midline of bilateral symmetry. We tested this possibility by direct visualization of 23 independent UHCPs in SqET4 animals, which showed that 14 UHCPs divided obliquely (Figure 3A,B and Supplementary Movie 2), suggesting that the orientation of UHCP division is not directly translated into bilateral symmetry. We further validated this conclusion by directly revealing the dynamics of UHCPs using double transgenics *Tg(Cldnb:lynGFP;SqET4)*, which express a membrane-targeted GFP in all supporting cells and a cytoplasmatic GFP in UHCPs and hair cells, allowing the evaluation of cellular behavior *in vivo* (Haas and Gilmour, 2006). Unexpectedly, we found that ~60% of UHCP divisions produced hair-cell pairs that rotated within the plane of the epithelium after progenitor cytokinesis (N=36). This is clearly demonstrated in the example shown in

Figure 3C and the Supplementary Movie 3, where at 276 minutes into the time series the immature hair-cell siblings begin to rotate within the plane of the epithelium, transiently and locally breaking the midline of mirror symmetry. This is most evident at 306 minutes into the time series. A complete inversion of the hair cells precisely realigns them along the neuromast's axis of planar polarity to reform mirror symmetry, evident at 730 minutes into the time series. Therefore, oriented UHCP divisions are not essential for directional regeneration or bilateral symmetry.

1.3.4 A polar compartment is neither a niche, nor it harbors stem cells

To further assess the relationship between regeneration anisotropy and bilateral symmetry, we deemed essential to determine the mechanism that mediates the localized acquisition of the UHCP fate. We focused on the polar compartments hypothesizing that their constituent cells either directly differentiate into UHCPs, or that they represent a stem-cell niche from where UHCPs originate. An alternative possibility is that a localized stem-cell population does not exist in the neuromast. An extension of this proposition is that the polar compartment is not a niche. We tested these hypotheses by continuous imaging of regenerating neuromasts at single-cell resolution for periods ranging between 32 and 48 hours using *Tg(Cldnb:lynGFP;SqET4)* double transgenic fish. We evaluated cellular behavior before and after UHCP development, and directly tracked cellular movement, proliferation and fate acquisition *in vivo*. Prospective UHCPs were identified retrospectively by playing the time series backward, and each labeled with a colored dot.

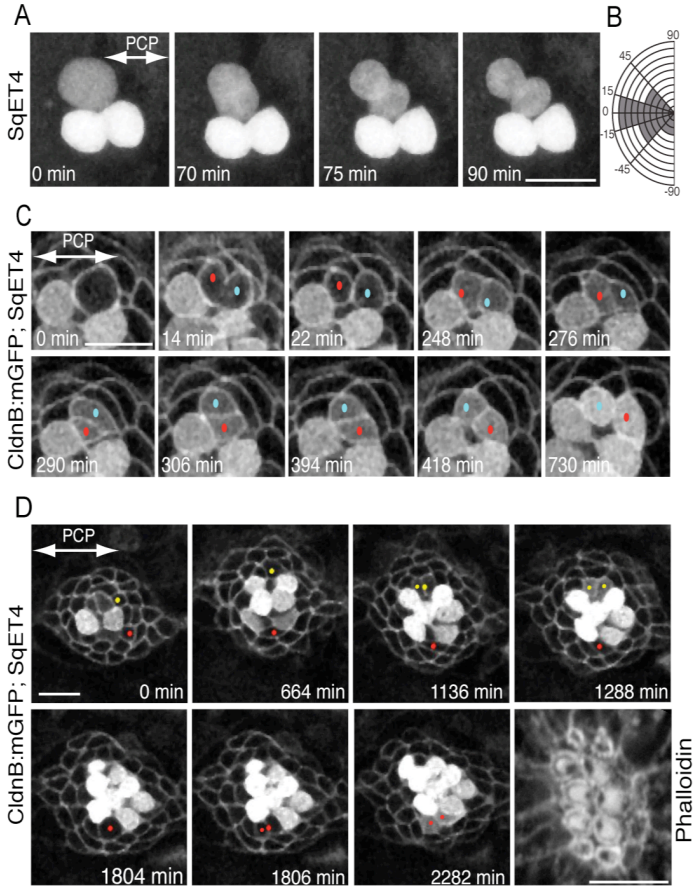

Figure 3. Orientation of UHCP divisions and planar cell inversion

(**A**) A 90-minute-long series of confocal images of a regenerating SqET4 neuromast revealing two GFP-positive hair cells aligned along the axis of planar polarity (double-headed arrow). An UHCP develops at the upper edge of the neuromast. Over the next hour, this UHCP commences mitosis and divides obliquelly into a pair of hair cells. (**B**) Quantification of the angle of division of UHCPs in 23 neuromasts, which indicates that the majority of UHCP divide obliquelly respect to the axis of planar polarity of the epithelium. (**C**) A twelve-hour-long series of confocal images of a regenerating neuromast of a double-transgenic *Tg(Cldnb:lynGFP;SqET4)* larva revealing two GFP-positive hair cells at the lower aspect of the image, and a UHCP at the top. Fourteen minutes into the time-series, this UHCP divides into two hair cells, each identified with a dot (red and blue). 264 minutes after cytokinesis (276'), the sibling hair cells begin to rotate around their contact point within the plane of the epithelium, which locally breaks the line of mirror symmetry (this is most evident at 306' into the time series). A complete inversion of the hair-cell pair eventually reforms the line of mirror symmetry and precise realigns the cells along the neuromast's axis of planar polarity (double-headed arrow in the first panel). (**D**) A 44-hour-long series of confocal images of a regenerating neuromast of a double-transgenic *Tg(Cldnb:lynGFP;SqET4)* larva reveals plasma-membrane GFP-positive supporting cells and cytoplasmatic GFP-positive hair cells and UHCPs. Two prospective UHCPs were identified retrospectively by playing the time series backwards, and each labelled with either a red or yellow dot. Their position was followed over time, showing that prospective UHCPs moved into the dorsal (yellow) and ventral (red) polar compartments,

where they became UHCP (weak cytoplasmatic GPF). Each UHCP eventually divided into a pair of hair cells. The last panel of the image is an actin staining, showing the resulting planar polarization of the epithelium. The neuromast's axis of planar polarity is indicated by a double-headed arrow in the first panel. Scale bars: 10 μm.

Cells were followed forward over time in all 10 successful long-term recordings, which consistently showed that although most neuromast cells do not change their relative position, some individual supporting cells relocated to the areas defined by the polar compartments, where they subsequently became UHCPs (Figure 3D and Supplementary Movie 4). This result shows that prospective UHCPs originate elsewhere in the neuromast. It also indicates that the polar compartments are not stem-cell niches. On the contrary, these compartments represent an environment that opposes a niche to permit the differentiation of UHCPs.

1.3.5 Notch signaling controls the production of hair-cell progenitors

Notch signaling is universally required for hair-cell development in vertebrates (Eddison et al., 2000; Haddon et al., 1998; Lanford et al., 1999; Ma et al., 2008). To understand the mechanism that underlies UHCP-fate acquisition we used as tools two complementary approaches that combined live imaging with genetic and pharmacological alterations of Notch signaling. First, we expressed a constitutively-active from of Notch (N^{ICD}) by heat-shock during regeneration using triple transgenics *Tg([hs70p:Gal4;UAS:N^{ICD}-Myc;SqET4)*, which blocked the production of UHCPs and hair cells (Figure 4A). In a converse experiment, we abrogated Notch activity by treating SqET4 fish with the γ-secretase inhibitor DAPT, which generated ectopic and supernumerary UHCPs and hair cells (Figure 4A,B) (Ma et al., 2008). These results suggest that a majority of supporting cells can become UHCPs upon loss of Notch signaling. To test this possibility directly we continuously imaged regenerating *Tg(Cldnb:lynGFP;SqET4)* fish under DAPT-treatment and found that UHCPs developed ectopically and in excess (Figure 4B-C and

Supplementary Movie 5). Importantly, loss of Notch broke directional regeneration and led to planar polarity defects (Figure 4B).

1.3.6 Compartmentalized Notch signaling controls regeneration anisotropy

Our previous results clearly show that Notch signaling controls the differentiation of UHCPs, but do not explain why UHCPs are produced within the polar compartments. The spatiotemporal development of UHCPs shadows the expression pattern of the hair-cell determination factors *deltaA* and *atoh1a* (Ma et al., 2008), suggesting that these genes are first expressed by the UHCPs. To directly test this possibility we imaged hair-cell regeneration in a double-transgenic line expressing a red-fluorescent protein under the transcriptional control of the Atoh1a promoter, combined with the UHCPs marker SqET4. Live imaging of *Tg(Atoh1a:TdTomato;SqET4)* fish showed that Atoh1a is expressed at low levels in some supporting cells that we regard as prospective progenitors (see below), and is strongly upregulated by the UHCPs at the dorsal or ventral part of parallel neuromasts, where the polar compartments are located (Figure 4D and Supplementary Movie 6). Cell expressing high levels of Atoh1a:TdTomato were also GFP(+) and divided to produce a pair of hair cells, indicating that Atoh1^{strong} cells are UHCPs. *atoh1* is a well-characterized negative transcriptional target of Notch (Itoh and Chitnis, 2001), suggesting that either Notch activity is low in the polar compartments, or that prospective progenitors become refractory to Notch signaling. Our previous live imaging analyses of regenerating *Tg(SqET4;cldnb:mGFP)* fish under DAPT treatment indicated that the majority of supporting cells can become UHCPs upon loss of Notch signaling. These results, together with the evidence that loss of Notch signaling expands *atoh1a* expression (Itoh and Chitnis, 2001; Ma et al., 2008), indicate that supporting cells are not intrinsically refractory to Notch. Thus, some supporting cells are able to express the UHCP fate within the

permissive environment of the polar compartments where Notch activity may be low or absent. *notch3* is the main receptor expressed in neuromasts and is dynamically regulated during hair-cell regeneration (Ma et al., 2008). To reveal the spatial expression pattern of *notch3* we used whole-mount fluorescent two-color *in situ* hybridization in combination with the UHCP markers *atoh1a* and *deltaA*. We found that *notch3* is strongly enriched in neuromast areas complementary to those expressing *deltaA* and *atoh1a* (Figure 4E-F). Importantly, *notch3* was absent from the areas representing the polar compartments. To directly assess Notch signaling status in neuromasts we used a validated red-fluorescent Notch sensor in combination with SqET4 (Parsons et al., 2009). Live imaging of neuromasts expressing this combination of markers showed that Notch activation occurs outside the polar compartments (Figure 4G). Collectively, these results indicate that Notch activity governs hair-cell regeneration anisotropy by preventing supporting cells from becoming progenitors outside the polar compartments.

1.3.7 Centrifugal movement of hair cells propagates planar polarity horizontally

During phase II of regeneration, the neuromast macula loses its oval shape to become rounder because the hair-cell population expands in a direction perpendicular to that of regeneration. Consequently, planar polarity propagates laterally across the epithelium (Lopez-Schier and Hudspeth, 2006) (Figure 1A,E). This may occur because hair cells move away from the midline, or because UHCPs begin to appear ectopically in the neuromast during this phase. To discriminate between these possibilities, we divided the neuromast by a Cartesian grid and gave positional values to

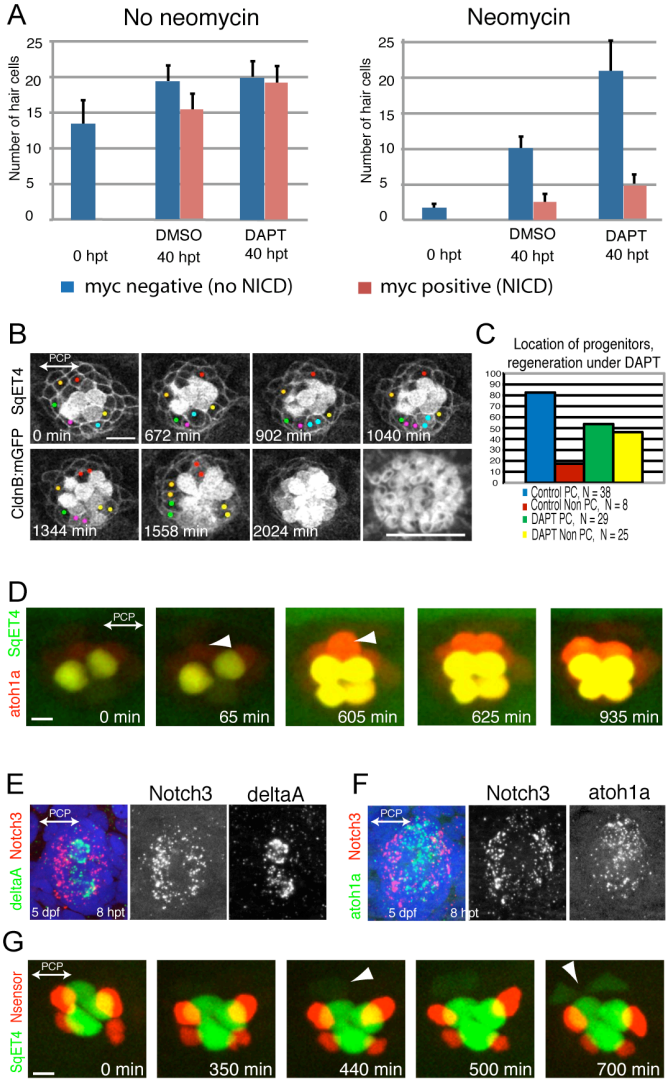

Figure 4. UHCP develop in polar compartments

(**A**) Quantifications of the average number of hair cells in samples that were treated with neomycin (right) or that were not treated (left), and later exposed to DMSO or DAPT, and that expressed (red) or did not express (blue) a constitutively-active form of Notch. It shows that DAPT induces the overproduction of hair cells, and this effect is suppressed by Notch activity. (**B**) A 34-hour-long time series of a regenerating *Tg(Cldnb:lynGFP; SqET4)* neuromast treated with DAPT. UHCPs were identified retrospectively by playing the time series backwards, and labelled with colored dots. UHCPs develop in excess producing pairs of hair cells ectopically. An actin staining shows the resulting defective planar polarization (last panel). (**C**) A graph showing the position of UHCPs relative to the polar compartments in control and DAPT-treated neuromasts during regeneration. More than 80% of UHCPs develop within the polar compartments in controls, compared to just over 50% in DAPT-treated samples (N=25). (**D**) Time series of a *Tg(Atoh1a:TdTomato ; SqET4)* double-transgenic

neuromast revealing GFP-positive UHCPs and hair cells (green), and Atoh1a-expressing cells (red). It shows the temporal gene-expression hierarchy. (**E**-**F**) Fluorescent whole-mount in situ hybridizations of regenerating neuromasts, revealing *notch3* (red) and *deltaA* (green) (**E**), and *notch3* (red) and *atoh1a* (green) (**F**). Cell nuclei are in blue. *notch3* is never expressed by the DeltaA(+) or Atoh1a(+) cells, and was absent from the polar compartments. (**G**) A 700-minute live imaging of a double-transgenic SqET4 (green) neuromast expressing a red-fluorescent Notch sensor (red). It shows that Notch signaling occurs outside the polar compartments.

the hair bundle of each hair cell to calculate the spatial distribution of each polarity (Figure 5A-D). This analysis showed that nearly 100% of the hair cells of each orientation were placed in separate compartments at either side of the vertical midline during phase I (Figure 5A,B).

A strongly biased distribution of polarities is maintained at either side of a vertical midline bisecting fully regenerated neuromasts (Figure 5C,D). Importantly, comparison of polarity distributions across a horizontal midline showed distributions of 52/48% in each compartment, indicating no polarity distribution bias between the dorsal and ventral halves of parallel neuromasts (Figure 5D). These observations support the possibility that the macula expands horizontally by a centrifugal movement of hair cells.

During hair-cell development, there is a temporal hierarchy of gene expression along which cells transition from SqET4^{-}/Atoh1a^{weak+} (prospective UHCPs) → SqET4^{+}/Atoh1a$^{strong+}$ (UHCPs and immature hair cells) → SqET4^{+}/Atoh1a^{-} (mature hair cells) (Figure 5E). We evaluated the expression of these markers in fully-regenerated neuromasts using triple transgenics *Tg(atoh1a:TdTomato;SqET4;Cldnb:mGFP)* and found that the oldest hair cells (SqET4^{+}/Atoh1a^{-}) were located at the periphery of the neuromast furthest from the midline of bilateral symmetry, whereas the youngest pairs (SqET4^{+}/Atoh1a$^{strong+}$) were central and described the typical direction of regeneration that connects the dorsal and ventral polar

compartments (N=9) (Figure 5F). DiAasp incorporation experiments that discriminate between immature and mature (mechanotransducing) hair cells revealed that older cells described a line perpendicular to that of the direction of regeneration (Figure 5G). Importantly, DiAsp(+) cells were always excluded from the polar compartments where the UHCPs and immature hair cells are preferentially located (Figure 5G). These results, together with the scarcity of UHCPs outside the polar compartments (Figures 3D and 4C), indicate that the horizontal expansion of planar polarity is not caused by the ectopic development of UHCPs, and that it is likely to occur because older hair cells that maintain their original orientation move away from the neuromast's midline towards its periphery.

1.4 Discussion

1.4.1 Hair-cell regeneration anisotropy and bilateral symmetry are functionally linked

During the initial phase of hair-cell regeneration in the zebrafish lateral line, a vertical midline bisects the neuromast epithelium into perfect mirror-symmetric plane-polarized halves. Each half contains hair cells of identical planar orientation but opposite to that of the confronting half. Hair-cell regeneration is strongly directional along the axis of bilateral symmetry. Our results explain the reason behind this reproducible behavior. It occurs because the development of UHCPs is spatially restricted to the dorsal or ventral polar compartments. The division of UHCPs into two hair cells, coupled with a consistent opposite planar orientation of the hair-cell siblings along a single axis, eventually defines the midline of mirror symmetry.

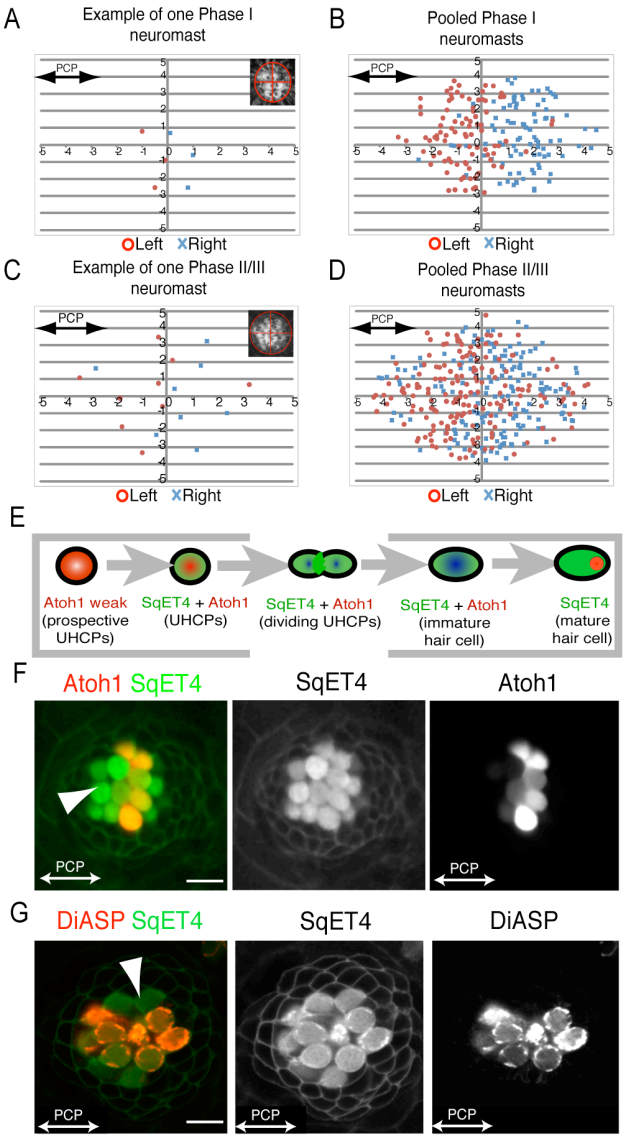

Figure 5. Local and global planar polarization of the neuromast epithelium

(**A**-**D**) Hair-cell planar polarity distribution in regenerating and mature neuromasts. Positional values of each polarity are plotted in a Cartesian plane. (**A**-**B**) Example of one neuromast (**A**) and pooled 20 neuromasts in Phase I (**B**). (**C**-**D**) Example of one neuromast (**C**) and pooled 22 neuromasts in Phase II/III (**D**). (**E**) Schematic transition of marker gene-expression in prospective UHCPs (weakly Atoh1a+ (pink)), UHCPs, immature and young hair cells (co-expressing SqET4 and Atoh1a (green/red)), and mature hair cells (exclusively SqET4+ (green)). (**F**) A *Tg(Atoh1a:TdTomato;SqET4)* neuromast exemplifies this transition (GFP(+) UHCPs and hair cells (green), and Atoh1a(+) cells (red). The white arrowhead indicates mature hair cells on the rostral part of this parallel neuromast. (**G**) DiAsp incorporation into hair cells of *Tg(Cldnb:lynGFP;SqET4)* neuromast, showing the exclusion of mature hair cells from the polar compartments. The white arrowhead indicates immature hair cells on the dorsal part of this parallel neuromast. Scale bars are 10 μm.

Live imaging demonstrates that oriented progenitor divisions are not essential for regeneration anisotropy. Therefore, bilateral symmetry is sustained by a strongly anisotropic regeneration process that relies on the stabilization of progenitor identity in permissive polar compartments. An additional important aspect of our results is that they conclusively demonstrate that the SqET4 transgenic line highlights *bona fide* hair-cell progenitors, whose proliferation is essential for hair-cell regeneration in the lateral line. This conclusion is further supported by a recent publication reporting that the promoter element of the *atp2b1a* gene is responsible for the expression pattern of the GFP in the SqET4 transgenic line, and that a morpholino-mediated knockdown of *atp2b1a* negatively affected the division of the hair-cell progenitors (Go, W. et al., 2010).

1.4.2 Regeneration anisotropy is not due to a localized stem-cell population

One explanation for the compartmentalized acquisition of UHCP identity is that the polar compartments are stem-cell niches. Live imaging indicates that this is unlikely because prospective UHCPs originate elsewhere in the neuromast. Thus, the polar compartments appear to be a permissive environment for the acquisition of UHCP identity by supporting cells. One possibility is that an intrinsic cell-fate determinant instructs some supporting cells to become UHCPs, and that intercellular signals prevent these cells from fully executing their differentiation until they reach a polar compartment. Previous results suggest that the source of hair-cell progenitors are the *sox2*(+) cells that reside basally in the neuromast epithelium (Hernandez et al., 2007). The observation that in the mouse, chick and zebrafish ears, the combinatorial activity of Sox2 and Notch control the development of pro-sensory patches, from where hair cells will eventually develop supports this proposition (Daudet et al., 2009; Millimaki

et al., 2010). Future experiments involving loss- and gain-of-function of *sox2* in the lateral line will allow to test this possibility directly.

1.4.3 Regeneration anisotropy depends on compartmentalized Notch signaling

What controls the spatiotemporal development of UHCP? When Notch activity was blocked in the whole organ by DAPT treatments, directional regeneration was broken, indicating that compartmentalized Notch signaling prevents the ectopic development of hair-cell progenitors. Using fluorescent sensors and live imaging we demonstrate that the polar compartments have low levels of Notch signaling. Because the localization of the polar compartments does not change over time, a consequence of UHCP development within them is the anisotropic regeneration of the hair cells. We have observed that hair-cell regeneration is always progressive. Live imaging of SqET4 fish showed that UHCP development alternate between the dorsal and ventral aspects of the neuromast. One explanation for the progressive development of UHCPs is that Atoh1a in the UHCPs and in young hair cells activates the expression of Notch ligands cell-autonomously. In turn, lateral inhibition originating from these cells would prevent the surrounding supporting cells from becoming new progenitors until hair cells have matured and lost *atoh1a* expression. This would decrease the number of cells expressing Notch ligands, allowing the organ to re-set and develop new UHCPs. It will be necessary to define the identity of the relevant Notch ligands and to manipulate their activity in a cell-specific manner to test this hypothesis.

1.4.4 The origin of axial references remains unknown

One outstanding question is the origin of axial references and whether they rely on long-range signals. If this were the case, disruptions of regeneration anisotropy should not affect epithelial planar polarity because hair cells

would be properly oriented regardless of their position in the epithelium. It follows that disruptions of Notch that break regeneration anisotropy should not cause planar-polarity defects in the epithelium. However, loss of Notch signaling randomizes hair-cell orientation, arguing against a role of long-range cues in polarizing the epithelium. We cannot currently rule out, however, the possibility that Notch signaling directly controls the establishment of axial references for planar polarity by affecting the expression, transport, or interpretation of long-range polarizing cues. Future experiments using iterative cycles of hair-cell ablation and regeneration, with an intervening blockade of Notch signaling, may be able to provide evidence for or against a role of Notch in the control of polarizing cues. An alternative possibility that could reconcile the effect of loss of Notch with a role of long-range polarization is that Notch signaling controls the positioning of the organelle that defines planar polarity in this tissue, the kinocilium of the hair cell. Under this scenario, loss of Notch would not allow kinocilia to respond to external polarizing cues. However, we believe that this is not likely because loss of Notch signaling in the mouse and the zebrafish ears produce normally polarized hair cells, which align in similar directions to their neighbours (Haddon et al., 1998; Lewis and Davies, 2002). Also, a disruption of the cell's internal machinery for planar polarity by loss of Notch should generate some hair cells with centrally located kinocilia, a phenotype that we have never observed. With our current knowledge, the most likely explanation for the planar polarity defects in neuromasts lacking Notch signaling is that supernumerary hair cells produce mechanical disturbances or packaging defects. Thus, a role for long-range polarizing signals at the origin of axial references remains a possibility.

1.4.5 Centrifugal hair-cell movement propagates planar polarity horizontally

Although hair-cell regeneration remains strongly anisotropic, the macula eventually expands symmetrically. This could be due to the development of UHCPs outside the polar compartments during Phases II and III. Alternatively, polar compartments may themselves relocate, or expand around the entire neuromast. Although these situations are possible, the weight of the evidence argues against them. First, the majority of UHCPs develop within the dorsal or ventral aspect of neuromasts in all three phases of regeneration, and the small percentage of UHCPs that could not be unambiguously located within these compartments would be insufficient to account for the rapid and widespread symmetric expansion of planar polarity. Second, we observed that peripheral hair cells were negative for Atoh1a, indicating that they are older that those located centrally or nearby the polar compartments. Therefore, we conclude that planar polarity is likely to propagate symmetrically because hair cells move away from the midline towards the periphery of the neuromast. It follows that the hair cells located peripherally along a line perpendicular to that of regeneration should be the oldest. Our results on DiAsp incorporation support this conclusion.

1.4.6 Planar cell inversions

Live imaging demonstrates that oriented progenitor divisions are not essential for regeneration anisotropy. In addition, we observed that the majority of hair-cell siblings rotate around their contact point immediately after UHCP cytokinesis. To the best of our knowledge, our data is the first description of "planar cell inversions". This remarkable cellular behavior could offer further mechanistic insights into the process that sustains bilateral symmetry during regeneration. It may reveal a general process that links epithelial polarity to external mechanical cues (Aigouy et al., 2010). It could also play a role in maintaining cellular orientation in plastic tissues with

high cellular turnover such as in the mammalian kidney, lung or brain ventricles (Fischer et al., 2006; Mirzadeh et al., 2010; Saburi et al., 2008; Yates et al., 2010).

1.5 Conclusion

In this study we employed transgenic sensors and markers of hair-cell progenitors, combined with high-resolution long-term *in toto* continuous live imaging, to demonstrate that hair-cell regeneration is strongly anisotropic, and that regeneration anisotropy is regulated by Notch signaling. The model that emerges from our results (summarized in Figure 6) suggests that bilateral symmetry is sustained by compartmentalized Notch activity, which governs regeneration anisotropy by permitting the stabilization of UHCP identity in the polar compartments. There are several examples of dynamic or stable compartments that allow cells to loose stemness and progress through a differentiation program (Mathur et al.; Voog et al., 2008). In the specific case of the lateral line, the polar compartments appear to oppose a niche by allowing supporting cells to become UHCPs. Further molecular dissection of this process in the zebrafish lateral line may provide deeper insights into the mechanisms that control the homeostasis of tissue architecture.

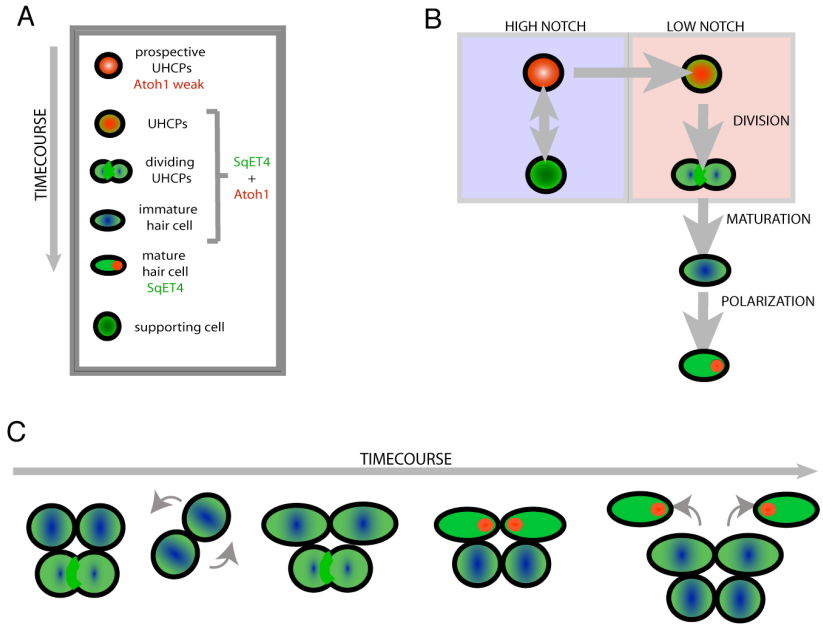

Figure 6. Model of epithelial planar polarization in the neuromast
(**A**) Scheme of the different cell types or cell status in the neuromast. Cellular identities are color-coded and the expression profile of the different markers is placed next to the cells. A grey arrow indicates the temporal transition along the differentiation path. (**B**) A schematic representation of the model of cell-fate acquisition in the neuromast, combining the temporal hierarchy of gene-expression relative to the areas of high (grey) or low (orange) Notch activity. (**C**) The temporal transition of hair cells from the division of their progenitor, through the planar inversions indicated by two curved grey arrows on the second scheme from the left, and the eventual realignment of polarized hair cells, shown by the red dots that represent the kinocilia. Two small grey arrows show the centrifugal movement of mature hair cells in the last schematic from the left, which propagates planar polarity across the epithelium

Chapter 2

The chromatin remodeling factor Brg1 is necessary for the development and homeostasis of the zebrafish lateral line

Filipe Pinto-Teixeira and Hernán López-Schier

Laboratory of Sensory Cell Biology & Organogenesis, Centre de Regulació Genòmica - CRG, c/Dr Aiguader 88, (08003) Barcelona, Spain

To be submitted

2.1 Abstract

The collective migration of cells is a crucial event in a wide variety of biological processes and its deregulation leads to several pathologic conditions such as developmental abnormalities and tumor metastasis. Collective cell migration is the product of several complex processes and therefore a major challenge of a migrating cohort is the coordination of multiple biological processes among its cells. This requires a broad coordination of gene expression, which can be achieved by genome-wide chromatin remodeling. Were we used the zebrafish deficient in *brg1* (*yng*) to address the role of the chromatin remodeling complex ATPase *brg1* during the posterior lateral line primordium (pLLp) migration. The pLLp is a group of about 100 cells that, as it collectively migrates caudally along the horizontal mioseptum, deposits the proneuromasts that will establish the posterior lateral line sensory system (pLL). Primordial cells display a mesenchymal behavior at the primordium leading edge, while rear cells become epithelialized into two to three epithelial rosettes that correspond to the proneuromast. As proneuromasts are periodically deposited at the trailing edge, Wnt signaling dependent progenitor cell proliferation at the leading edge assures the addition of new cells for additional rosettes to be formed, whose assembly is under the control of Fgf signaling in the adjacent trailing part of the primordium. Here we show that Brg1 activity is necessary for pLL morphogenesis. In the lack of *brg1*, primordial cells are unable to coordinate their migratory behavior and the pLLp shows a deficient migration. Additionally, we show that *brg1* regulates the pLLp homeostasis by maintaining progenitor cells in the leading edge and the proliferative capacity of the primordium, which altogether result in the development of a truncated lateral line. These findings reveal an until now unappreciated role of *brg1* during mechanosensoy organ formation in the zebrafish.

2.2 Introduction

Collective cell migration is a fundamental process that underlies tissue remodeling both during embryonic development, wound repair and cancer metastasis (Aman and Piotrowski, 2009a; Friedl and Gilmour, 2009; Rorth, 2007) The transition from a stationary to a migratory state by cells often requires a broad and coordinated reprogramming of gene expression, which can be achieved by genome-wide chromatin remodeling.

Chromatin remodeling complexes play a crucial role in transcriptional regulation and participate in diverse processes such as cell proliferation, apoptosis, differentiation, embryonic patterning and tumorigenesis. The SWI/SNF (mating type switching sucrose nonfermenting) chromatin remodeling complexes use the energy provided by ATP hydrolysis to locally disrupt nucleosome position facilitating transcription factors to access the DNA (Kingston and Narlikar, 1999; Muchardt and Yaniv, 2001; Randazzo et al., 1994). SWI/SNIF complexes contain either one of the two ATPase subunits Brahma (Brm) or Bhrama-related gene 1 (Brg1). While Brm or Brg1 containing complexes share most of its other subunits, they have different target gene specificity (Kadam and Emerson, 2003).

Unraveling the role of chromatin remodeling complexes in regulating collective cell migration might therefore prove essential for our understanding of morphogenesis and importantly for cancer research, as several human cancers metastase as groups of cells (Friedl, 2004; Friedl and Gilmour, 2009; Hegerfeldt et al., 2002).

The primordium of the posterior lateral-line system in the zebrafish has proven to be a powerful *in vivo* model for collective cell migration that combines the ease with which it can be imaged with the genetic tools available in the zebrafish (Dambly-Chaudiere et al., 2003; Ghysen and Dambly-Chaudiere, 2007; Lopez-Schier, 2010; Ma and Raible, 2009). The lateral line is a system present in some aquatic vertebrates that allows the animal to perceive directional water movements (Ghysen and Dambly-

Chaudiere, 2004). The functional units of the system are the neuromasts, composed by sensory hair cells, innervated by sensory neurons that project to the central nervous system (Alexandre and Ghysen, 1999; Metcalfe et al., 1985) and surrounding supporting cells (Montgomery, 1997; Raible and Kruse, 2000). In the zebrafish the posterior lateral line (pLL) develops from the posterior lateral line primordium (pLLp), a complex entity of roughly 100 cells that migrates collectively along each flank of the embryo as it periodically deposits the mechanosensory organ progenitors, the proneuromast (Gompel et al., 2001; Kimmel et al., 1995; Metcalfe et al., 1985). The pLLp is a polarized entity with a mesenchymal leading group of around 25 cells followed by two to three epithelial rosettes at various stages of maturation that correspond to the proneuromast that will be deposited as discrete groups from the trailing end of the migrating primordium (Lecaudey et al., 2008). Rosette formation in the leading edge and proneuromast regular deposition are maintained by a paracrine feedback mechanism involving a Wnt signaling center in the leading edge and a counteracting domain of FGF activity in the trailing adjacent cells (Aman and Piotrowski, 2008; Aman and Piotrowski, 2009b; Ma and Raible, 2009). Activation of Wnt signaling in the leading cells of the pLLp induces the expression of the *fgf3* and *fg10* secreted Fgf ligands and simultaneously drives the expression of the Fgfr antagonistic *sef* in the first third of the pLLp, thereby preventing the activation of the Fgf pathway in the leading domain of the pLLp, limiting it to the trailing cells. Meanwhile, Fgf activity in the trailing domain induces the expression of the Wnt diffusible inhibitor *dkk1*, thereby restricting Wnt signaling to the leading cells and establishing a coupled mutually inhibitory interaction between the Fgf and Wnt networks (Aman and Piotrowski, 2008).

While Fgf signaling is responsible for the epithelialization and maturation of the rosettes, as well as differentiation of neuromast cells (Lecaudey et al., 2008; Nechiporuk and Raible, 2008), Wnt signaling, through Lef1 activity, is essential to maintain the progenitor cell population in the leading tip, that

replenishes the pLLp through compensatory homeostatic cell proliferation as proneuromast are deposited at the trailing edge (McGraw et al., 2011; Nechiporuk and Raible, 2008; Valdivia et al., 2011). The pLLp is therefore a complex system where cell proliferation, differentiation, epithelialization and compartmentalized gene expression must be finely maintained to allow coordinated multicellular movement in a tissue that is under constant remodeling.

Our observation that *brg1* is expressed in the neuromasts of the zebrafish lateral line system and that *brg1* mutants lack a full complements of neuromasts in the posterior lateral line prompted us to analyze the role of *brg1* in the development of a functional lateral-line system. In this study, we show that Brg1 activity is necessary to maintain the pLLp homeostasis by maintaining progenitor cells in the leading edge and the proliferative capacity of the primordium. Additionally, we show that *brg1* mutant primordial cells are unable to coordinate their migratory behavior, which results in a deficient migration of the pLLp. Furthermore, we show that *brg1* plays a fundamental role in the functional homeostasis of the lateral line being necessary for the production and proper polarization of a full complement of hair cells in neuromasts.

2.3 Results

2.3.1 *brg1* is expressed in the migrating primordium and in the neuromasts of the lateral line

brg1 has been shown to be a maternally given mRNA with ubiquitous expression until 24 hours post-fertilization (hpf), after which it becomes mostly restricted to the anterior part of the embryo, with stronger expression in the telenchephalon, cerebellum and hindbrain regions (Eroglu et al., 2006; Gregg et al., 2003; Haas and Gilmour, 2006) (Figure 1A). We further extended these observations and found that *brg1* is also expressed in the

posterior lateral line primordium (pLLp), as revealed by whole mount FISH at 36 hpf, with stronger expression in the leading front (Figure 1A,B) and in deposited neuromasts (Supplementary Figure 1) (Gregg et al., 2003).

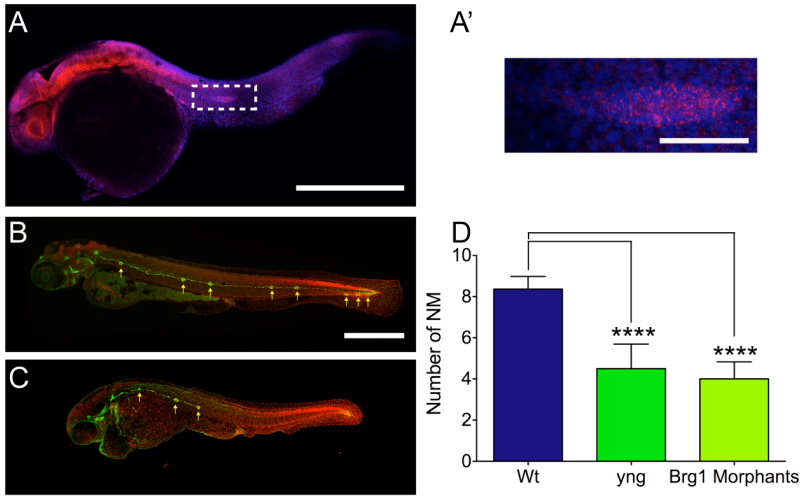

Figure 1. ***brg1*** **is required for posterior lateral line development.**
(**A**) At 24 hpf, *brg1* is expressed the anterior part of the embryo, with stronger expression in the telenchephalon, cerebellum and hindbrain regions (Eroglu et al., 2006; Gregg et al., 2003; Haas and Gilmour, 2006) and also in the pLLp (detail in **A'**) as revealed by whole mount FISH. (**B**-**C**) Lateral views of wild-type (**B**) and *yng* mutant (**C**) 3 dpf zebrafish bearing the SqEt20 transgene. (**C**) Quantification of the number of neuromasts in wild-type, *yng* mutants and *brg1* morphants at 3 dpf. *yng* mutants and morphants have significantly less neuromast then the wild-type (N-wild-type=N-*yng*=N-morphants=30,1-Way-anova P< 0.05, Bonferroni's Multiple comparison test p<0,05). Scale bar is 100 μm in (**A**), 50 μm in (**A'**) and 500 μm in (**B**).

2.3.2 Zebrafish mutants for *brg1* develop a truncated posterior lateral line

Fully differentiated hair cells of the zebrafish lateral line can be selectively labeled with the vital dye DiAsp making it easy to visualize the distribution of neuromasts (Collazo et al., 1994) Initial observations of the pLL in *brg1* mutants (*yng*) zebrafish at 5 dpf revealed the lack of DiAsp positive cells in the most posterior part of the trunk and tail of the fish, suggesting that either *yng* mutants develop a truncated lateral line and/or the last deposited neuromast degenerate or do not harbor a population of fully differentiated hair cells (Supplementary Figure 2). To clarify these observations we

analyzed *yng* mutants bearing the SqEt20 transgene, which expresses GFP in the neuromast supporting cells (Hernandez et al., 2007; Parinov et al., 2004; Wibowo et al., 2011), to examine the posterior lateral line neuromast population. At 3 dpf, wild-type embryos showed an average of five neuromasts deposited in a periodic pattern over the trunk (L1 to L5) with two to three additional proneuromasts deposited at the tip of the tail, where the pLLp stops migrating. In *yng* mutants the number of deposited neuromasts was reduced with the last neuromast being deposited half way to the tip of the tail (Figure 1B-D). The number of deposited neuromasts did not change from 3 dpf to 6 dpf (Supplementary Figure 3) and we did not observe the development of the proneuromasts deposited from the secondary primordium (data not shown). These observations suggest that the neuromast population in *brg1* mutants is derived entirely from Prim1 and that the lack of most posterior neuromasts is not due to reduced neuromast survival. To confirm that the observed phenotype was indeed due to the lack of *brg1* we injected two non overlapping morpholinos specifically targeting *brg1* into one to two cell stage embryos which phenocopied the *yng* mutant (Figure 1D), demonstrating that the lack of *brg1* is responsible for the lateral line defects identified in the *yng* mutant.

2.3.3 *brg1* is necessary for lateral line homeostasis

To assess for neuromast differentiation we analyzed *yng* mutants neuromast at 5 dpf carrying either the SqEt20 transgene or double transgenic *Tg(SqEt4;cldnb:lyngFP)*, which expresses cytoplasmatic and membrane-targeted EGFP in, respectively, the hair cells and the pLL system (Haas and Gilmour, 2006; Lopez-Schier and Hudspeth, 2006; Parinov et al., 2004; Wibowo et al., 2011). The analysis of these lines showed that *yng* mutant neuromasts contain both supporting and hair cells. In wild-type *Tg(SqEt20)* animals the expression of GFP is heterogeneous with low or absent GFP areas, located at the dorsal and ventral aspects of the neuromast that coincide

with domains free of Notch expression. These domains have been implicated in the stabilization of hair cell progenitor identity and establishment of bilateral symmetry in the lateral line, hence named polar compartments (Wibowo et al., 2011).

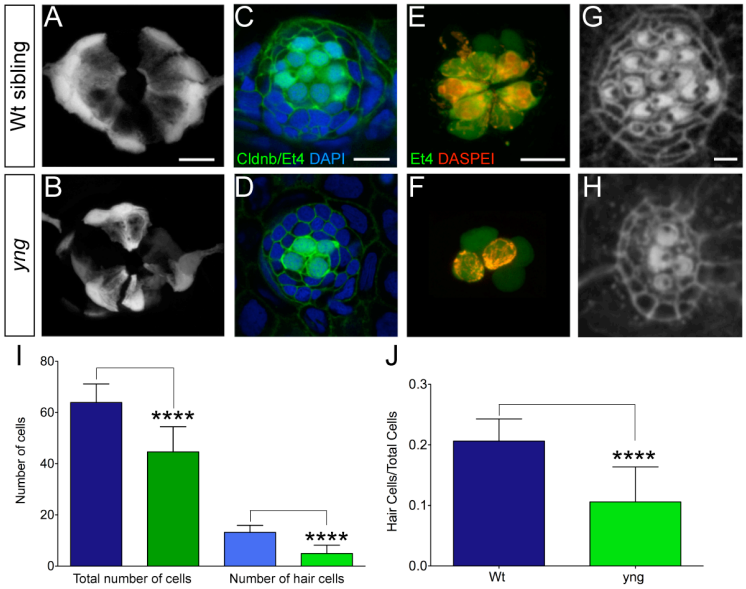

Figure 2. *brg1* **is required for the homeostasis of the zebrafish lateral line.**
(**A**-**B**) Expression of the SqEt20 transgene in wild-type (**A**) and *yng* mutants (**B**), where the polar compartments are aberrantly defined. (**C**-**D**) The analysis of 5 dpf *Tg(SqEt4/cldnb:lynGFP) yng* mutants and wild-type larvae reveals that *yng* mutants bear smaller neuromasts (N-wild-type = 54 and N-*yng* = 25, Mann–Whitney U = 94.50, , P < 0.05 two-tailed) and less hair cells (Mann-Whitney U = 45.50, N-wild-type = 54 and N-*yng* = 25, P < 0.05 two-tailed) (**C**) then their wild-type siblings (**D**), quantification in (**I**). Hair cell index in (**J**) (Mann–Whitney U = 99, N-wild-type = 54 and N-*yng* = 25, P < 0.05 two-tailed). Blue bars correspond to wild-type and green bars to *yng*. (**E**-**F**) DiAsp incorporation into hair cells of a *Tg(SqEt4)* wild-type (**E**) and *yng* (**F**) neuromast reveals that hair cells eventually fully differentiate in *yng* mutants, but the sensory epithelium is defective in its planar polarization as evidenced by an acting staining of the epithelium, wild-type (**G**) and *yng* mutant (**H**). Scale bar is 10 μm in (**A**), (**C**) and (**E**) and 2 μm in (**G**).

In *Tg(SqEt20) yng* mutants, the GFP expression pattern is aberrant, with polar compartments badly defined, suggesting that hair cells production and epithelial architecture could be affected in the mutant condition (Figure 2A-B). Additionally, the analysis of the *Tg(SqET4;cldnb:lynEGFP) yng* mutants at 5 dpf revealed that deposited neuromasts are smaller compared to the wild-type siblings, and bore a reduced hair-cell population (Figure 2C,D,I,J).

Albeit hair-cells are functional, as shown from the incorporation of the vital dye DiAsp (Figure 2 E-F), and shown normal apical basal polarity, they are defective in their planar polarization, as revealed by an acting staining of the hair cells stereocilia bundle (Figure 2 G-H). Because the lack of *brg1* as been associated with increased apoptosis (Eroglu et al., 2006), we assessed whether apoptosis could explain the reduced number of hair cells. By performing a TUNEL assay we could not find any evidence for increased apoptosis in *yng* mutant neuromasts, suggesting that the reduced hair cell number in *yng* mutants is not due to increased hair-cell degeneration (Supplementary Figure 5) but most probably a consequence of reduced hair cell production. Together, these results show that Brg1 activity is necessary for the homeostasis of the zebrafish lateral line.

2.3.4 *brg1* is required for coordinated cell migration in the pLLp

To further assess the nature of the pLL morphogenesis defect in *yng* mutants we quantified neuromast distribution in wild-type animals and *yng* mutants at 3 dpf. This analysis revealed that *yng* mutant's neuromasts are stereotypically located at somite boundaries as in wild-type animals but more anteriorly deposited and more closely spaced (Figure 3 A,B). In order to address the role of *brg1* in neuromast production we performed time lapse imaging of the migrating pLLp in *Tg(cldnb:lyngGFP) yng* mutants. At the onset of pLLp migration, the primordium of *yng* mutants is indistinguishable from the wild-type condition, with the same number of cells and a front group of mesemchymal like cells followed by 2 or 3 rosettes. These observations suggest that pLLp specification and formation is not affected in *yng* mutants, and neither is its polarization as the primordium forms rosettes and eventually migrates. However time-lapse analysis reveals that the pLLp does not migrate at a constant pace in *yng* mutants (Figure 3 C,D and Movies 1 and 2). In wild-type primordia cells maintain their relative position through migration. In *yng* primordia, we observed that migrating cells show extensive

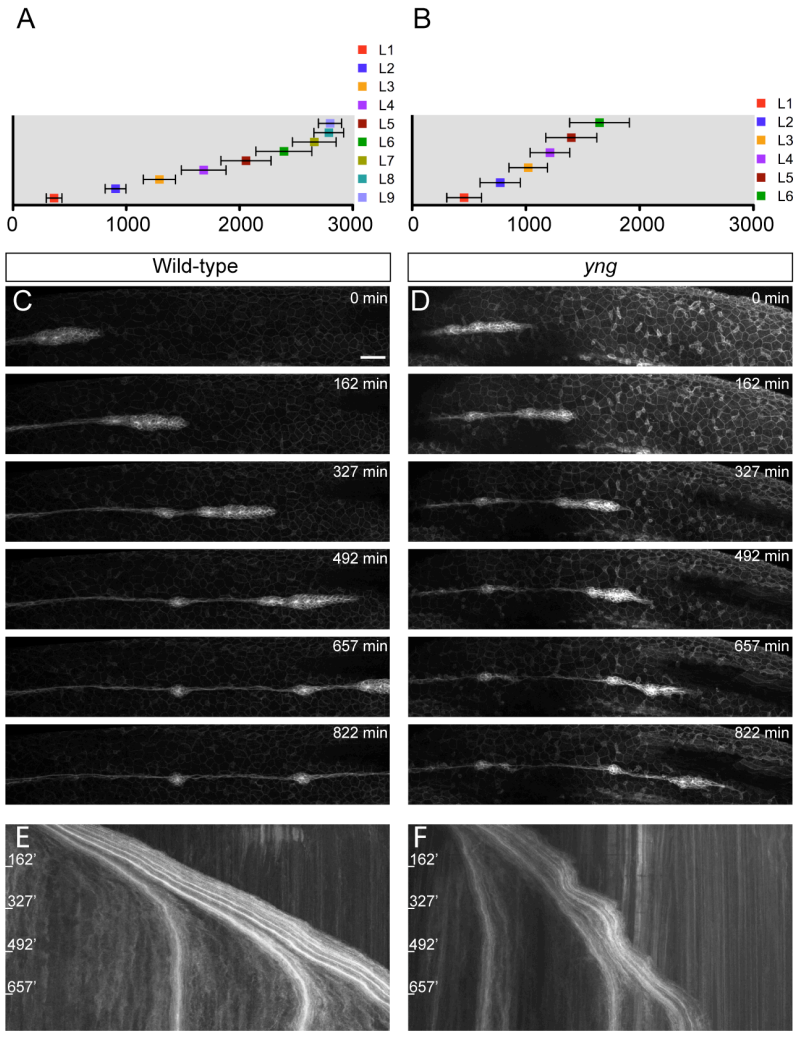

Figure 3. Abnormal primordium migration leads to a loss of terminal neuromast in the *yng* mutant.

(**A**-**B**) Axial positions of deposited neuromasts in wild-type (**A**) and *yng* mutants (**B**). The position of deposited neuromasts in *yng* mutants is significantly shifted anteriorly (N-wild-type = 30 and N-*yng* = 18, Mann–Whitney U = 121, P<0.05 two-tailed). (**C**-**D**) Stills from time-lapse movies of primordium migration in wild-type and *yng* mutants embryos expressing the *Tg(cldnb:lynGFP)* and the corresponding kymographs for the wild-type in (**E**) and *yng* (**F**). Wild-type and *yng* embryos were imaged after the deposition of the neuromast L1 (see the corresponding Movies 1 and 2 in the supplementary material). Scale bars are 50 μm.

uncoordinated movement with the leading part of the pLLp often stalling in front of the rosettes that keep migrating (compare kymographs in (Figure 3E,F).

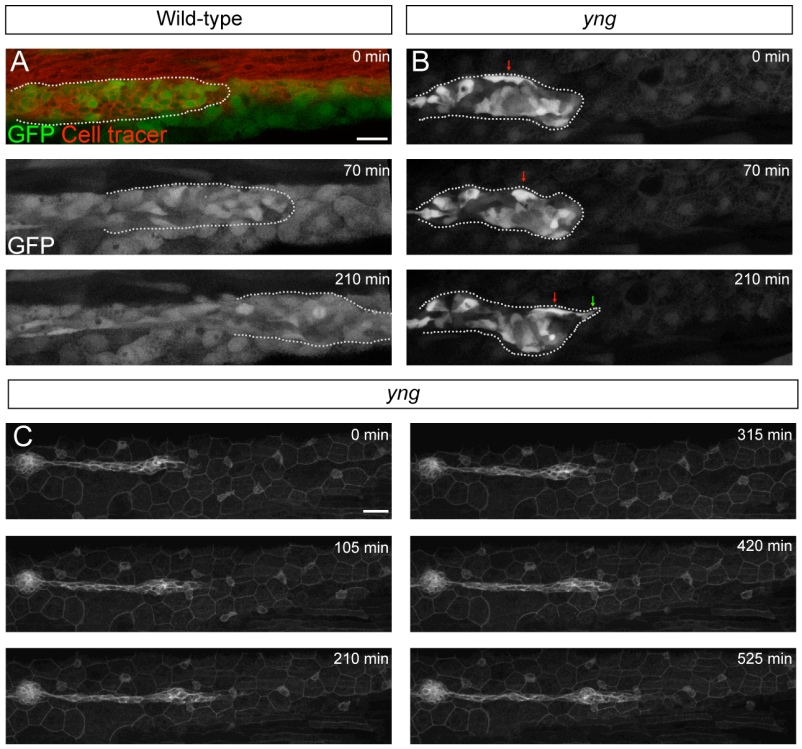

Figure 4. *yng* **primordial cells do not retain their relative position**
(**A**-**B**) Stills of time lapses of wild-type (**A**) and *yng* mutant (**B**) *Tg(SqEt20)* primordia. The *Tg(SqEt20)* line expresses GFP is a mosaic fashion in all cells of the pLLp. In the first image of panel (**A**) cell membranes are labeled with Cell-Tracer. (**B**) In *yng* mutants, primordial cells to not maintain their relative position with trailing cells moving to the leading edge (red arrow), and producing lamelipodia that extend caudally (green arrow). See corresponding movies 3 and 4. (**C**) *yng* primordia at the end of migration with the remaining primordial cells extending caudally behind the last deposited neuromast. See corresponding movie 5. Scale bars are 50 μm.

Additionally, by imaging the primordia of *Tg(SeqEt20)* animals, which express GFP in a mosaic fashion in all cells of the primordium (Figure 4A), we found that as *yng* primordia stall during migration, cells tumble and change their relative position, with cells from the trailing region eventually moving to the leading edge, a situation never observed in wild-type primordia. (Figure 4B and movies 3 and 4). These observations indicate that

the lack of *brg1* does not block primordium migration but strongly compromises its migratory persistence and neuromast deposition. As proneuromasts are deposited the pLLp eventually runs out of cells with the remaining cells not incorporated in the last deposited proneuromast extending caudally (Figure 4C and movie 5).

2.3.5 Rosette maturation and proneurogenic cell fate acquisition is delayed in *yng* mutants

While primordium formation is not affected in *yng* mutants we observed a defect in rosette formation at later stages, with a delay in the central accumulation of ClaudinB (Figure 5A,B) and of N-Cadherin to the central junctions of the maturing rosettes, eventually occurring further away form the leading tip (Figure 5 C-E).

Proneuromast formation is under the control of two distinct Fgf signaling systems that operate in the leading and trailing ends of the pLLp. In the leading third, a Wnt-dependent Fgf signaling system regulates proneuromast formation by driving *atoh1a* and *deltaA* expression and rosette assembly (Itoh and Chitnis, 2001; Lecaudey et al., 2008; Nechiporuk and Raible, 2008). *atoh1a* and *deltaA* are specifically expressed in foci in the center of the rosettes, complementary to *notch3*, which is broadly expressed in the pLLp with foci of no expression in the center of the rosettes (Itoh and Chitnis, 2001). As the expression of *atoh1a* becomes stabilized, an additional Atoh1a-dependent Fgf signaling center is established, assuring the maintenance of focal Fgf signaling centers in the maturing rosettes (Matsuda and Chitnis, 2010). While we saw no differences in the expression of *fgf10* and *fgfr1* between *yng* mutants and wild-type siblings (Figure 5F-I), we found that *fgf3* was misexpressed in the mutant condition, being expressed in the trailing part and strongly downregulated in the leading front of the primordium, as revealed by whole mount *in situ* hibridization at 26 hpf (Figure 5J-K). Consistent with the upregulation of this Fgf ligand we found that *pea3*

expression was consistently upregulated in *yng* mutants, expanding to the leading domain and reducing the extent of the *pea3* expression-free zone with respect to the overall length of the primordium (Figure 5L, M, R). Additionally, while we saw no differences in *notch3* expression between both conditions (Figure 5N,O), *atoh1a* expression was restricted to one focus in the trailing part in *yng* mutant's pLLp (Figure 5P,Q). Altogether these observations show that both rosette formation and hair cell progenitor specification are delayed in *yng* mutants most probably due to disrupted Fgf signaling (see discussion).

2.3.6 Brg1 activity is needed to maintain cell proliferation and primordium homeostasis by regulating progenitor cell identity

We reasoned that the pLLp in *yng* mutants could become depleted of cells due to an increase of the number of cells in deposited proneuromast. However, we saw no differences in the cell number of wild-type animals and *yng* mutants proneuromasts as they were just about to be deposited (Supplementary Figure 5).

Wnt signaling controls cell proliferation in the pLLp (Aman et al., 2011). Additionally, Wnt signaling, trough Lef1 activity, is required for progenitor cell identity in the leading tip responsible for feeding the primordium with new cells, maintaining its homeostasis during migration, so that in the lack of *lef1* a truncated lateral line with fewer and more anteriorly deposited neuromasts is formed (McGraw et al., 2011; Valdivia et al., 2011). Based on the analysis of *lef1* mutants, Valdivia *et al* proposed that proneuromast deposition depends on the relative size of the pLLp compartments and of a factor(s) in the leading edge by which trailing cells judge their relative location in the pLLp (Valdivia et al., 2011).

As cells proliferate in the trailing zone and new cells are continuously produced in the leading edge, trailing edge cells are further moved away from

the leading zone. Eventually, the most rostral rosette will eventually be out of the range of the factor(s) at the leading edge, which triggers its deposition. As in *yng* mutants the pLLp becomes depleted of cells as proneuromasts are deposited we asked if this could be a consequence of disrupted Wnt signaling. We assessed the expression of *axin2* and *lef1*, whose expression is Wnt dependent and restricted to the leading tip cells of the pLLp (Aman and Piotrowski, 2008). While *lef1* expression was undistinguishable between *yng* mutants and wild-type siblings we found that *axin2* is not expressed in the pLLp of *yng* mutants (Figure 6A-D), suggesting that Brg1 mediates Wnt activity by regulating the expression of a subset of its efector genes. We reasoned that the reduction of Wnt activity would have consequences in the proliferative activity of the pLLp in *yng* mutants. By performing one hour pulse BrdU at 26 hpf we found a 50% reduction of proliferation in *yng* mutants primordia compared to the wild-type siblings (Figure 6E-G). Additionally, we could not find evidence for increased apoptosis in *yng* mutant primordia, as revealed by a TUNEL assay (Supplementary Figure 6), suggesting that the observed cell depletion in the mutant condition is not due to increased apoptosis but instead to reduced cell proliferation in the pLLp. While we could not find evidence for the downregulation of *lef1* in *yng* mutants, the deposition of more closely spaced neuromasts at a more anterior axial position, and primordium cell depletion is remarkably similar to the *lef1* mutant condition (McGraw et al., 2011; Valdivia et al., 2011).

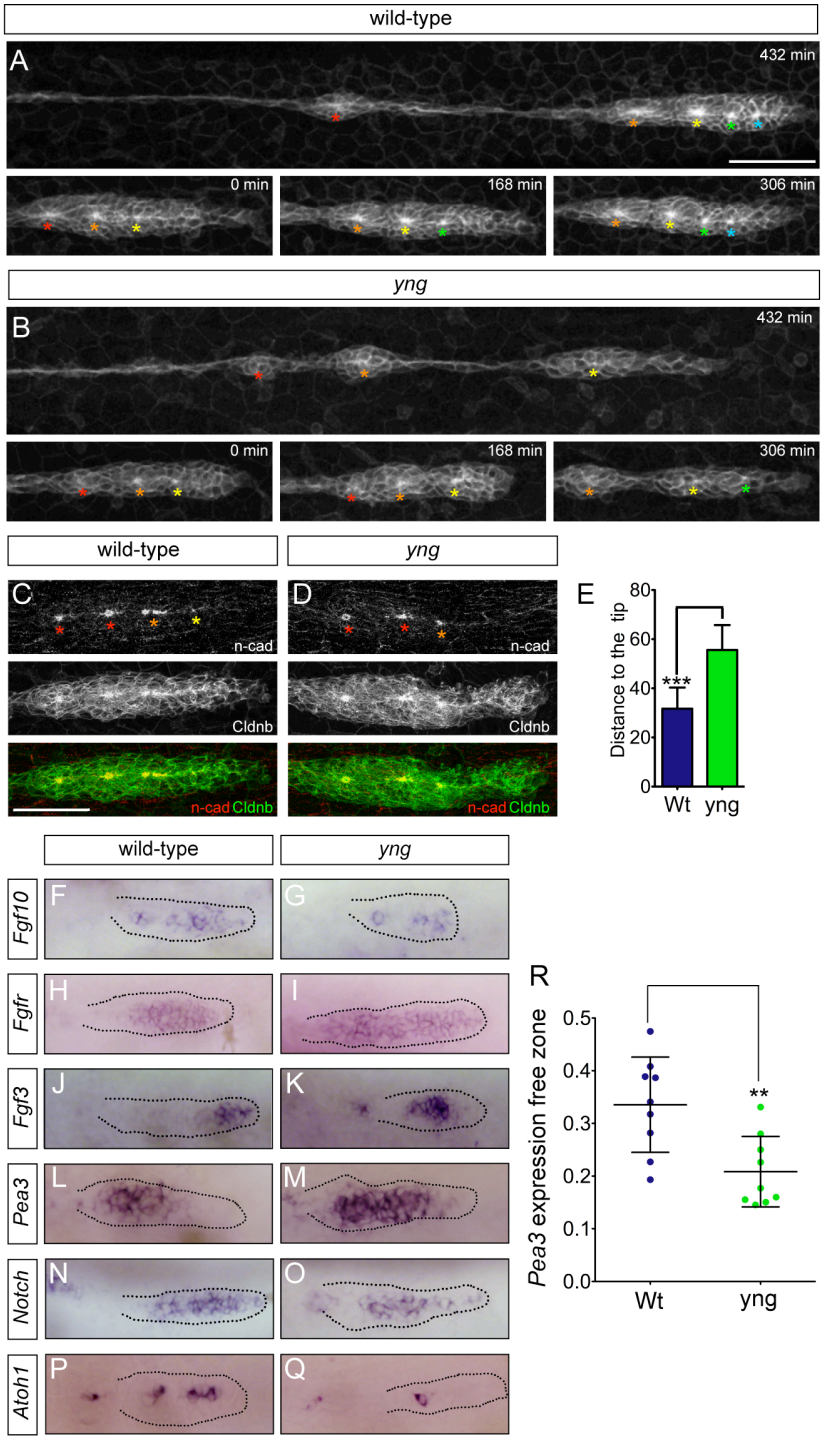
wild-type
A
432 min
0 min
168 min
306 min
yng
B
432 min
0 min
168 min
306 min
wild-type
yng
C
D
n-cad
Cldnb
n-cad Cldnb
E
Distance to the tip
80
60
40
20
0
***
Wt
yng
wild-type
yng
Fgf10
Fgfr
Fgf3
Pea3
Notch
Atoh1
F
G
H
I
J
K
L
M
N
O
P
Q
R
Pea3 expression free zone
0.5
0.4
0.3
0.2
0.1
0.0
**
Wt
yng

Figure 5. Loss of Brg1 activity causes a delay in proneuromast maturation.
(**A**-**B**) Stills from time-lapse movies of primordium migration in wild-type and *yng* mutants embryos expressing the *Tg(cldnb:lynGFP)* depicting the accumulation of ClaudinB and rosette formation. *yng* mutants show a delay in the central accumulation of ClaudinB and reduced rosette formation. Over the course of 432 minutes the primordium in the wild-type generated two new rosettes (green and blue asterix) while the *yng* mutant primordia started the production of one single rosette, as depicted from the accumulation of ClaudinB at minute 306 (green asterix) (see the corresponding Movies 6 and 7 in the supplementary material). (**C**,**D**) n-cadherin accumulation is delayed in *yng* mutants (**D**) when compared with wild-type siblings (C) at 28hpf, eventually occurring further away from the leading tip of the primordium (**E**) (N = 9 for both conditions, Mann–Whitney U = 2.5, P<0.05 two-tailed). (**F**-**Q**) RNA *in situ* hybridization of factors required for proneuromast formation and maturation. (**R**) Quantification of the *Pea3*-free expression domain at 28hpf (N = 9 for both conditions, Mann–Whitney U = 9, P<0.05 two-tailed). Scale bars are 50 μm.

Brg1 was showed to interact with β-catenin in the activation of the transcription factor TCF/LEF and its downstream target genes (Barker et al., 2001; Griffin et al., 2011; Park et al., 2009). We reasoned that Brg1 activity might be needed in the regulation of Lef1 transcription activity, and therefore the lack of *brg1* would affect the maintenance of progenitor cells in the leading tip of the pLLp, which could explain the similar observed phenotypes in *yng* and *lef1* mutants. To test this hypothesis, we photoconverted Kaede-expressing cells at the leading tip in 24 hpf *Tg(cldnb:lynEGFP)* wild-type animals and *yng* mutants. At 38 hpf we observed that in the wild-type siblings all the primordium was labeled (red) as well as the last deposited neuromast (Figure 6 H,I). In *yng* mutants labeled cells also retained the ability to move into the trailing zone as labeled cells where found across the primordium and eventually in the last deposited neuromast. Additionally, labeled cells where not retained in the leading edge, suggesting that Brg1 activity is required for progenitor cell maintenance in the leading tip (Figure 6 J,K).

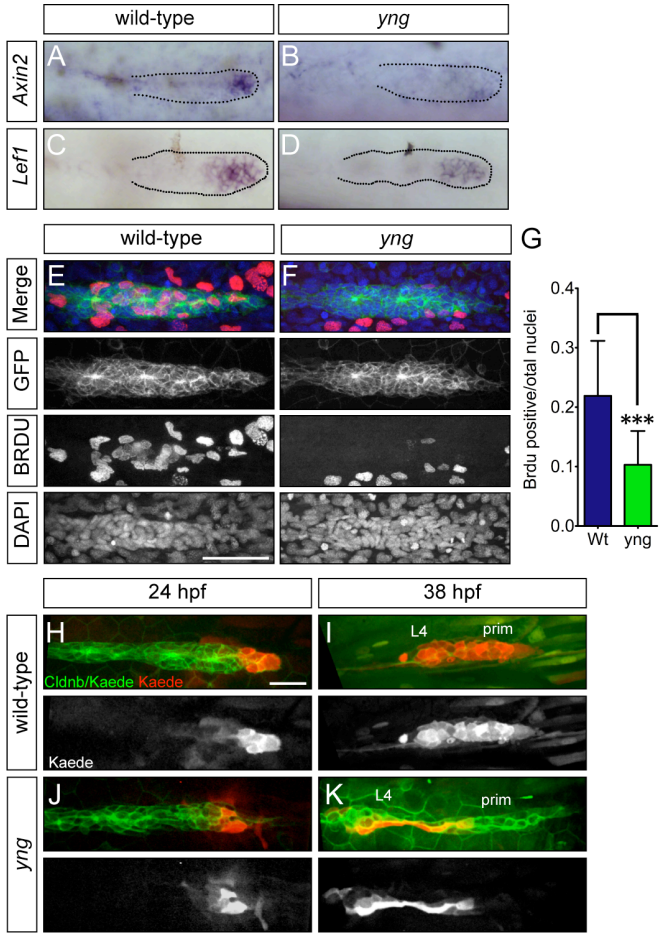

Figure 6. Brg1 activity is needed to maintain primordium homeostasis.
(**A**-**D**) Wnt downstream target genes *lef1* and *axin2* are expressed in the tip of the pLLp (**A**) and **C**). In *yng* mutants embryos pLLp at 26 hpf *Lef1* expression is undistinguishable from the wild-type condition (**A** and **C**) , *axin2* is not expressed in *yng* mutants pLLp (**B** and **D**). (**E**-**F**) Cell proliferation analysis in wild-type (**E**) and *yng* mutants (**F**) in *Tg(cldnb:lynGFP)* embryos. (**G**) BRDU incorporation index for wild-type siblings and *yng* mutants at 26 hpf. (N-wild-type = 28, N-yng = Mann–Whitney U = 94 , P<0.05 two-tailed). Kaede photoconverted leading edge cells at 24 hpf in wild-type (**H**) and *yng* mutants (**J**) and assessed at 38 hpf (**I**,**K**).
Scale bars are 50 μm.

2.3.7 *brg1* is needed for *cxcr4b* chemokine receptor expression in the pLLp

The pLLp in *yng* mutants does not migrate at a constant speed, with extensive uncoordination between its leading and trailing cells and often stalling during migration. To gain further insight on the molecular basis of

pLLp migration arrest in *yng* mutants we assessed for the expression of the *sdf1a* chemokine and its receptors, *cxcr4b* and *cxcr7b*, whose polarized expression in the migrating primordium is essential for effective pLLp migration and morphogenesis (Dambly-Chaudiere et al., 2007; Haas and Gilmour, 2006; Valentin et al., 2007). While the *sdf1a* expression pattern was undistinguishable between wild-type animals and *yng* mutants (Supplementary Figure 7A,B), the expression of *cxcr4b* at 26 hpf was strongly reduced but still present (Supplementary Figure 7C-D), consistent with the capacity of *yng* mutant primordia to migrate. It has been suggested the existence of an antagonistic interaction between *cxcr4b* and *cxcr7b* (Dambly-Chaudiere et al., 2007), by which Cxcr4b activity in the leading cells of the primordium represses *cxcr7b* expression. This observation has however been questioned (Valentin et al., 2007). We therefore assessed for the expression of *cxcr7b* in *yng* mutants at 26 hpf, a time by which we have shown that *cxcr4b* expression was strongly reduced. We could not find any significant change in *cxcr7b* expression in *yng* mutants (Supplementary Figure 7E,F), which supports the view that Cxcr4b activity does not inhibit *cxcr7b* expression and suggests that additional factors prevent the expansion of *cxcr7b* in the leading part of the pLLp. As both *cxcr4b* and progenitor cells are needed at the leading edge, we asked if the observed pLLp migration defects in *yng* mutants could be recovered in mosaic primordia containing few wild-type cells in the leading tip, and therefore test for the specific requirement of *brg1* in the leading tip cells. By performing gastrula-stage transplants of rodamine labeled wild-type donor cells we obtained eight mosaic *yng* embryos with wild-type cells localized in the pLLp, three of which with clusters of 4-6 wild-type cells in the leading tip domain. In all samples the primordium always runned out of cells stopping migrating prematurely during migration, as in *yng* mutants (Figure 7 and movie 6).

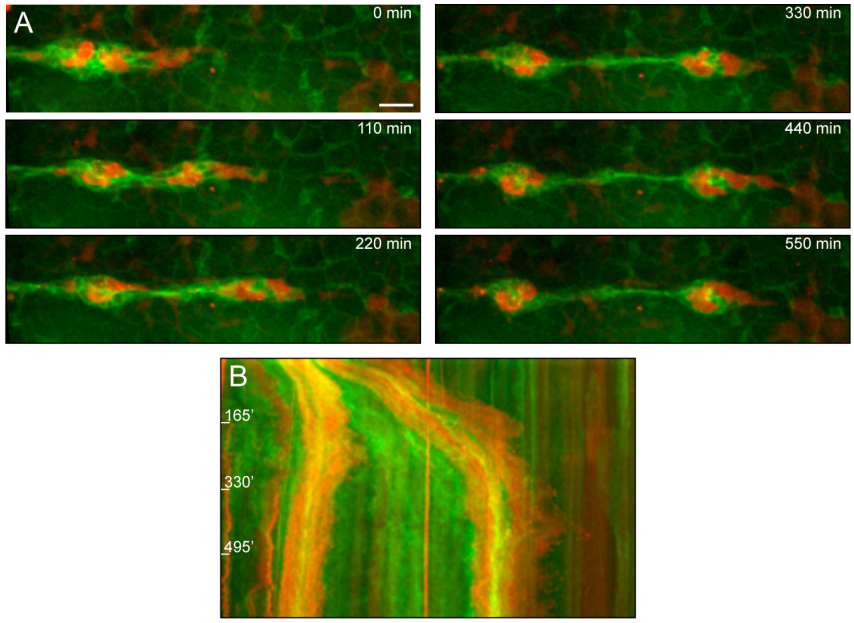

Figure 7. Mosaic clone analysis.
(**A**) Stills from a time lapse movies of a *Tg(cldnb:lynGFP) yng* mutant host that received *Tg(cldnb:lynGFP)* wild-type donor cells (rhodamine dextran, red), and the corresponding kymograph in (**B**). At the beginning of the time lapse, by 28 hpf, the primordium contains donor cells in the leading zone and in the rosettes. The presence of wild-type cells does not recover primordium migration. Scale bar is 50 μm.

2.4 Discussion

In this study we have characterized the defective morphogenesis of the pLL system in the *yng* mutant, that lacks the SWI/SNIF complex ATPase *brg1*. We show that in the lack of *brg1* primordial cells are unable to coordinate their migratory behavior and that the pLLp migrates aberrantly. Brg1 activity is required to maintain progenitor cells in the leading tip and for the regulation of proliferation in the pLLp, and therefore for its homeostasis. Furthermore, we show that *brg1* mutant primordia show a delayed rosette formation and maturation and, as a consequence, are unable to efficiently renewal rosettes as proneuromasts are deposited in the trailing edge, with the primordium eventually becoming depleted of cells and stalling prematurely on its journey. Additionally, we show that at later stages Brg1 activity is

essential for the development of a functional lateral line as *yng* mutants neuromasts bore a reduced and deficiently polarized sensorial epithelium.

2.4.2 Brg1 activity is needed for proper mesenchymal to epithelial transition

In *yng* mutants, as fewer cells are added at the leading edge, fewer cells are then available to form additional rosettes, consistent with the observed delayed rosette formation. Fgf signaling has been shown to promote proneuromast formation so that when inhibited, rosettes are not formed (Lecaudey et al., 2008; Nechiporuk and Raible, 2008). The upregulation of Fgf signaling using the *Tg(hsp70:fgf3)*, has been shown to deplete the migrating primordium of rosettes, which reassemble in higher number nine hours upon the heat shock treatment, suggesting that discrete spots of Fgf are needed for the seeding and maintenance of the rosettes (Lecaudey et al., 2008). Here we show that the *fgf3* ligand is absent in *yng* mutants primordia leading edge, and ectopically expressed in the pLLp trailing domain, disrupting the *fgf* discrete spots expression pattern. Additionally, we saw an expansion of the Fgf target *pea3*, however, we could not find evidence for increased epitelialization due to the increase of Fgf signaling. . By time lapse analysis of *Tg(cldnb:lynGFP) yng* mutants we observed a delay in rosette formation and that rosettes apical constrictions were unstable but proneuromasts are eventually deposited. In *yng* mutants, primordium migration lasts over ten to thirteen hours, with the primordium getting exhausted of cells during the process, which might explain why we could not see overproduction of rosettes. Consistent with a role for *brg1* in regulating rosette assembly and maturation is the observation that *atoh1a* expression was restricted to one focus in the trailing part in *yng* mutant's pLLp. It is tempting to suggest that Delta/Notch signaling, and hence hair cell specification is the internal checkpoint proposed by Lecaudey *et al* (Lecaudey et al., 2008). The interdependence of the Notch/Fgf signaling pathways

assures the stability of the migration process(Matsuda and Chitnis, 2010), which might also explain the high conservation of embryonic pLL patterns across teleosts (Gamba et al., 2010; Pichon and Ghysen, 2004; Sapede et al., 2002).

2.4.1 *brg1* dependent proliferation maintains the homeostasis of the pLLp

Progenitor-cell identity is regulated by Wnt signaling through Lef1, whose activity is necessary for the specification and/or maintenance of the progenitor population in the leading edge. In the absence of *lef1*, progenitor cells are prematurely incorporated into proneuromast and the primordium gets depleted of its leading cells, leaving an insufficient number of cells to renewal rosettes after the first proneuromasts have been deposited. As a consequence, *lef1* mutants develop a truncated and shorter lateral line (McGraw et al., 2011; Valdivia et al., 2011). Based on these observations, Valdivia *et al* postulated that neuromast deposition might be inhibited by unknown factors produced at the leading edge. As trailing cells get further away from the leading tip due to continuous cell proliferation, the proneuromast at the trailing edge is eventually instructed to be deposited when out of the range of the signaling factors (Valdivia et al., 2011). The downregulation of the Wnt efector gene *tcf7* has no effects in pLLp morphogenesis (Aman et al., 2011; McGraw et al., 2011), however, its abrogation in a *lef1* mutant background enhances the severity of the *lef1* phenotype, reducing the number of deposited neuromasts and shifting their axial level position more anteriorly when compared to *lef1* mutants (McGraw et al., 2011). While these observations show that *lef1* and *tcf7* have partial functional redundancy in the migrating pLLp, their combined loss is not as severe as that caused by the global loss of Wnt signaling, which strongly disrupts pLLp patterning and proliferation affecting its organization (Aman and Piotrowski, 2008). Additionally, loss of Lef1 function does not fully

rescue pLLp migration in *apc* mutants (Valdivia et al., 2011). Altogether these observations suggest that Wnt signaling is mediated by multiple downstream effectors in the pLLp. We showed that *axin2* is downregulated in the absence of *brg1*, further supporting a role for *brg1* in mediating the activity of Wnt signaling in the pLLp. *axin2* is a component of the canonical Wnt signal transduction machinery, where it serves as a scaffold for the β-catenin destruction complex (Kikuchi, 1999; Luo and Lin, 2004). As its expression is induced by Wnt/β-catenin signaling, *axin2* mediates a negative-feedback mechanism by which the response to Wnt signals can be regulated (Jho et al., 2002; Leung et al., 2002; Lustig et al., 2002). In zebrafish mutants for *apc*, Wnt signaling is constitutively active, which results in the global expression of both *axin2* and *lef1* in the pLLp (Aman and Piotrowski, 2008). However, in *yng* mutants, we could not see an expansion of *lef1* expression at 26 hpf, suggesting the maintenance of a negative-feedback mechanism at that stage. In mouse it has been shown that both Axin1 and Axin2 proteins are functionally equivalent (Chia and Costantini, 2005), with only *axin2* being transcriptionally upregulated by canonical Wnt signaling. Though the expression of *axin1* has not been described in the pLLp, we hypothesize that *Axin1* might be expressed in the pLLp which could explain the maintenance of a negative-feedback mechanism in the absence of *Axin2* in *yng* mutants.

Using lineage analyses and BrdU incorporation assays we show that Brg1 activity regulates the proliferative capacity of the pLLp and the maintenance of progenitor cells in the leading edge. Another possibility is that *brg1* is required for the specification of maintenance of progenitor cell fate. Supporting this possibility is the observation that *brg1* was shown to be required for murine stem cell maintenance (Matsumoto et al., 2006), for the self renewal of embryonic stem cells (Kidder et al., 2009) and in adults, *brg1* expression has been mostly observed in cells with high turnover rates or that constantly proliferate (Reisman et al., 2005). Mosaic analysis aimed at testing the specific requirement of *brg1* in leading cells did not recovered *yng* mutant

primordium migration, that always became depleted of cells and stopped migrating prematurely. Further studies addressing the role of *brg1* in the leading and trailing domains of the pLLp will help in understanding our results. In conclusion we have demonstrated a previously unreported role for *brg1* during mechanosensory organ formation in the zebrafish.

2.5 Supplementary Material

Supplementary Figure 1. *brg1* expression in the pLL at 3 dpf
(**A**) *brg1* is expressed the anterior part of the embryo, with stronger expression in the telenchephalon, cerebellum and hindbrain regions and also in the lateral line neuromasts. (**B**) Detail of *brg1* expression in neuromasts. *brg* is broadly expressed in deposited neuromasts.

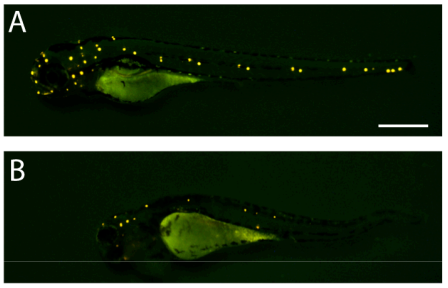

Supplementary Figure2. DiAsp staining of the lateral line
Fluorescent image of a wild-type zebrafish larva (**A**) and an *yng* mutant (**B**) at 4 dpf with neuromasts labelled with DiAsp. Scale bar is 500µm.

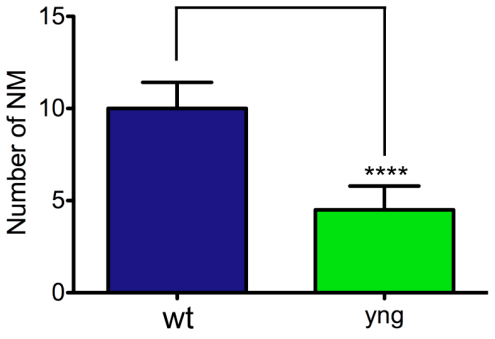

Supplementary Figure 3. Number of neuromasts in wild-type and *yng* mutants at 6 dpf
(Student's t-test, N=30 p<0,05).

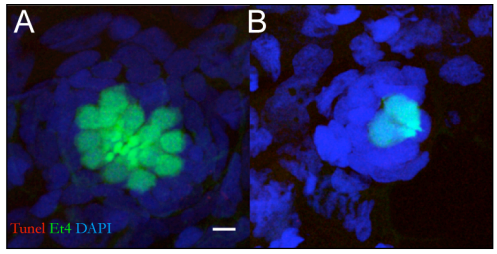

Supplementary Figure 4. Tunel assay at 6 dpf
(**A**) wild-type neuromast and (**B**) *yng* neuromast at 5 dpf. Scale bar is 5 μm.

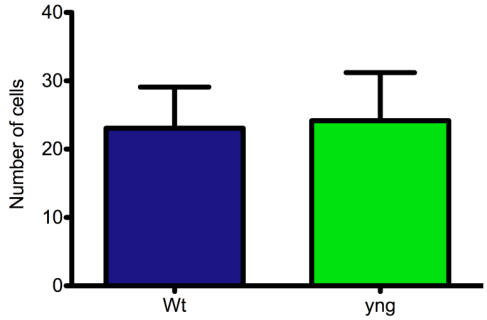

Supplementary Figure 5. Number of cells per proneuromast about to be deposited at the trailing edge of the pLLp. (Mann–Whitney U = 121, N = 20 for both conditions, P < 0.05 two-tailed)

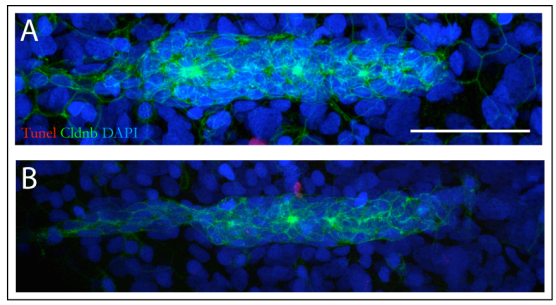

Supplementary Figure 6. Tunel Assay
(**A**) Wild-type primordium and *yng* primordium (**B**) at 26hpf. Scale bar is 50 μm.

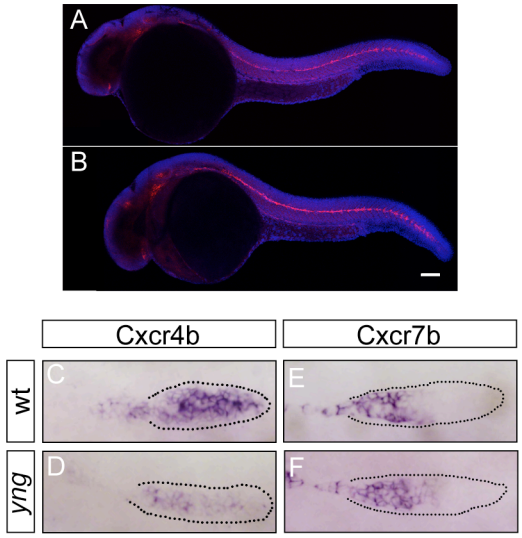

Supplementary Figure 7. ***cxcr4b*** **is downregulated in yng mutants.**
Whole-mount FISH for *sdf1a* in wild-type (**A**) and *yng* mutant (**B**) at 26 hpf. Chromogenic whole-mount in situ hybridization for *cxcr4b* in wild-type (**C**) and *yng* (**D**) and *cxcr7b* in wild-type (**E**) and *yng* (**F**). Scale bar is 100 μm.

General discussion and future directions

Functional role of a compartmentalized organization in hair-cell regeneration.

In chapter 1 I showed that hair-cell regeneration in the zebrafish lateral line relies on the mitotic proliferation of UHCP's whose differentiation is controlled by compartmentalized Notch activity in the lateral line neuromasts.

A fundamental question in regenerative stem cell biology is how stem cell behavior is controlled during development and in adulthood, in the maintenance of tissue homeostasis and regeneration. The organization of stem cells in spatially well defined microenvironments, or niches, has been described as a general feature by which organ growth, homeostasis and regeneration is orquestrated (Greco and Guo, 2010). Stem cells have been described as slow cycle or quiescent populations that eventually re-enter the cell cycle when requested to assure the cell turnover necessary for tissue homeostasis (Foudi et al., 2009; Tumbar et al., 2004; Wilson et al., 2008). However, stem cells must as well maintain tissues with high turnover rates and, importantly, upon injury, stem cells must rapidly contribute to the regeneration of the damaged tissue, which depending on its nature and intensity could potentially results in the uncontrolled request of the entire stem cell population, leading to its exhaustion. It has recently been suggested that the bi-compartmentalization of stem cells might represent a general strategy by which only a few stem cells are requested to sustain tissue regeneration while others are maintained assuring the maintenance of the population (Greco and Guo, 2010). Among others (Barker et al., 2007; Passegue et al., 2005; Venezia et al., 2004), the hair follicle is perhaps the most evident example of such bi compartmentalization, that is translated in a two step process by which hair follicles regenerate. In a first step the dermal papilla signals to the hair germ cells, initiating hair follicle growth, followed by a second step where bulge cells are activated and assure the maintenance of the hair follicle regeneration process (Greco et al., 2009).

In *Drosophila*, neuronal differentiation has been shown to be regulated by Notch signaling, whose activity maintains a proliferative precursor population, while it's down regulation induces neuronal differentiation (Chitnis, 1995). This mechanism was shown to be conserved in vertebrates (Austin et al., 1995; Dorsky et al., 1995; Henrique et al., 1997; Myat et al., 1996; Weinmaster et al., 1991) where, for instance, in the retina, Notch compartmentalization along the apical-basal axis of the neuroepithelium regulates neurogenesis (Del Bene et al., 2008; Jadhav et al., 2006; Nelson et al., 2006). During development, the nuclei of neuronal progenitors moves apical-basaly along the columnar neuroepithelium, a process known as interkinetic nuclear migration (INM), therefore being exposed to different levels of Notch activity. If a progenitor nucleus stays close to the apical side it will encounter high levels of Notch and, as a consequence, daughter cells will likely remain proliferative. Conversely, more basally located nuclei will be exposed to reduced Notch levels, favouring cell cycle exit and neuronal differentiation (Del Bene et al., 2008). In this way Notch, signaling cooperates with INM coordinating cell cycle control and differentiation so that only a fraction of the neuronal progenitors exit the cell cycle at any given time, generating, according to their competence state, the correct proportion of each cell type, while a subset of progenitors is maintained for subsequent waves of neurogenesis (Del Bene et al., 2008).

I showed that putative UHCP's originate across the lateral-line neuromasts but their fate acquisition is limited to the Notch free polar compartments, suggesting that these to not hold a specific stem cell population but rather behave as a permissive compartment, providing further evidence that fate acquisition might be determined by the cell environment (Barroca et al., 2009; Nystul and Spradling, 2007). Whether cell movement is unidirectional or if cells move out of the polar compartments remains unknown. Further studies elucidating the interchange of cells between the polar compartments and other parts of the neuromasts, depending on the organ physiology, will

help elucidate how cell fate plasticity and differentiation are regulated in the zebrafish neuromast, in particular how is hair progenitor cell competence regulated and how does this contributes to the specific translocation of hair-cell progenitors to the polar compartments? The observation that regenerated hair cells derive from *sox2*-positive supporting cells (Hernandez et al., 2007) suggests that, like in ear of zebrafish (Sweet et al., 2011), chick (Neves et al., 2007) and mice (Dabdoub et al., 2008; Kiernan et al., 2005b) progenitor fate competence is regulated by the combined activity of Sox and Notch signaling. Additionally Fgf has been shown to interact with Sox2 and Atoh1 enhancing the competence of non sensory regions of the otic vesicle to respond to Atoh1 (Sweet et al., 2011). In the zebrafish pLLp Fgf signaling controls Atoh1a expression in the pLLp and is active in neuromasts both during development and during hair-cell regeneration (our unpublished data). How these players interact during hair-cell development and regeneration in the pLL remains unknown. We hypothesize that putative UHCP's translocation to the polar compartment depends on their competence and therefore mediated by the combined activity of Sox2 and Notch. The identification of the relevant Notch ligands and further gain and loss of function of these genes combined with live imaging of reported lines of Notch activity during the regenerative process will allow to test this hypothesis and elucidate how are UHCP's spatiotemporally controlled. Moreover, the identification of additional cell markers will allow to ask for cell heterogeneity in the supporting cell population and test their contribution in the regenerative potential of the neuromast.

Hair cells dance the twist

A standing question in hair cell development is whether individual hair cells are generated with their final polarity vector already defined or sensory patch remodeling or cell rotation account for the final orientation of the hair cells (Lewis J, 2002). The unpredictable orientation of newborn hair cells in the chick basilar papilla suggested that hair cells final orientation depends on their interaction with the overlaying tectorial membrane, whose shearing movements over the newborn hair bundles would align them relatively to the sensory epithelium. However it seems unlikely that a similar mechanism could account for the establishment of hair cell polarity in the lateral line neuromasts, which obviously lack a tectorial membrane.

Upon UHCP division the centrosommes of the newborn hair cells are located in opposite poles. However, centrosomes have their final location on the opposite side of the cell, where the kinocilium will be located in the fully differentiated hair cell. This could be due to either centrosome migration inside the cell or cell rotation. Here I describe a previous unknown behavior by which sibling hair cells rotate on the plane of the epithelium over their contact point. Whether planar cell inversions account for the establishment of hair cell polarity and therefore the maintenance of bilateral symmetry in the neuromasts remains unknown. The combination of the *Tg(Et4;cldnb:lynGFP)* lines with a red fluorescent marker fused to centrine would allow to follow centriole movement during hair cell development and regeneration and understand how bilateral symmetry is established at the cellular level.

The observation that upon ablation of the entire hair cell population the first pair of newborn hair cells is properly oriented suggests that polarity establishment does not depend on the presence of mature hair cells that would instruct newborn hair cells to orient along the same axis. However how sibling hair cells affect each other polarity remains unknown. The

ablation of one sister hair cell just upon UHCP division would allow to ask for any crosstalk between newborn hair cell by which polarity is defined.

Planar Cell Polarity and Hair Cell Polarity

The organization of the sensory epithelium in the mammalian inner ear is disrupted in several Planar Cell Polarity (PCP) mutants (Curtin et al., 2003; Montcouquiol et al., 2003), however not all PCP mutants seem to have planar defects in the ear unless when combined with mutations in family related members: *fz3;fz6* double mutants and *dvl1;dvl2* double mutants have a disrupted sensory epithelium (Wang et al., 2005; Wang et al., 2006) while single mutants for each individual gene show a normal PCP, suggesting some level of redundancy between PCP elements. The zebrafish *trilobite* mutant lacks the PCP *vangl2* gene. In this mutant condition UCHP division and differentiation in the polar compartments does not seem affected, new born hair cells show disrupted hair cell polarity (Lopez-Schier and Hudspeth, 2006). How do mutations in other PCP components affect hair cell polarity in the zebrafish lateral line and which disturbed cellular processes underlie the disruption of the epithelium organization? It has recently been shown that PCP dependent cell adhesion underlies the coordinated organization of progenitor cells in the zebrafish laterality organ (Kupffer's vesicle, KV) (Oteiza et al., 2010), providing a clear example of the need of a precise control of progenitor cells during vertebrate organogenesis. The KV is the first organ to be formed in the zebrafish embryo and whose function, in a similar fashion to its mouse homolog, the ventral node, relies on the presence of polarized ciclia to regulate the extracellular flow of Nodal by which laterality of asymmetric gene expression and consequent organ chirality is established (Essner et al., 2005) .By inhibiting the PCP components *wnt11* and *pricle1a*, Oteiza *et al* showed that the Kupffer's vesicle progenitor cells show reduced cell-cell adhesion during vesicle formation, which results in impaired convergence and organization of the progenitor

cells. As a consequence, misshapen vesicles with shortened cilia are formed, strongly affecting the organ functionality. Does PCP signaling regulate cell adhesion in the zebrafish lateral line neuromasts? In particular, is the localization of UCHP's in the polar compartment mediated by PCP dependent cell adhesion? Additionally how do planar cell inversions account for the establishment of hair cell polarity and how is this novel cellular behavior regulated? I foresee the possibility that the asymmetric distribution of PCP elements in the newborn hair cells might instruct their polarity and regulate its establishment by controlling planar cell inversions as a result of deferential cell-cell adhesion between newborn hair cells and the surrounding supporting cells. Understanding the role of planar cell inversions in the establishment of hair cell polarity and the characterization of this behavior in different PCP mutants with defective hair cell polarity might corroborate this hypothesis.

Brg1 activity is needed for the development of a functional lateral line system

During lateral line development, neuromast cells undergo a developmental program that involves specification, survival, and differentiation of both hair and supporting cells. Hair cells specification and differentiation is associated with the expression of transcription factors of the pro-neural class such as *atoh1* and *neuroD* (Itoh and Chitnis, 2001; Sarrazin et al., 2010). Though *yng* mutants are able to differentiate hair cells, their production is strongly compromised and the sensorial epithelium is not properly polarized. Consistent with our results is the observation that the expression of several downstream pro-neural genes, including *atoh2a*, and *neurod2,* is significantly suppressed in *yng* mutants, as revealed by whole embryo factorial microarray analysis at 52 hpf (Leung et al., 2008).

It has been shown that Notch compartmentalization regulates hair-cell production in the pLLp and maintains the neuromast functional epithelial mirror symmetry by restricting hair-cell progenitor differentiation to Notch

free compartments (Wibowo et al., 2011). Additional studies addressing the role of *brg1* in regulating the expression of Notch signaling elements and the proliferative capacity of hair-cell progenitors are needed to dissect the role of *brg1* in the homeostasis of a functional lateral line.

The role of *brg1* in the morphogenesis of the lateral line

brg1 is an important modulator of transcription regulation. Not surprisingly, we show that Brg1 activity is essential for the proper morphogenesis of the lateral line by affecting multiple cellular events. We provide evidence that Brg1 activity is needed to maintain progenitor cells at the leading edge of the primordium. If *brg1* is needed to specify or maintain progenitor identity remains unknown. It has recently been shown that progenitor cell identity is regulated by Wnt signaling through Lef1 activity. We could not find evidence for disrupted *lef1* expression in *yng* mutants at early stages of migration (26 hpf). However we found that, at the same stage, *axin2*, a downstream target of Wnt signaling, and itself a negative regulator of Wnt activity, was not expressed in the pLLp of yng mutants. This shows that, at this stage of development, an *axin2* independent mechanism restricts *lef1* expression in the leading tip cells. The Wnt effector genes *tcf7l1a* and *tcf7l1b* are expressed in the trailing domain on the pLLp. It has been proposed that Tcf7l1a and Tcf7l1b activity could be responsible for the establishment of the boundary between leading and trailing zones by inhibiting Wnt signaling in the trailing zone (Valdivia et al., 2011). Further studies addressing the expression of *tcf7l1a* and *tcf7l1b* in *yng* mutants and their function in the pLLp will help in understand how *brg1* is required in the regulation of Wnt signaling during lateral line morphogenesis. Another possibility is that *brg1* regulates the maintenance of progenitor cells in the leading front of the primordium by regulating cellular adhesion, as there is evidence that *brg1* is required for the expression of cell-adhesion proteins (Reisman et al., 2009). *cadherin2*, is expressed in the leading region of the primordium (Kerstetter et

al., 2004; Matsuda and Chitnis, 2010), and its downregulation leads to the development of a truncated lateral line with neuromasts more closely spaced. Further studies addressing the ex pression of *cadherin2* in *yng* mutants might help corroborating this hypothesis.

SWI/SNF complexes and lateral line morphogenesis

SWI/SNF complexes are fundamental players in the regulation of an extensive number of often unrelated pathways and not surprisingly their misregulation has been associated with cancer development, in particular with the loss of *brg1* and *brm* occurring in 20% of bladder, colon, breast, melanoma and other cancers (Glaros et al., 2008; Reisman et al., 2009; Reisman et al., 2003; Roberts and Orkin, 2004). SWI/SNF complexes have then been recognized for their role in tumor suppression. Additionally *brg1* has been shown to be a critical regulator of the tumor suppressor gene *p53*, supporting a role for *brg1* in the control of cell proliferation (Naidu et al., 2009). However, SWI/SNF complexes have also been described as positive regulators of the cell cycle with distinct subsets of SWI/SNIF complexes showing opposing roles in cell-cycle, control dependent on the their Arid family subunit composition. Arid1A containing complexes are involved in cell-cycle repression while Arid1B is a determinant of cell proliferation (Nagl et al., 2007). It will be interesting to indentify which SWI/SNF complexes are recruited in the pLLp during lateral line development and in particular how they account for the regulation of progenitor cell maintenance/identity and proliferation.

Making sense of the *yng* mutant

We show that in the lack of Brg1 activity leading cells are not retained in the front of the primordium, being prematurely incorporated in the proneuromasts. *yng* mutant primordia show an uncoordinated migration between tip and trailing cells. Additionally, as the primodium stalls during

migration, primodial cells do not maintain their relative position, with trailing cells eventually moving to the leading front of the primordium. Why does the primordium stalls in *yng* primordia? And how is the primordium able to resume its migration. We found that the *cxcr4b* receptor was strongly downregulated in *yng* mutants. Whether Brg1 regulates *cxcr4b* directly or indirectly remains unknown. However the maintenance of *cxcr4b* expression suggests the maintenance of a Brg1-non-mediated *cxcr4b* transcription. Can the staling behavior be a consequence of the reduced *cxcr4b* expression?

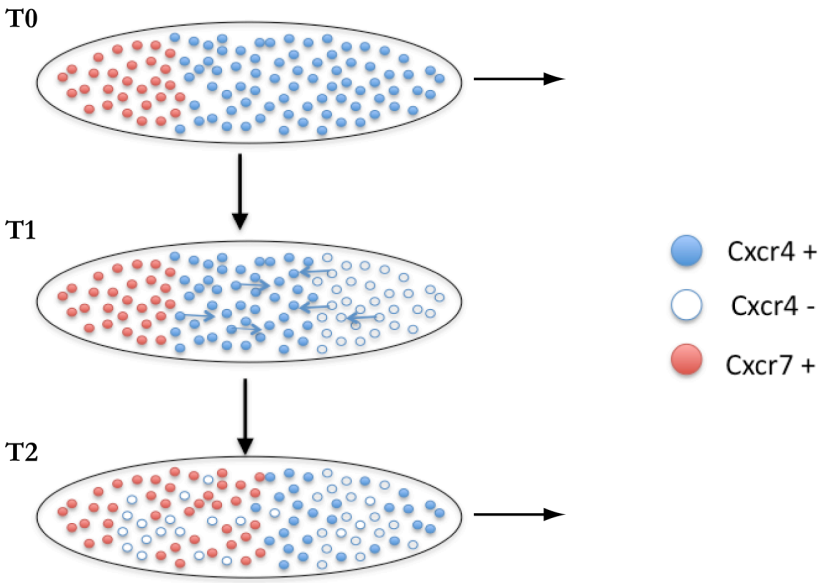

Figure 11. Proposed model
The movement of a few trailing Cxcr4b positive cells to the leading edge would be able to resume primordium migration.

Receptor endocytosis upon ligand binding is a widespread mechanism by which degradation, recycling, localization and availability of the receptor at the cell surface can be controlled, by which signaling activity can be regulated. Additionally, the activation of Cxcr4b as been show to induce its own transcription, acting as a positive feedback loop, assuring the turnover of the receptor at the cell membrane (Helbig et al., 2003). Therefore, an inefficient positive feedback loop and/or defective sorting of the receptor in

the recycling or degradative pathways is likely to affect efficient receptor turnover. It is possible that the staling behavior results from a deficient receptor turnover due to reduced Brg1-mediated *cxcr4b* transcription. This would decrease the availability of the receptor at the cell membrane, downregulating Cxcr4b dependent signaling activity and, as a consequence, the primordium would stop migrating. It as been suggested a differential activation of Cxcr4b upon Sdf1a binding across the pLLp, with higher activation at the leading edge (Valentin, 2009). Therefore, *brg1* mutant trailing cells are more likely to have available Cxcr4b at the cell membrane. At this stage, the movement of a few trailing cells to the leading edge would be able to resume primordium migration (Figure 11). Consistent with this possibility is the observation that as few as four wild-type cells at the leading tip can rescue the migration of *cxcr4b*-deficient pLLp. The movement of trailing cells to the front of the primordium further helps understanding why in primordia where leading cells were photoconverted at the beginning of migration, non-photoconverted cells are found at the leading tip at latter stages. This occurs because as leading progenitor cells are incorporated in the proneuromasts, more rostral non-photoconverted cells move to the leading tip.

A standing question is why in our mosaic clone analysis, lateral line morphogenesis is not restored in *yng* mutants. This observation suggests that Brg1 might be needed not only in the leading cells but also in the trailing cells, where it is also expressed. Supporting this hypothesis is our observation that the Estrogen Receptor 3 (*esr3*), which is expressed in the trailing domain of the pLLp and absent from the leading domain, is strongly downregulated in *yng* mutants (data not shown). In the zebrafish retina brg1 acts in a non-cell-autonomous manner (Link et al., 2000). While our results do not fully support a non-cell-autonomous requirement for *brg1* in the pLLp, they suggest this can be the case. A non-cell autonomous requirement can be rescued by the presence of wild-type cells in tissues where the ratio of mutants cells is low. If at higher number, the mutant cells might impose the

mutant phenotype on the surrounding wild type cells and rescue is not achieved. . Further studies addressing the role of *brg1* in the leading and trailing domains of the pLLp and mosaic clone analysis with a higher contribution of wild-type cells in *yng* pLLp, as well as clonal analysis of *brg1* mutant cells in wild-type primordia will help in understanding our results.

Making use of Brg1

Due do its nature as part of a chromatin remodeling complex Brg1 is a good candidate to use in Co-Ip and Chip-Seq, which would allow the identification of both transcription factors and their downstream targets. Due to the reduced size of the primordium, roughly 100 cells, the success of such a strategy depends on the capacity to obtain enough biological material.

Another possibly is to perform a factorial microarray analysis designed for searching Brg1-regulated pLLp genes. The efficiency of such approach as recently been showed through the combined use of the *Tg(cldnb:lynGFP)* larvae, fluorescence activated cell sorting and microarray analysis, by which a repertoire of genes expressed in the migrating primordium were indentified (Gallardo et al., 2011). This would aid in better understanding the role or *brg1* and the genetic regulatory circuits that control lateral line morphogenesis.

Conclusions

From chapter 1:

- The mitotic division of UHCPs is essential for hair cell regeneration.
- Hair-cell regeneration anisotropy and bilateral symmetry are functionally linked in the zebrafish lateral line neuromasts. Bilateral symmetry is sustained by compartmentalized Notch activity, which governs regeneration anisotropy by permitting the stabilization of UHCP identity in the polar compartments.
- Regeneration anisotropy is not due to a localized stem-cell population. Our results provide evidence that prospective UHCP's do not originate from a specific location in the neuromast. Therefore, polar compartments are not stem-cell niches, on the contrary, these compartments represent an environment that opposes a niche to permit the differentiation of UHCPs.
- Centrifugal movement of hair cells propagates planar polarity horizontally. Although hair-cell regeneration remains strongly anisotropic, the macula eventually expands symmetrically. Our data supports a model by wich planar polarity is likely to propagate symmetrically because mature hair cells move away from the midline towards the periphery of the neuromast.
- The orientation of UHCPs divisions is dispensable for bilateral symmetry.

From chapter 2:

I demonstrated a previously unreported role for *brg1* during mechanosensory organ formation in the zebrafish. I show that:

- *brg1* mutant primordia develop a truncated lateral line system
- In the lack of Brg1, primordial cells are unable to coordinate their migratory behavior and the pLLp migrates aberrantly.

- Brg1 activity is required to maintain progenitor cells in the leading tip and for the regulation of proliferation in the pLLp, and therefore for its homeostasis.
- *brg1* mutant primordia show a delayed rosette formation and maturation
- Brg1 activity is essential for the development of a functional lateral line as *yng* mutants neuromasts bore a reduced and deficiently polarized sensorial epithelium.

Materials and Methods

Fish maintenance, transgenic and mutant strains

Fish were maintained under standard conditions and experiments were performed in accordance with protocols approved by the PRBB Ethical Committee of Animal Experimentation. Eggs were collected from natural spawning and maintained at 28ºC and staged according to Kimmel et al. (Kimmel et al., 1995)

Table 1. Zebrafish transgenic lines used

Zebrafish	Note	Publication
Tg(SqET4)	Enhancer trap line with EGFP expression under the control of the *atp2b1a* gene promoter marking UHPC's and mature hair cells of the the zebrafish lateral	Parinov *et al.,* 2004
Tg(SqET20)	Enhancer trap line with EGFP expression in interneuromast cells and in the neuromast supporting cell population, with stronger expression in the external mantle cells and showing areas with low levels of green fluorescence located at both poles of a line perpendicular to the neuromast's axis of planar cell polarity	Parinov *et al.,* 2004; Hernández *et al*, 2007.

Tg(cldnb:lynEGFP)	8 kb cldnb promoter driving the expression of lynEGFP in all cells of the migrating pLLP, whose expression is retained in the interneuromast cells and in deposited neuromast.	Haas & Gilmour, 2006
Tg(atoh1a:tdTomato)	The *Tg(atoh1a:tdTomato)* line was constructed from the zC247L22 BAC and dTomato cDNACell	
Tp1(bglob:hmgb1-mCherry)	A *tp1blgob* element consisting of 6 copies of the TP1 promoter (12 Rbp-Jκ binding sites), upstream of the rabbit β-globin minimal promoter drives the expression of *mCherry*.	Parsons et al., 2009
Tg(hsp70:Gal4;UAS:Nicd-myc)		A gift from P. Chapouton; Scheer and Campos-Ortega, 1999

Heat-shock treatments

All embryos obtained from crossing heterozygous transgenic fish carrying the hsp70 promoter were incubated at the desired developmental stage at 39 °C for 30 min in groups of 30-40 embryos in 2 ml eppendorf tubes

containing a total volume of 1000 µl E3 fish medium. Upon incubation embryos were returned to petri dishes containing E3 fish medium at 28°C where they recovered till fixation at the desired time point.

Morpholinos

All morpholinos used in this study were diluted in sterile miliQ water and were prepared and injected at 1 cell stage embryos.

Table 2. Morpholino oligos that are used in this thesis.

Morpholinos	Sequences	Concentration	Source
Brg1Mo1	5'-CATGGGTGGGTCAG GAGTGGACATC-3'	30µM	Balak et al 1990; Greegg et al 2003
Brg1Mo2	5'-CTCAGCAGAGCCAGA AGTGAGAGGC-3'	30µM	Gregg *et al*, 2003

Whole-mount *in situ* hybridization

High resolution in situ hybridization (ISH) to whole-mount zebrafish embryos (modified from (Thisse and Thisse, 2008)

A - Probe synthesis .

Component	Amount per reaction	Final
Linear Template DNA	2.5µl	100-200 ng
5x Transcription buffer	1µl	1X
DTT 0.1M	0.5µl	10 mM
DIG-RNA labeling mix (UTP)	0.5 µl	
RNASEin (40U/µl)	0.25 µl	10 U
T3 or T7 RNA polymerase (20U/µl)	0.25 µl	5U

1. Mix and incubate 2 hours at 37°C. Add 2 µl RNAse free DNAse I and 18 µl sterile water.
2. Mix and incubate for 30 min at 37°C.
3. Stop the reaction by adding 1 µl sterile 0.5 M EDTA and 9 µl sterile water.
4. Place a Sigmaspin Post Reaction Purification column on top of a microfuge tube. Centrifuge 15 sec at 750 g.
5. Break the base of the column and discard lid. Spin 2 min at 750 g.
6. Place the column on a new microfuge tube. Add the RNA template on top of the resin.

7. Centrifuge 4 min at 750 g. Discard the column and test 1µl on an agarose gel.
8.

B – Embryo / Larva collection, chorion removal, fixation, storage

1. Collect the eggs. Incubate the eggs at 28.5°C in Petri dishes containing E3 fish medium until the desired developmental stage is reached. If post-gastrulation stages are to be examined, the formation of melanin pigmentation can be prevented by replacing the regular E3 fish medium with 0.0045% 1-Phenyl-2-Thiourea (PTU) solution prepared in E3 medium at the end of gastrulation. For larva and embryos older than 24 hours post fertilization (hpf) change this medium once a day.
2. Dechorionate embryos of the appropriate developmental stage(s) and fix in 4% paraformaldehyde in PBS overnight at 4°C in groups of 30 embryos per eppendorf tube in a rolling wheel.
3. Dehydrate the embryos in 100% methanol for 15 min at room temperature.
4. Place the eggs at -20°C in 100 % methanol for at least two hours before use. Embryos can be kept at -20°C in methanol for several months.

C – In situ hybridization

Step 1: Embryos rehydratation

1.	1 x 5 min	100% Methanol
2.	1 x 5 min	75% Methanol -25% 0,1%PBST
3.	1 x 5 min	50% Methanol -50% 0,1%PBST
4.	1 x 5 min	25% Methanol -75% 0,1%PBST
5.	3 x 10 min	0,1%PBST

Step 2: Embryos permeabilization

1. Digestion with proteinase K (PK). Final solution at 10 µg/ml in PBT (test appropriate time for every new batch of PK)

For embryos at 75 % epiboly (Gastrula)	0 - 30 sec
For embryos from 5-6 somites (ES)	1 min
For embryos from 18-20 somites (MS)	3 min
For embryos of 24 h	10 min
For embryos of 36 h	20 min
For embryos of 48 h and later	30 min

2. Postfixation (stop the proteinase K digestion) for 20 min in 4% PFA-PBS
3. Washes:
   - 3 x 10 min in 0,1%PBT
4. Transfer embryos into 2 ml sterile eppendorf tubes

Step 3: Embryos prehybridization

Incubation from 2 to 5 hours at 65°C in 0.5 to 1 ml of hybridization mix (HM). For 50 ml of HM:

	Volume	Final
Formamide	25,0 ml	50% formamide
20 x SSC	12,5 ml	5 x SSC
Heparin 5 mg/ml	0,5 ml	50 µg/ml
tRNA 50 mg/ml	0,5 ml	500 µg/ml
Tween 20 20%	0,25 ml	0,1%

Acide citrique 1M	0,46 ml	-> pH 6
H_2O	to 50 ml	

Possible storage in HM for weeks at -20°C or at + 4°C for one day

Step 4: Hybridization

Add the antisense DIG labeled RNA:

1. Remove the HM used for the prehybridization and replace with 200 µl of HM containing 30 - 100 ng of probe (1 - 2 µl of probe synthesis)
2. Incubate O/N at 65°C in a water bath

Step 5: Probe Removal

1. 1 x quickly with HM (without tRNA and heparin) at 65°C
2. 10 min 75% HM + 25% 2xSSC at 65°C
3. 10 min 50% HM + 50% 2xSSC at 65°C
4. 10 min 25% HM + 75% 2xSSC at 65°C
5. 10 min in 2xSSC at 65°C
6. 30 min in 0.2 x SSC at room temperature (RT)
7. 10 min 75 % 0.2xSSC + 25% 0,1%PBST at RT
8. 10 min 50 % 0.2xSSC + 50% 0,1%PBST at RT
9. 10 min 25 % 0.2xSSC + 75% 0,1%PBST at RT
10. 10 min 0,1%PBST at RT

Step 6: Preincubation of embryos for Antibody labeling

Incubate embryos from 2-4 hours under agitation in Blocking Solution (BSA 2 mg/ml - 2% Sheep serum in 0,1%PBST)

Step 7: Incubation with Alkaline phosphatase anti DIG/Fluorescein antibody

Dilute the correspondent Antibody 1/5,000 - 10,000 in 500 µl of Blocking Solution and incubate overnight at 4°C with agitation

Step 8 – Washes/labeling reaction

Washes (remove unbound Antibodies)

1. Quick wash in 0.1%PBT at RT
2. 6 x 15 min in 0.1%PBT at RT under gentle agitation
3. 3 x 5 min at room temperature in alkaline tris buffer

Alkaline Tris buffer :

	Volume	Final
Tris HCl pH 9,5 1M	10 ml	100 mM
MgCl2 1	5 ml	50 mM
NaCl 5M	2 ml	100 mM
Tween 20 20%	0,5 ml	0,1%l
H2O	to 50 ml	

Labeling

Move the embryos to 12 well plates and replace the alkaline tris buffer with 2ml of labeling mix freshly prepared. Let the reaction occur in the dark, looking under a dissecting scope every 15 min for the first hour then every ½ h or 1hour after the first hour of reaction.

Stop the reaction by replacing the labeling mix with PBS pH 5,5 EDTA 1 mM (3 washes, 1 quick and 2 under gentle agitation) and store at 4°C in PBS pH 5,5 EDTA 1 mM in the dark (labeled embryos can be kept for years).

For imaging wash embryos 3x 10 min in 0,1%PBST with the last wash with DAPI diluted 1/500 to better identify the primordium and neuromasts boundaries when imaging. Transfer the embryos to 100% glycerol and store at 4ºC. This can be achieved by filling a 2ml eppendorf with 1ml of glycerol and gently transfer the embryos in the minimum amount of PBST to the

glycerol's surface. The embryos will get incorporated in the glycerol during the next 48 hours after which the PBST at the surface should be removed.

Labelling mix :

225 µl NBT + 50 ml Alkaline Tris buffer + 175 µl BCIP

Stock Solutions :

NBT: 50 mg Nitro Blue Tetrazolium dissolved in 0.7 ml de N,N-dimethylformamide anhydrous and 0.3 ml of water (store at -20°C)

BCIP : 50 mg of 5-Bromo 4-Chloro 3-indolyl Phosphate dissolved in 1 ml of N,N-dimethylformamide anhydrous (store at -20°C)

Step 9: Mounting

To mount the embryos, 3 (for embryos after 24 hpf) or 4 (for embryos before 24h) cover slips of thickness are glued together using a drop of super glue (cyanoacrylate) to make a bridge. A drop of glycerol containing the embryo is placed in the middle of the slide between two cover slips bridges and covered with a larger cover slip (24 x 40 mm).

Whole-mount fluorescent *in situ* hybridization

Modified from **Zebrafish Whole Mount High-Resolution Double Fluorescent In Situ Hybridization**, Tim Brend and Scott A. Holley Department of Molecular, Cellular and Developmental Biology, Yale University

Steps 1 to 3 are equal to the previously described Chromogenic ISH

Step 4: Hybridization

1. Remove all but 50 µl of the preHYB, but make sure to keep the embryos completely submerged.

2. Add 1-2 μl of each riboprobe (digoxygenin- and fluorescein-labeled riboprobes) to the embryos and mix by gently flicking the tube. The amount of probe is typically 1-2μl from a 20μl probe synthesis reaction. Given that fluorescein is light-sensitive, the tubes should be wrapped in aluminum foil or otherwise exposed to minimal light from this point forward.
3. Incubate the embryos overnight at 65 °C.

Step 5: Probe Removal

Note that the solutions from this point forward lack detergent. Elimination of detergent appears to help the staining reactions but does cause the embryos to become rather sticky. Remove the riboprobe.

1. Wash 1 x 30 min at 65 °C in HYB-.
2. Wash for 15 minutes at 65 °C in 75% HYB-/25% 2xSSC.
3. Wash for 15 minutes at 65 °C in 50% HYB-/50% 2xSSC.
4. Wash for 15 minutes at 65 °C in 25% HYB-/75% 2xSSC.
5. Wash for 15 minutes at 65 °C in 2xSSC.
6. Wash for 30 minutes 65 °C in 0.2 x SSC.

Step 6: Anti-Fluorescein antibody incubation

1. Block for at least 1 hour at RT in 500μl of a solution of 1x maleic acid buffer plus 2% blocking reagent (see reagents section).
2. Add the anti-Fluorescein-POD antibody, as supplied by Roche, at a 1:500 dilution in the blocking solution.
3. Incubate overnight at 4°C. During this incubation lay the eppendorf tube on its side.
4. Wash 4 x 20 minutes in 1x maleic acid buffer. Wash twice for 5 minutes each in PBS.

Step 7: Detection of the fluorescein-labeled probe

1. Incubate 30-60 minutes in TSA Plus Fluorescein Solution. (Spin down TSA substrate before making staining solution. For the reaction, dilute tyramide reagent 1:50 in Perkin Elmer amplification diluent buffer.) During this incubation lay the microcentrifuge tube on its side. Reaction time must be determined empirically for each probe. Unfortunately, the staining reaction cannot be visually monitored as the substrate is fluorescent, and one will see ubiquitous green fluorescence throughout the staining reaction.
2. Wash for 10 minutes each in 30%, 50%, 75% and 100% methanol in PBS.
3. Incubate in a solution of 1% H202 in methanol for 30 minutes to inactivate the first peroxidase.
4. Wash 10 minutes each in 75%, 50% and 30% methanol in PBS. Then wash twice for 10 minutes each in PBS. It is important that all of the methanol be removed.

Step 8: Anti-digoxygenin antibody incubation

1. Block the embryos again for at least 1 hour at RT in a solution of 1x maleic acid buffer plus 2% blocking reagent.
2. Add the anti-DIG POD antibody as supplied by Roche at a 1:1000 dilution in above blocking solution
3. Incubate overnight at 4^{o}C. During this incubation lay the eppendorf tube on its side.
4. Wash 4 x 20 minutes in 1x maleic acid buffer. Wash twice for 5 minutes each in PBS.

Step 9: Detection of the digoxygenin-labeled probe

1. Incubate 30-60 minutes in TSA Plus Cy5 Solution (Spin down TSA substrate before making staining solution. For the reaction, dilute the

tyramide reagent 1:50 in amplification diluent buffer). During this incubation lay the microcentrifuge tube on its side. Reaction time must be determined empirically for each probe.

2. Wash three times for 10 minutes each in PBST with the last wash with DAPI diluted 1/500.

Step 10: Mounting

1. Incubate the embryos for 10 minutes each in 25% and 50% glycerol in PBST. Clear overnight in 75% glycerol at 4°C.
2. The yolk can produce significant background fluorescence and therefore embyros should be deyolked before flat mounting them on a microscope slide.

Fish imaging

For whole-mount ISH, embryos were mounted in 100% glycerol and photographed on an Olympus BX61 microscope using a 20X dry objective with transmission light. Whole embryo images were acquired on a Leica MZ10 stereomicroscope. Fluorescent images were acquired using either a Leica SP5 or SPE or an Andor microscope using 10X and 20X dry objective or 40X and 60X oil immersion objective. Images were processed using Imaris and/or ImageJ software packages, and assembled with Adobe Photoshop CS2 and Adobe Illustrator CS2. For time-lapse imaging, staged and dechorionated embryos were anesthetized with 0,02% tricaine and mounted in 1% low-melting-point agarose on a glass-bottom culture dish (MatTek). Z-stack series were aquired every 2-10 min intervals. All movies were processed using Imaris and ImageJ software.

Notes on the tyramide signal amplification

Alexa-Tyramide substrates stain well using the Perkin Elmer amplification diluent buffer, but using the staining buffer provided with the

Invitrogen/Molecular Probes Kits. Additionally Cy5 fluorescence is eliminated by subsequent Methanol/H2O2 treatment while fluorescein and Alexa-647 are unaffected. Cy3 may also be adversely affected by the Methanol/H2O2 treatment as it is structurally related to Cy5. For this reason, Cy3 and Cy5 TSA reactions should only be used for the second staining reaction in a double fluorescent in situ protocol.

Cell cycle inhibitor treatments

Compounds for cell cycle inhibitors were used as described before (Murphey *et al.,* 2006). Larva were treated for the desired period with the drugs described in table 2 dissolved in E3 medium with 1% DMSO at 28.5ºC medium. Zebrafish strains used were SqET4 and *Tg(Brn3c:GFP)* to quantify the number of hair cells. For statistical analysis, at least 10 larvae were used and around 70 neuromasts were analyzed. For time-lapse confocal microscopy larvae were mounted in 1% low melting point agarose (see Imaging procedures).

Table 2. Minimum effective doses of known cell cycle inhibitors.

Compunds	NIH3T3 cells	AB9 cells	Zebrafish embryos	Zebrafish larvae
Aphidicolin (DMSO)	7.4 μM	7.4 μM	259 μM	100 μM
Genistein (DMSO)	47 μM	93 μM	93 μM	25 μM
Nocodazole (DMSO)	150 nM	ND	150 nM	150 nM

Mimosine (10% $NaHCO_3$)	200 μM	200 μM	-2000 μM	-2000 μM
Okadeic acid (DMSO)	0.06 μM	6 μM	-6 μM	-6 μM
Taxol (DMSO)	10 μM	10 μM	-100 μM	-100 μM
Colchicine (H_2O)	200 μM	ND	1000 μM	1000 μM

* All compounds were purchased from Calbiochem (San Diego, CA, USA)

Neomycin treatments

Zebrafish larvae were treated in E3 fish medium containing 250μM neomycin for 45 minutes at room temperature. After treatments larvae were washed several times with E3 fish medium using a small diameter strainer to wash out residual neomycin. Larvae were allowed to recover from the neomycin treatment for 2 hours before live imaging and/or treatment with other drugs to avoid high mortality.

DAPT treatments

(adapted from Geling *et al.,* 2002)

1. Prepare 10 mM DAPT stock solution in 100% DMSO.
2. Dechorionate embryo or larvae.
3. Set up the treatments and control solutions. Add the DAPT stock solution into E3 medium to get 50-100 μM final solutions. NOTE: DAPT will precipitate if not warmed at RT.
4. Swirl dishes to thoroughly mix.

5. Transfer embryo or larvae to the treatment dishes and incubate until the desired developmental stages.
6. Wash briefly and fix embryo or larvae in 4% PFA overnight at 4°C. For time lapse movies, mount larvae in 1% low melting point agarose in the presence of a 10 μM DAPT solution and 0,02% tricaine.

Vital Dye, Phalloidin and Alkaline phosphatase stainings

Vital Dye

For vital labeling of the hair cells zebrafish larvae were immersed in 5 μg/ml of DiAsp (Invitrogen, Carlsbad, CA, USA) in E3 medium for 5 minutes at room temperature and then washed several times to remove the excess of dye.

Phalloidin staining

For phalloidin staining, samples were fixed in 4% PFA overnight at 4°C then washed several times in 0.1% PBST and incubated in phalloidin-Alexa 568 or Alexa 488 (Invitrogen) diluted 1:20 in 0.1% PBST overnight at 4°C. Samples were washed several times in 0.1% PBST before being mounted in Vectashield Mounting Medium (Vector Laboratories).

Alkaline phosphatase staining

Zebrafish larvae were fixed in 4%PFA for 1-4 hours at RT after which they were washed 3X for 10 minutes in 0,1% PBST. They were finally stained in a staining buffer solution (see procedure above for Alkaline Tris buffer) for *in situ* hybridization. Reaction time can vary from sample to sample, from 1 minute to 15 minutes. The reaction was stopped by washing 3X for 10 minutes in 0,1% PBST and the larvae stored at 4°C.

Whole mount assay for cell proliferation

Dechorionate embryos of the desired stage and incubate in 10mM BrdU, made up in Embryo Medium with 15% DMSO at 6 to 8 degrees for 20 minutes by putting the petri dish resting on top of ice.

1. Allow embryos to develop to the desired age.
2. Fix in 4% PFA, several hours at RT, or ON at 4ºC.
3. Remove PFA, wash embryos 2X in 100% methanol. Store the embryos in fresh methanol at -20ºC for at least overnight. Embryos can be stored Indefinitively at -20°C.
4. Rehydrate using a graded Methanol/PBST series: 75%, 50%, 25% and wash 3x10 min in 0,1%PBST.
5. Incubate at RT in 2N HCl for 1 hour.
6. Rinse 3 x 10 minutes in 0,1%PBST.
7. Incubate at least 2 hours in BRDU blocking solution, rocking or shaking gently.
8. Incubate 4 hours, or more (RT), in anti-BrdU, 1:150, (or ON at 4ºC), rocking or shaking gently.
9. Rinse several times, then wash 4 x 30 min each in 0,1%PBST rocking or shaking gently.
10. Incubate at least 2 hours in blocking solution, rocking or shaking gently.
11. Incubate 2 hours or more with the appropriate fluorescent labeled secondary antibody 1:150 in 0,1%PBST (or ON at 4ºC).
12. Rinse several times, then wash 4 x 30 minutes each in 0,1%PBST rocking or shaking.
13. Store embryo or larvae in 0,1%PBST plus mounting medium, Vectashiled with or without DAPI.

Reagents

- PBS-D-Tw: PBS + 1% DMSO + 0.1% Tween-20
- 4% PF: 4% paraformaldehyde, 50 mM NaPO4, pH 7.4.
- 10mM BrdU: made up in embryo medium with 1% or 15% DMSO according to the stages of the embryos or larvae.
- 2 N HCl, in water.
- 10 mg/ml proteinase K stock.
- Anti-BrdU antibody and appropriate secondary antibody and detection system.
- Blocking Solution: PBST + 1% BSA + 2% Normal Goat Serum.

Tunel Assay

Step 1: Fixation

1. Fix embryos overnight at 4°C in 4% paraformaldehyde (PFA) in PBS.
2. Remove PFA and wash 3 x 10 minutes in 0,1%PBST RT.
3. Manually dechorionate embryos in PBS in a glass depression plate using watchmaker forceps. After dechorionation, embryos are transferred using a fire-polished glass Pasteur pipette as they may stick to polypropylene pipettes.
4. Transfer embryos through a series of 25%, 50% and 75% methanol in PBS for 5 minutes each.
5. Replace liquid with 100% methanol, incubate 5 minutes and then replace with fresh methanol.
6. Place embryos at -20°C for a minimum of one hour. (Better if overnight.)
7. Wash embryos for 5 minutes each in 75%, 50%, 25% methanol in 0,1%PBST at RT. Wash twice for 5 minutes each in 0,1%PBST at RT.

Step 2: ProteinaseK treatment and Postfixation

1. Digest with proteinase K (10 μg/ml in 0,1%PBST) at RT for 20 minutes

to permeabilize the embryos. (The incubation time depends on the age of the embryos as younger stages are more sensitive. It also depends on the batch of enzyme.) For somitogenesis stage embryos permeabilize for 3-4 minutes and for larvae stages permeabilize for 20 min. During this incubation lay the microcentrifuge tube on its side.

2. Rinse briefly in 0,1%PBST and wash once for 5 minutes in 0,1%PBST.
3. Fix again for 20 minutes in 4% PFA in 0,1%PBST at RT.
4. Wash twice, for 5 minutes each, in 0,1%PBST at RT.

Step 3: Tunel reaction mix

1. Incubate embryos for 60 minutes in TUNEL buffer at RT.
2. Replace TUNEL buffer with TUNEL reaction mix, a 9:1 ratio of TUNEL buffer-TUNEL enzyme for 3 hours at 37°C in darkness. For a positive control: incubate embryos with DNase solution (1 µl DNase, 5 µl DNase buffer, 44 µl miliQ for 15 min at 37°C). Rinse briefly in 0,1%PBST and wash once for 5 min in 0,1%PBST. Incubate embryos in TUNEL reaction mix. For a negative control: incubate embryos only in TUNEL buffer.
3. Wash embryos 2x 30 minutes in 0,1%PBST at RT with the last wash with DAPI 1:500 and store embryos in 0,1%PBST with vectashield at 4°C.

Whole mount antibody staining

1. Remove chorions for embryos older than 18 somites.
2. Fix embryos in 4% formaldehyde in PBS 1-2 hours 25°C, or overnight 4°C.
3. Dechorionate embryos that are younger than 18 somites.
4. Transfer the embryos to 100% methanol and store them overnight at 20°C, or for longer period.
5. Rehydrate embryos for 5 minutes each in 75%, 50%, 25% methanol in

0,1%PBST at RT. Wash twice for 5 minutes each in 0,1%PBST at RT.

6. Block in antibody blocking buffer (650 µL/tube; 10% sheep serum, in
7. PBS containing 0.5% BSA, and 1% DMSO (optional)) for 2-4 hours at room temperature, or overnight at 4 °C with rocking agitation.
8. Dilute the primary antibody to desired concentration in antibody blocking buffer. Remove blocking buffer from embryos and replace with diluted antibody solution. Incubate overnight at 4 °C with rocking agitation.
9. Wash 5x 20 min in 0,1%PBST at RT.
10. Dilute secondary antibody 1/200 in 0,1%PBST. Remove blocking buffer from embryos and replace with diluted secondary antibody solution and incubate overnight at 4ºC.
11. Wash 5x 20 min in 0,1%PBST at RT and store in 0,1%PBST with Vectashield.

Reagents

Paraformaldehyde

10X PBS

Tween20

Primary antibody

Alexa-Fluor conjugated secondary antibody

BSA

DMSO (optional)

Methanol

Normal Sheep Serum (heat inactivated at 56 °C for 30 minutes)

Mounting embryos or larvae for time-lapse videomicroscopy

1. Prepare a 1% solution of low melting point agarose in Embryo Medium by heating in a boiling water bath or in a microwave oven. This solution remains liquid at 37-40ºC but quickly hardens when cooled.
2. Anesthetize the larvae in 0,02% tricaine in E3 medium and transfer them in a small drop of medium onto the imaging disk.
3. Cover the larvae with the low melting agarose and, using a fine hair mounted on a needle holder, position the embryo at the appropriate angle and allow the agar to harden.
4. After the agar hardens place 3 ml of E3 medium containing 0,02% tricaine over the agar block.

Kaede photoconvertion

The progeny of *Tg(cldnb:lynGFP)* fish was injected at the one-cell stage with 200 pg of Kaede mRNA. The Kaede fluorophore was photo-converted at 24 hpf using 405 nm laser and 60x objective in a Leica Sp5 system. Images were taken in an Andor System using a 40x objective.

Transplantations experiments

All host and Donor embryos expressed the *Tg(cldnb:lynGFP)*. Donor zygotes were injected with fixable rhodamine dextran (Invitrogen) at 1 cell stage. Host embryos were obtained from the cross of fish heterozygous for *Brg1*. Donor fish were obtained from wild-type crosses. Dechorionated donor and host embryos were mounted in an agarose transplantation chamber and 25-30 donor cells were inserted into the presumptive placodal domain of a shield-staged host embryo. All host embryos received donor cells in the left side, whereas the right side served as control.

References

Adler, H. J. and Raphael, Y. (1996). New hair cells arise from supporting cell conversion in the acoustically damaged chick inner ear. *Neurosci Lett* **205**, 17-20.

Aigouy, B., Farhadifar, R., Staple, D. B., Sagner, A., Roper, J. C., Julicher, F. and Eaton, S. (2010). Cell flow reorients the axis of planar polarity in the wing epithelium of Drosophila. *Cell* **142**, 773-86.

Alexandre, D. and Ghysen, A. (1999). Somatotopy of the lateral line projection in larval zebrafish. *Proc Natl Acad Sci U S A* **96**, 7558-62.

Aman, A., Nguyen, M. and Piotrowski, T. (2011). Wnt/beta-catenin dependent cell proliferation underlies segmented lateral line morphogenesis. *Dev Biol* **349**, 470-82.

Aman, A. and Piotrowski, T. (2008). Wnt/beta-catenin and Fgf signaling control collective cell migration by restricting chemokine receptor expression. *Dev Cell* **15**, 749-61.

Aman, A. and Piotrowski, T. (2009a). Cell migration during morphogenesis. *Dev Biol* **341**, 20-33.

Aman, A. and Piotrowski, T. (2009b). Multiple signaling interactions coordinate collective cell migration of the posterior lateral line primordium. *Cell Adh Migr* **3**, 365-8.

Aman, A. and Piotrowski, T. (2010). Cell migration during morphogenesis. *Dev Biol* **341**, 20-33.

Austin, C. P., Feldman, D. E., Ida, J. A., Jr. and Cepko, C. L. (1995). Vertebrate retinal ganglion cells are selected from competent progenitors by the action of Notch. *Development* **121**, 3637-50.

Axelrod, J. D. (2009). Progress and challenges in understanding planar cell polarity signaling. *Semin Cell Dev Biol* **20**, 964-71.

Baena-Lopez, L. A., Baonza, A. and Garcia-Bellido, A. (2005). The orientation of cell divisions determines the shape of Drosophila organs. *Curr Biol* **15**, 1640-4.

Baird, R. A., Steyger, P. S. and Schuff, N. R. (1996). Mitotic and nonmitotic hair cell regeneration in the bullfrog vestibular otolith organs. *Ann N Y Acad Sci* **781**, 59-70.

Baird, R. A., Torres, M. A. and Schuff, N. R. (1993). Hair cell regeneration in the bullfrog vestibular otolith organs following aminoglycoside toxicity. *Hear Res* **65**, 164-74.

Balabanian, K., Lagane, B., Infantino, S., Chow, K. Y., Harriague, J., Moepps, B., Arenzana-Seisdedos, F., Thelen, M. and Bachelerie, F. (2005). The chemokine SDF-1/CXCL12 binds to and signals through the orphan receptor RDC1 in T lymphocytes. *J Biol Chem* **280**, 35760-6.

Balak, K. J., Corwin, J. T. and Jones, J. E. (1990). Regenerated hair cells can originate from supporting cell progeny: evidence from phototoxicity and laser ablation experiments in the lateral line system. *J Neurosci* **10**, 2502-12.

Barker, N., Hurlstone, A., Musisi, H., Miles, A., Bienz, M. and Clevers, H. (2001). The chromatin remodelling factor Brg-1 interacts with beta-catenin to promote target gene activation. *EMBO J* **20**, 4935-43.

Barker, N., van Es, J. H., Kuipers, J., Kujala, P., van den Born, M., Cozijnsen, M., Haegebarth, A., Korving, J., Begthel, H., Peters, P. J. et al. (2007). Identification of stem cells in small intestine and colon by marker gene Lgr5. *Nature* **449**, 1003-7.

Barroca, V., Lassalle, B., Coureuil, M., Louis, J. P., Le Page, F., Testart, J., Allemand, I., Riou, L. and Fouchet, P. (2009). Mouse differentiating spermatogonia can generate germinal stem cells in vivo. *Nat Cell Biol* **11**, 190-6.

Becker, P. B. and Horz, W. (2002). ATP-dependent nucleosome remodeling. *Annu Rev Biochem* **71**, 247-73.

Beites, C. L., Kawauchi, S., Crocker, C. E. and Calof, A. L. (2005). Identification and molecular regulation of neural stem cells in the olfactory epithelium. *Exp Cell Res* **306**, 309-16.

Bermingham, N. A., Hassan, B. A., Price, S. D., Vollrath, M. A., Ben-Arie, N., Eatock, R. A., Bellen, H. J., Lysakowski, A. and Zoghbi, H. Y. (1999). Math1: an essential gene for the generation of inner ear hair cells. *Science* **284**, 1837-41.

Bianco, A., Poukkula, M., Cliffe, A., Mathieu, J., Luque, C. M., Fulga, T. A. and Rorth, P. (2007). Two distinct modes of guidance signalling during collective migration of border cells. *Nature* **448**, 362-5.

Boldajipour, B., Mahabaleshwar, H., Kardash, E., Reichman-Fried, M., Blaser, H., Minina, S., Wilson, D., Xu, Q. and Raz, E. (2008). Control of chemokine-guided cell migration by ligand sequestration. *Cell* **132**, 463-73.

Bourne, H. R. and Weiner, O. (2002). A chemical compass. *Nature* **419**, 21.

Brigande, J. V. and Heller, S. (2009). Quo vadis, hair cell regeneration? *Nat Neurosci* **12**, 679-85.

Brignull, H. R., Raible, D. W. and Stone, J. S. (2009). Feathers and fins: non-mammalian models for hair cell regeneration. *Brain Res* **1277**, 12-23.

Brooker, R., Hozumi, K. and Lewis, J. (2006). Notch ligands with contrasting functions: Jagged1 and Delta1 in the mouse inner ear. *Development* **133**, 1277-86.

Bultman, S., Gebuhr, T., Yee, D., La Mantia, C., Nicholson, J., Gilliam, A., Randazzo, F., Metzger, D., Chambon, P., Crabtree, G. et al. (2000). A Brg1 null mutation in the mouse reveals functional differences among mammalian SWI/SNF complexes. *Mol Cell* **6**, 1287-95.

Cafaro, J., Lee, G. S. and Stone, J. S. (2007). Atoh1 expression defines activated progenitors and differentiating hair cells during avian hair cell regeneration. *Dev Dyn* **236**, 156-70.

Cairns, B. R., Kim, Y. J., Sayre, M. H., Laurent, B. C. and Kornberg, R. D. (1994). A multisubunit complex containing the SWI1/ADR6, SWI2/SNF2, SWI3, SNF5, and SNF6 gene products isolated from yeast. *Proc Natl Acad Sci U S A* **91**, 1950-4.

Chardin, S. and Romand, R. (1995). Regeneration and mammalian auditory hair cells. *Science* **267**, 707-11.

Chen, P., Johnson, J. E., Zoghbi, H. Y. and Segil, N. (2002). The role of Math1 in inner ear development: Uncoupling the establishment of the sensory primordium from hair cell fate determination. *Development* **129**, 2495-505.

Chezar, H. H. (1930). Studies on the lateral-line system of amphibia II. Comparative cytology and innervation of the lateral-line organs in the Urodela. *J. Comp. Neurol.* **50**, 159-175.

Chia, I. V. and Costantini, F. (2005). Mouse axin and axin2/conductin proteins are functionally equivalent in vivo. *Mol Cell Biol* **25**, 4371-6.

Chitnis, A. B. (1995). The role of Notch in lateral inhibition and cell fate specification. *Mol Cell Neurosci* **6**, 311-21.

Collado, M. S., Burns, J. C., Hu, Z. and Corwin, J. T. (2008). Recent advances in hair cell regeneration research. *Curr Opin Otolaryngol Head Neck Surg* **16**, 465-71.

Collazo, A., Fraser, S. E. and Mabee, P. M. (1994). A dual embryonic origin for vertebrate mechanoreceptors. *Science* **264**, 426-30.

Corwin, J. T. (1981). Postembryonic production and aging in inner ear hair cells in sharks. *J Comp Neurol* **201**, 541-53.

Corwin, J. T. (1985). Perpetual production of hair cells and maturational changes in hair cell ultrastructure accompany postembryonic growth in an amphibian ear. *Proc Natl Acad Sci U S A* **82**, 3911-5.

Corwin, J. T. and Cotanche, D. A. (1988). Regeneration of sensory hair cells after acoustic trauma. *Science* **240**, 1772-4.

Cotanche, D. A., Saunders, J. C. and Tilney, L. G. (1987). Hair cell damage produced by acoustic trauma in the chick cochlea. *Hear Res* **25**, 267-86.

Curtin, J. A., Quint, E., Tsipouri, V., Arkell, R. M., Cattanach, B., Copp, A. J., Henderson, D. J., Spurr, N., Stanier, P., Fisher, E. M. et al. (2003). Mutation of Celsr1 disrupts planar polarity of inner ear hair cells and causes severe neural tube defects in the mouse. *Curr Biol* **13**, 1129-33.

Dabdoub, A., Puligilla, C., Jones, J. M., Fritzsch, B., Cheah, K. S., Pevny, L. H. and Kelley, M. W. (2008). Sox2 signaling in prosensory domain specification and subsequent hair cell differentiation in the developing cochlea. *Proc Natl Acad Sci U S A* **105**, 18396-401.

Dambly-Chaudiere, C., Cubedo, N. and Ghysen, A. (2007). Control of cell migration in the development of the posterior lateral line: antagonistic interactions between the chemokine receptors CXCR4 and CXCR7/RDC1. *BMC Dev Biol* **7**, 23.

Dambly-Chaudiere, C., Sapede, D., Soubiran, F., Decorde, K., Gompel, N. and Ghysen, A. (2003). The lateral line of zebrafish: a model system for the analysis of morphogenesis and neural development in vertebrates. *Biol Cell* **95**, 579-87.

Daudet, N., Gibson, R., Shang, J., Bernard, A., Lewis, J. and Stone, J. (2009). Notch regulation of progenitor cell behavior in quiescent and regenerating auditory epithelium of mature birds. *Dev Biol* **326**, 86-100.

David, N. B., Sapede, D., Saint-Etienne, L., Thisse, C., Thisse, B., Dambly-Chaudiere, C., Rosa, F. M. and Ghysen, A. (2002). Molecular basis of cell migration in the fish lateral line: role of the chemokine receptor CXCR4 and of its ligand, SDF1. *Proc Natl Acad Sci U S A* **99**, 16297-302.

Davis, R. I., Ahroon, W. A. and Hamernik, R. P. (1989). The relation among hearing loss, sensory cell loss and tuning characteristics in the chinchilla. *Hear Res* **41**, 1-14.

Deisboeck, T. S. and Couzin, I. D. (2009). Collective behavior in cancer cell populations. *Bioessays* **31**, 190-7.

Del Bene, F., Wehman, A. M., Link, B. A. and Baier, H. (2008). Regulation of neurogenesis by interkinetic nuclear migration through an apical-basal notch gradient. *Cell* **134**, 1055-65.

Denman-Johnson, K. and Forge, A. (1999). Establishment of hair bundle polarity and orientation in the developing vestibular system of the mouse. *J Neurocytol* **28**, 821-35.

Devenport, D. and Fuchs, E. (2008). Planar polarization in embryonic epidermis orchestrates global asymmetric morphogenesis of hair follicles. *Nat Cell Biol* **10**, 1257-68.

Devreotes, P. and Janetopoulos, C. (2003). Eukaryotic chemotaxis: distinctions between directional sensing and polarization. *J Biol Chem* **278**, 20445-8.

Dijkgraaf, S. (1963). The functioning and significance of the lateral line organ. *Biology Reviews* **38**.

Dormann, D. and Weijer, C. J. (2001). Propagating chemoattractant waves coordinate periodic cell movement in Dictyostelium slugs. *Development* **128**, 4535-43.

Dorsky, R. I., Rapaport, D. H. and Harris, W. A. (1995). Xotch inhibits cell differentiation in the Xenopus retina. *Neuron* **14**, 487-96.

Dufourcq, P., Roussigne, M., Blader, P., Rosa, F., Peyrieras, N. and Vriz, S. (2006). Mechano-sensory organ regeneration in adults: the zebrafish lateral line as a model. *Mol Cell Neurosci* **33**, 180-7.

Duncan, L. J., Mangiardi, D. A., Matsui, J. I., Anderson, J. K., McLaughlin-Williamson, K. and Cotanche, D. A. (2006). Differential expression of unconventional myosins in apoptotic and regenerating chick hair cells confirms two regeneration mechanisms. *J Comp Neurol* **499**, 691-701.

Eddison, M., Le Roux, I. and Lewis, J. (2000). Notch signaling in the development of the inner ear: lessons from Drosophila. *Proc Natl Acad Sci U S A* **97**, 11692-9.

Eroglu, B., Wang, G., Tu, N., Sun, X. and Mivechi, N. F. (2006). Critical role of Brg1 member of the SWI/SNF chromatin remodeling complex during neurogenesis and neural crest induction in zebrafish. *Dev Dyn* **235**, 2722-35.

Essner, J. J., Amack, J. D., Nyholm, M. K., Harris, E. B. and Yost, H. J. (2005). Kupffer's vesicle is a ciliated organ of asymmetry in the zebrafish

embryo that initiates left-right development of the brain, heart and gut. *Development* **132**, 1247-60.
Fischer, E., Legue, E., Doyen, A., Nato, F., Nicolas, J. F., Torres, V., Yaniv, M. and Pontoglio, M. (2006). Defective planar cell polarity in polycystic kidney disease. *Nat Genet* **38**, 21-3.
Forge, A., Li, L. and Nevill, G. (1998). Hair cell recovery in the vestibular sensory epithelia of mature guinea pigs. *J Comp Neurol* **397**, 69-88.
Foudi, A., Hochedlinger, K., Van Buren, D., Schindler, J. W., Jaenisch, R., Carey, V. and Hock, H. (2009). Analysis of histone 2B-GFP retention reveals slowly cycling hematopoietic stem cells. *Nat Biotechnol* **27**, 84-90.
Friedl, P. (2004). Prespecification and plasticity: shifting mechanisms of cell migration. *Curr Opin Cell Biol* **16**, 14-23.
Friedl, P. and Gilmour, D. (2009). Collective cell migration in morphogenesis, regeneration and cancer. *Nat Rev Mol Cell Biol* **10**, 445-57.
Friedl, P., Hegerfeldt, Y. and Tusch, M. (2004). Collective cell migration in morphogenesis and cancer. *Int J Dev Biol* **48**, 441-9.
Friedl, P. and Weigelin, B. (2008). Interstitial leukocyte migration and immune function. *Nat Immunol* **9**, 960-9.
Gallardo, V. E., Liang, J., Behra, M., Elkahloun, A., Villablanca, E. J., Russo, V., Allende, M. L. and Burgess, S. M. (2011). Molecular dissection of the migrating posterior lateral line primordium during early development in zebrafish. *BMC Dev Biol* **10**, 120.
Gamba, L., Cubedo, N., Ghysen, A., Lutfalla, G. and Dambly-Chaudiere, C. (2010). Estrogen receptor ESR1 controls cell migration by repressing chemokine receptor CXCR4 in the zebrafish posterior lateral line system. *Proc Natl Acad Sci U S A* **107**, 6358-63.
Ghysen, A. and Dambly-Chaudiere, C. (2004). Development of the zebrafish lateral line. *Curr Opin Neurobiol* **14**, 67-73.
Ghysen, A. and Dambly-Chaudiere, C. (2007). The lateral line microcosmos. *Genes Dev* **21**, 2118-30.
Glaros, S., Cirrincione, G. M., Palanca, A., Metzger, D. and Reisman, D. (2008). Targeted knockout of BRG1 potentiates lung cancer development. *Cancer Res* **68**, 3689-96.
Gompel, N., Cubedo, N., Thisse, C., Thisse, B., Dambly-Chaudiere, C. and Ghysen, A. (2001). Pattern formation in the lateral line of zebrafish. *Mech Dev* **105**, 69-77.
Gong, Y., Mo, C. and Fraser, S. E. (2004). Planar cell polarity signalling controls cell division orientation during zebrafish gastrulation. *Nature* **430**, 689-93.
Greco, V., Chen, T., Rendl, M., Schober, M., Pasolli, H. A., Stokes, N., Dela Cruz-Racelis, J. and Fuchs, E. (2009). A two-step mechanism for stem cell activation during hair regeneration. *Cell Stem Cell* **4**, 155-69.
Greco, V. and Guo, S. (2010). Compartmentalized organization: a common and required feature of stem cell niches? *Development* **137**, 1586-94.

Gregg, R. G., Willer, G. B., Fadool, J. M., Dowling, J. E. and Link, B. A. (2003). Positional cloning of the young mutation identifies an essential role for the Brahma chromatin remodeling complex in mediating retinal cell differentiation. *Proc Natl Acad Sci U S A* **100**, 6535-40.

Griffin, C. T., Curtis, C. D., Davis, R. B., Muthukumar, V. and Magnuson, T. (2011). The chromatin-remodeling enzyme BRG1 modulates vascular Wnt signaling at two levels. *Proc Natl Acad Sci U S A* **108**, 2282-7.

Haas, P. and Gilmour, D. (2006). Chemokine signaling mediates self-organizing tissue migration in the zebrafish lateral line. *Dev Cell* **10**, 673-80.

Haddon, C., Jiang, Y. J., Smithers, L. and Lewis, J. (1998). Delta-Notch signalling and the patterning of sensory cell differentiation in the zebrafish ear: evidence from the mind bomb mutant. *Development* **125**, 4637-44.

Haddon, C., Mowbray, C., Whitfield, T., Jones, D., Gschmeissner, S. and Lewis, J. (1999). Hair cells without supporting cells: further studies in the ear of the zebrafish mind bomb mutant. *J Neurocytol* **28**, 837-50.

Haines, L., Neyt, C., Gautier, P., Keenan, D. G., Bryson-Richardson, R. J., Hollway, G. E., Cole, N. J. and Currie, P. D. (2004). Met and Hgf signaling controls hypaxial muscle and lateral line development in the zebrafish. *Development* **131**, 4857-69.

Harris, J. A., Cheng, A. G., Cunningham, L. L., MacDonald, G., Raible, D. W. and Rubel, E. W. (2003). Neomycin-induced hair cell death and rapid regeneration in the lateral line of zebrafish (Danio rerio). *J Assoc Res Otolaryngol* **4**, 219-34.

Hava, D., Forster, U., Matsuda, M., Cui, S., Link, B. A., Eichhorst, J., Wiesner, B., Chitnis, A. and Abdelilah-Seyfried, S. (2009). Apical membrane maturation and cellular rosette formation during morphogenesis of the zebrafish lateral line. *J Cell Sci* **122**, 687-95.

Hegerfeldt, Y., Tusch, M., Brocker, E. B. and Friedl, P. (2002). Collective cell movement in primary melanoma explants: plasticity of cell-cell interaction, beta1-integrin function, and migration strategies. *Cancer Res* **62**, 2125-30.

Helbig, G., Christopherson, K. W., 2nd, Bhat-Nakshatri, P., Kumar, S., Kishimoto, H., Miller, K. D., Broxmeyer, H. E. and Nakshatri, H. (2003). NF-kappaB promotes breast cancer cell migration and metastasis by inducing the expression of the chemokine receptor CXCR4. *J Biol Chem* **278**, 21631-8.

Henrique, D., Hirsinger, E., Adam, J., Le Roux, I., Pourquie, O., Ish-Horowicz, D. and Lewis, J. (1997). Maintenance of neuroepithelial progenitor cells by Delta-Notch signalling in the embryonic chick retina. *Curr Biol* **7**, 661-70.

Hernandez, P. P., Moreno, V., Olivari, F. A. and Allende, M. L. (2006). Sub-lethal concentrations of waterborne copper are toxic to lateral line neuromasts in zebrafish (Danio rerio). *Hear Res* **213**, 1-10.

Hernandez, P. P., Olivari, F. A., Sarrazin, A. F., Sandoval, P. C. and Allende, M. L. (2007). Regeneration in zebrafish lateral line neuromasts:

expression of the neural progenitor cell marker sox2 and proliferation-dependent and-independent mechanisms of hair cell renewal. *Dev Neurobiol* **67**, 637-54.
Huang, X. and Saint-Jeannet, J. P. (2004). Induction of the neural crest and the opportunities of life on the edge. *Dev Biol* **275**, 1-11.
Hudspeth, A. J. (1985). The cellular basis of hearing: the biophysics of hair cells. *Science* **230**, 745-52.
Hudspeth, A. J. (1989). How the ear's works work. *Nature* **341**, 397-404.
Itoh, M. and Chitnis, A. B. (2001). Expression of proneural and neurogenic genes in the zebrafish lateral line primordium correlates with selection of hair cell fate in neuromasts. *Mech Dev* **102**, 263-6.
Jadhav, A. P., Cho, S. H. and Cepko, C. L. (2006). Notch activity permits retinal cells to progress through multiple progenitor states and acquire a stem cell property. *Proc Natl Acad Sci U S A* **103**, 18998-9003.
Jho, E. H., Zhang, T., Domon, C., Joo, C. K., Freund, J. N. and Costantini, F. (2002). Wnt/beta-catenin/Tcf signaling induces the transcription of Axin2, a negative regulator of the signaling pathway. *Mol Cell Biol* **22**, 1172-83.
Jones, J. E. and Corwin, J. T. (1993). Replacement of lateral line sensory organs during tail regeneration in salamanders: identification of progenitor cells and analysis of leukocyte activity. *J Neurosci* **13**, 1022-34.
Jones, J. E. and Corwin, J. T. (1996). Regeneration of sensory cells after laser ablation in the lateral line system: hair cell lineage and macrophage behavior revealed by time-lapse video microscopy. *J Neurosci* **16**, 649-62.
Kadam, S. and Emerson, B. M. (2003). Transcriptional specificity of human SWI/SNF BRG1 and BRM chromatin remodeling complexes. *Mol Cell* **11**, 377-89.
Kadonaga, J. T. (1998). Eukaryotic transcription: an interlaced network of transcription factors and chromatin-modifying machines. *Cell* **92**, 307-13.
Kametani, Y. and Takeichi, M. (2007). Basal-to-apical cadherin flow at cell junctions. *Nat Cell Biol* **9**, 92-8.
Kelley, M. W. (2006). Regulation of cell fate in the sensory epithelia of the inner ear. *Nat Rev Neurosci* **7**, 837-49.
Kelley, M. W. (2007). Cellular commitment and differentiation in the organ of Corti. *Int J Dev Biol* **51**, 571-83.
Kerstetter, A. E., Azodi, E., Marrs, J. A. and Liu, Q. (2004). Cadherin-2 function in the cranial ganglia and lateral line system of developing zebrafish. *Dev Dyn* **230**, 137-43.
Khavari, P. A., Peterson, C. L., Tamkun, J. W., Mendel, D. B. and Crabtree, G. R. (1993). BRG1 contains a conserved domain of the SWI2/SNF2 family necessary for normal mitotic growth and transcription. *Nature* **366**, 170-4.
Kidder, B. L., Palmer, S. and Knott, J. G. (2009). SWI/SNF-Brg1 regulates self-renewal and occupies core pluripotency-related genes in embryonic stem cells. *Stem Cells* **27**, 317-28.

Kiernan, A. E., Cordes, R., Kopan, R., Gossler, A. and Gridley, T. (2005a). The Notch ligands DLL1 and JAG2 act synergistically to regulate hair cell development in the mammalian inner ear. *Development* **132**, 4353-62.
Kiernan, A. E., Pelling, A. L., Leung, K. K., Tang, A. S., Bell, D. M., Tease, C., Lovell-Badge, R., Steel, K. P. and Cheah, K. S. (2005b). Sox2 is required for sensory organ development in the mammalian inner ear. *Nature* **434**, 1031-5.
Kikuchi, A. (1999). Modulation of Wnt signaling by Axin and Axil. *Cytokine Growth Factor Rev* **10**, 255-65.
Kimmel, C. B., Ballard, W. W., Kimmel, S. R., Ullmann, B. and Schilling, T. F. (1995). Stages of embryonic development of the zebrafish. *Dev Dyn* **203**, 253-310.
Kingston, R. E. and Narlikar, G. J. (1999). ATP-dependent remodeling and acetylation as regulators of chromatin fluidity. *Genes Dev* **13**, 2339-52.
Laguerre, L., Ghysen, A. and Dambly-Chaudiere, C. (2009). Mitotic patterns in the migrating lateral line cells of zebrafish embryos. *Dev Dyn* **238**, 1042-51.
Laguerre, L., Soubiran, F., Ghysen, A., Konig, N. and Dambly-Chaudiere, C. (2005). Cell proliferation in the developing lateral line system of zebrafish embryos. *Dev Dyn* **233**, 466-72.
Lanford, P. J., Lan, Y., Jiang, R., Lindsell, C., Weinmaster, G., Gridley, T. and Kelley, M. W. (1999). Notch signalling pathway mediates hair cell development in mammalian cochlea. *Nat Genet* **21**, 289-92.
Lecaudey, V., Cakan-Akdogan, G., Norton, W. H. and Gilmour, D. (2008). Dynamic Fgf signaling couples morphogenesis and migration in the zebrafish lateral line primordium. *Development* **135**, 2695-705.
Lecuit, T. and Le Goff, L. (2007). Orchestrating size and shape during morphogenesis. *Nature* **450**, 189-92.
Ledent, V. (2002). Postembryonic development of the posterior lateral line in zebrafish. *Development* **129**, 597-604.
Lemon, B., Inouye, C., King, D. S. and Tjian, R. (2001). Selectivity of chromatin-remodelling cofactors for ligand-activated transcription. *Nature* **414**, 924-8.
Leung, J. Y., Kolligs, F. T., Wu, R., Zhai, Y., Kuick, R., Hanash, S., Cho, K. R. and Fearon, E. R. (2002). Activation of AXIN2 expression by beta-catenin-T cell factor. A feedback repressor pathway regulating Wnt signaling. *J Biol Chem* **277**, 21657-65.
Leung, Y. F., Ma, P., Link, B. A. and Dowling, J. E. (2008). Factorial microarray analysis of zebrafish retinal development. *Proc Natl Acad Sci U S A* **105**, 12909-14.
Lewis J, D. A. (2002). Planar cell polarity in the inner ear: how do hair cells acquire their oriented structure?
. *J Neurobiol* **53**, 190-201.
Lewis, J. and Davies, A. (2002). Planar cell polarity in the inner ear: how do hair cells acquire their oriented structure? *J Neurobiol* **53**, 190-201.

Li, Q., Shirabe, K. and Kuwada, J. Y. (2004). Chemokine signaling regulates sensory cell migration in zebrafish. *Dev Biol* **269**, 123-36.
Link, B. A., Fadool, J. M., Malicki, J. and Dowling, J. E. (2000). The zebrafish young mutation acts non-cell-autonomously to uncouple differentiation from specification for all retinal cells. *Development* **127**, 2177-88.
Lopez-Schier, H. (2004). Regeneration: did you hear the news? *Curr Biol* **14**, R127-8.
Lopez-Schier, H. (2010). Fly fishing for collective cell migration. *Curr Opin Genet Dev* **20**, 428-32.
Lopez-Schier, H. and Hudspeth, A. J. (2006). A two-step mechanism underlies the planar polarization of regenerating sensory hair cells. *Proc Natl Acad Sci U S A* **103**, 18615-20.
Lopez-Schier, H., Starr, C. J., Kappler, J. A., Kollmar, R. and Hudspeth, A. J. (2004). Directional cell migration establishes the axes of planar polarity in the posterior lateral-line organ of the zebrafish. *Dev Cell* **7**, 401-12.
Lowenstein, O. (1967). Lateral Line Detectors *Indiana University Press*.
Lu, P., Sternlicht, M. D. and Werb, Z. (2006). Comparative mechanisms of branching morphogenesis in diverse systems. *J Mammary Gland Biol Neoplasia* **11**, 213-28.
Luo, W. and Lin, S. C. (2004). Axin: a master scaffold for multiple signaling pathways. *Neurosignals* **13**, 99-113.
Luster, A. D. (1998). Chemokines--chemotactic cytokines that mediate inflammation. *N Engl J Med* **338**, 436-45.
Lustig, B., Jerchow, B., Sachs, M., Weiler, S., Pietsch, T., Karsten, U., van de Wetering, M., Clevers, H., Schlag, P. M., Birchmeier, W. et al. (2002). Negative feedback loop of Wnt signaling through upregulation of conductin/axin2 in colorectal and liver tumors. *Mol Cell Biol* **22**, 1184-93.
Ma, E. Y. and Raible, D. W. (2009). Signaling pathways regulating zebrafish lateral line development. *Curr Biol* **19**, R381-6.
Ma, E. Y., Rubel, E. W. and Raible, D. W. (2008). Notch signaling regulates the extent of hair cell regeneration in the zebrafish lateral line. *J Neurosci* **28**, 2261-73.
Martens, J. A. and Winston, F. (2003). Recent advances in understanding chromatin remodeling by Swi/Snf complexes. *Curr Opin Genet Dev* **13**, 136-42.
Mathur, D., Bost, A., Driver, I. and Ohlstein, B. A transient niche regulates the specification of Drosophila intestinal stem cells. *Science* **327**, 210-3.
Matsuda, M. and Chitnis, A. B. Atoh1a expression must be restricted by Notch signaling for effective morphogenesis of the posterior lateral line primordium in zebrafish. *Development* **137**, 3477-87.

Matsuda, M. and Chitnis, A. B. (2010). Atoh1a expression must be restricted by Notch signaling for effective morphogenesis of the posterior lateral line primordium in zebrafish. *Development* **137**, 3477-87.
Matsumoto, S., Banine, F., Struve, J., Xing, R., Adams, C., Liu, Y., Metzger, D., Chambon, P., Rao, M. S. and Sherman, L. S. (2006). Brg1 is required for murine neural stem cell maintenance and gliogenesis. *Dev Biol* **289**, 372-83.
McGraw, H. F., Drerup, C. M., Culbertson, M. D., Linbo, T., Raible, D. W. and Nechiporuk, A. V. (2011). Lef1 is required for progenitor cell identity in the zebrafish lateral line primordium. *Development* **138**, 3921-30.
Metcalfe, W. K. (1985). Sensory neuron growth cones comigrate with posterior lateral line primordial cells in zebrafish. *J Comp Neurol* **238**, 218-24.
Metcalfe, W. K., Kimmel, C. B. and Schabtach, E. (1985). Anatomy of the posterior lateral line system in young larvae of the zebrafish. *J Comp Neurol* **233**, 377-89.
Millimaki, B. B., Sweet, E. M. and Riley, B. B. (2010). Sox2 is required for maintenance and regeneration, but not initial development, of hair cells in the zebrafish inner ear. *Dev Biol* **338**, 262-9.
Mirzadeh, Z., Han, Y. G., Soriano-Navarro, M., Garcia-Verdugo, J. M. and Alvarez-Buylla, A. (2010). Cilia organize ependymal planar polarity. *J Neurosci* **30**, 2600-10.
Miura, H., Kusakabe, Y. and Harada, S. (2006). Cell lineage and differentiation in taste buds. *Arch Histol Cytol* **69**, 209-25.
Mogilner, A. and Keren, K. (2009). The shape of motile cells. *Curr Biol* **19**, R762-71.
Montcouquiol, M., Rachel, R. A., Lanford, P. J., Copeland, N. G., Jenkins, N. A. and Kelley, M. W. (2003). Identification of Vangl2 and Scrb1 as planar polarity genes in mammals. *Nature* **423**, 173-7.
Montgomery, J., Baker, C. & Carton, G. . (1997). The lateral line can mediate rheotaxis in fish. *Nature* **389**,
.
Montgomery, J., Carton, G., Voigt, R., Baker, C. and Diebel, C. (2000). Sensory processing of water currents by fishes. *Philos Trans R Soc Lond B Biol Sci* **355**, 1325-7.
Muchardt, C. and Yaniv, M. (2001). When the SWI/SNF complex remodels...the cell cycle. *Oncogene* **20**, 3067-75.
Myat, A., Henrique, D., Ish-Horowicz, D. and Lewis, J. (1996). A chick homologue of Serrate and its relationship with Notch and Delta homologues during central neurogenesis. *Dev Biol* **174**, 233-47.
Nagl, N. G., Jr., Wang, X., Patsialou, A., Van Scoy, M. and Moran, E. (2007). Distinct mammalian SWI/SNF chromatin remodeling complexes with opposing roles in cell-cycle control. *EMBO J* **26**, 752-63.
Naidu, S. R., Love, I. M., Imbalzano, A. N., Grossman, S. R. and Androphy, E. J. (2009). The SWI/SNF chromatin remodeling subunit

BRG1 is a critical regulator of p53 necessary for proliferation of malignant cells. *Oncogene* **28**, 2492-501.
Nakayama, T., Mutsuga, N. and Tosato, G. (2007). FGF2 posttranscriptionally down-regulates expression of SDF1 in bone marrow stromal cells through FGFR1 IIIc. *Blood* **109**, 1363-72.
Nechiporuk, A. and Raible, D. W. (2008). FGF-dependent mechanosensory organ patterning in zebrafish. *Science* **320**, 1774-7.
Nelson, B. R., Gumuscu, B., Hartman, B. H. and Reh, T. A. (2006). Notch activity is downregulated just prior to retinal ganglion cell differentiation. *Dev Neurosci* **28**, 128-41.
Neves, J., Kamaid, A., Alsina, B. and Giraldez, F. (2007). Differential expression of Sox2 and Sox3 in neuronal and sensory progenitors of the developing inner ear of the chick. *J Comp Neurol* **503**, 487-500.
Nicolson, T. (2005). The genetics of hearing and balance in zebrafish. *Annu Rev Genet* **39**, 9-22.
Nie, Z., Xue, Y., Yang, D., Zhou, S., Deroo, B. J., Archer, T. K. and Wang, W. (2000). A specificity and targeting subunit of a human SWI/SNF family-related chromatin-remodeling complex. *Mol Cell Biol* **20**, 8879-88.
Nunez, V. A., Sarrazin, A. F., Cubedo, N., Allende, M. L., Dambly-Chaudiere, C. and Ghysen, A. (2009). Postembryonic development of the posterior lateral line in the zebrafish. *Evol Dev* **11**, 391-404.
Nystul, T. and Spradling, A. (2007). An epithelial niche in the Drosophila ovary undergoes long-range stem cell replacement. *Cell Stem Cell* **1**, 277-85.
Oteiza, P., Koppen, M., Krieg, M., Pulgar, E., Farias, C., Melo, C., Preibisch, S., Muller, D., Tada, M., Hartel, S. et al. (2010). Planar cell polarity signalling regulates cell adhesion properties in progenitors of the zebrafish laterality organ. *Development* **137**, 3459-68.
Owens, K. N., Cunningham, D. E., MacDonald, G., Rubel, E. W., Raible, D. W. and Pujol, R. (2007). Ultrastructural analysis of aminoglycoside-induced hair cell death in the zebrafish lateral line reveals an early mitochondrial response. *J Comp Neurol* **502**, 522-43.
Parent, C. A. (2004). Making all the right moves: chemotaxis in neutrophils and Dictyostelium. *Curr Opin Cell Biol* **16**, 4-13.
Parinov, S., Kondrichin, I., Korzh, V. and Emelyanov, A. (2004). Tol2 transposon-mediated enhancer trap to identify developmentally regulated zebrafish genes in vivo. *Dev Dyn* **231**, 449-59.
Park, J. I., Venteicher, A. S., Hong, J. Y., Choi, J., Jun, S., Shkreli, M., Chang, W., Meng, Z., Cheung, P., Ji, H. et al. (2009). Telomerase modulates Wnt signalling by association with target gene chromatin. *Nature* **460**, 66-72.
Parsons, M. J., Pisharath, H., Yusuff, S., Moore, J. C., Siekmann, A. F., Lawson, N. and Leach, S. D. (2009). Notch-responsive cells initiate the secondary transition in larval zebrafish pancreas. *Mech Dev* **126**, 898-912.
Passegue, E., Wagers, A. J., Giuriato, S., Anderson, W. C. and Weissman, I. L. (2005). Global analysis of proliferation and cell cycle gene

expression in the regulation of hematopoietic stem and progenitor cell fates. *J Exp Med* **202**, 1599-611.
Peterson, C. L. and Tamkun, J. W. (1995). The SWI-SNF complex: a chromatin remodeling machine? *Trends Biochem Sci* **20**, 143-6.
Pichon, F. and Ghysen, A. (2004). Evolution of posterior lateral line development in fish and amphibians. *Evol Dev* **6**, 187-93.
Platt, C. (1977). Hair cell distribution and orientation in goldfish otolith organs. *J Comp Neurol* **172**, 283-87.
Raible, D. W. and Kruse, G. J. (2000). Organization of the lateral line system in embryonic zebrafish. *J Comp Neurol* **421**, 189-98.
Randazzo, F. M., Khavari, P., Crabtree, G., Tamkun, J. and Rossant, J. (1994). brg1: a putative murine homologue of the Drosophila brahma gene, a homeotic gene regulator. *Dev Biol* **161**, 229-42.
Reisman, D., Glaros, S. and Thompson, E. A. (2009). The SWI/SNF complex and cancer. *Oncogene* **28**, 1653-68.
Reisman, D. N., Sciarrotta, J., Bouldin, T. W., Weissman, B. E. and Funkhouser, W. K. (2005). The expression of the SWI/SNF ATPase subunits BRG1 and BRM in normal human tissues. *Appl Immunohistochem Mol Morphol* **13**, 66-74.
Reisman, D. N., Sciarrotta, J., Wang, W., Funkhouser, W. K. and Weissman, B. E. (2003). Loss of BRG1/BRM in human lung cancer cell lines and primary lung cancers: correlation with poor prognosis. *Cancer Res* **63**, 560-6.
Rida, P. C. and Chen, P. (2009). Line up and listen: Planar cell polarity regulation in the mammalian inner ear. *Semin Cell Dev Biol* **20**, 978-85.
Ridley, A. J., Schwartz, M. A., Burridge, K., Firtel, R. A., Ginsberg, M. H., Borisy, G., Parsons, J. T. and Horwitz, A. R. (2003). Cell migration: integrating signals from front to back. *Science* **302**, 1704-9.
Roberson, D. W., Alosi, J. A. and Cotanche, D. A. (2004). Direct transdifferentiation gives rise to the earliest new hair cells in regenerating avian auditory epithelium. *J Neurosci Res* **78**, 461-71.
Roberts, C. W. and Orkin, S. H. (2004). The SWI/SNF complex--chromatin and cancer. *Nat Rev Cancer* **4**, 133-42.
Rorth, P. (2003). Communication by touch: role of cellular extensions in complex animals. *Cell* **112**, 595-8.
Rorth, P. (2007). Collective guidance of collective cell migration. *Trends Cell Biol* **17**, 575-9.
Rorth, P. (2009). Collective cell migration. *Annu Rev Cell Dev Biol* **25**, 407-29.
Rouse, G. W. and Pickles, J. O. (1991). Paired development of hair cells in neuromasts of the teleost lateral line. *Proc Biol Sci* **246**, 123-8.
Rubel, E. W., Dew, L. A. and Roberson, D. W. (1995). Mammalian vestibular hair cell regeneration. *Science* **267**, 701-7.
Ryals BM, R. E. (1988). Hair cell regeneration after acoustic trauma in adult Coturnix quail. *Science*, 1774-1776.

Ryals, B. M. and Rubel, E. W. (1988). Hair cell regeneration after acoustic trauma in adult Coturnix quail. *Science* **240**, 1774-6.
Saburi, S., Hester, I., Fischer, E., Pontoglio, M., Eremina, V., Gessler, M., Quaggin, S. E., Harrison, R., Mount, R. and McNeill, H. (2008). Loss of Fat4 disrupts PCP signaling and oriented cell division and leads to cystic kidney disease. *Nat Genet* **40**, 1010-5.
Sapede, D., Gompel, N., Dambly-Chaudiere, C. and Ghysen, A. (2002). Cell migration in the postembryonic development of the fish lateral line. *Development* **129**, 605-15.
Sarrazin, A. F., Nunez, V. A., Sapede, D., Tassin, V., Dambly-Chaudiere, C. and Ghysen, A. (2010). Origin and early development of the posterior lateral line system of zebrafish. *J Neurosci* **30**, 8234-44.
Song, J., Yan, H. Y. and Popper, A. N. (1995). Damage and recovery of hair cells in fish canal (but not superficial) neuromasts after gentamicin exposure. *Hear Res* **91**, 63-71.
Stone, J. S. and Cotanche, D. A. (1994). Identification of the timing of S phase and the patterns of cell proliferation during hair cell regeneration in the chick cochlea. *J Comp Neurol* **341**, 50-67.
Strobeck, M. W., Reisman, D. N., Gunawardena, R. W., Betz, B. L., Angus, S. P., Knudsen, K. E., Kowalik, T. F., Weissman, B. E. and Knudsen, E. S. (2002). Compensation of BRG-1 function by Brm: insight into the role of the core SWI-SNF subunits in retinoblastoma tumor suppressor signaling. *J Biol Chem* **277**, 4782-9.
Strutt, H. and Strutt, D. (2009). Asymmetric localisation of planar polarity proteins: Mechanisms and consequences. *Semin Cell Dev Biol* **20**, 957-63.
Sweet, E. M., Vemaraju, S. and Riley, B. B. (2011). Sox2 and Fgf interact with Atoh1 to promote sensory competence throughout the zebrafish inner ear. *Dev Biol* **358**, 113-21.
Takeuchi, J. K., Lickert, H., Bisgrove, B. W., Sun, X., Yamamoto, M., Chawengsaksophak, K., Hamada, H., Yost, H. J., Rossant, J. and Bruneau, B. G. (2007). Baf60c is a nuclear Notch signaling component required for the establishment of left-right asymmetry. *Proc Natl Acad Sci U S A* **104**, 846-51.
Takeuchi, J. K., Lou, X., Alexander, J. M., Sugizaki, H., Delgado-Olguin, P., Holloway, A. K., Mori, A. D., Wylie, J. N., Munson, C., Zhu, Y. et al. (2010). Chromatin remodelling complex dosage modulates transcription factor function in heart development. *Nat Commun* **2**, 187.
Thisse, C. and Thisse, B. (2008). High-resolution in situ hybridization to whole-mount zebrafish embryos. *Nat Protoc* **3**, 59-69.
Torres, M. and Giraldez, F. (1998). The development of the vertebrate inner ear. *Mech Dev* **71**, 5-21.
Trotter, K. W. and Archer, T. K. (2008). The BRG1 transcriptional coregulator. *Nucl Recept Signal* **6**, e004.

Tumbar, T., Guasch, G., Greco, V., Blanpain, C., Lowry, W. E., Rendl, M. and Fuchs, E. (2004). Defining the epithelial stem cell niche in skin. *Science* **303**, 359-63.

Valdivia, L. E., Young, R. M., Hawkins, T. A., Stickney, H. L., Cavodeassi, F., Schwarz, Q., Pullin, L. M., Villegas, R., Moro, E., Argenton, F. et al. (2011). Lef1-dependent Wnt/{beta}-catenin signalling drives the proliferative engine that maintains tissue homeostasis during lateral line development. *Development* **138**, 3931-41.

Valentin, G. (2009). Chemokine receptors orchestrate collective cell migration in the zebrafish lateral line. *PhD Thesis*.

Valentin, G., Haas, P. and Gilmour, D. (2007). The chemokine SDF1a coordinates tissue migration through the spatially restricted activation of Cxcr7 and Cxcr4b. *Curr Biol* **17**, 1026-31.

Van Haastert, P. J. and Devreotes, P. N. (2004). Chemotaxis: signalling the way forward. *Nat Rev Mol Cell Biol* **5**, 626-34.

Venezia, T. A., Merchant, A. A., Ramos, C. A., Whitehouse, N. L., Young, A. S., Shaw, C. A. and Goodell, M. A. (2004). Molecular signatures of proliferation and quiescence in hematopoietic stem cells. *PLoS Biol* **2**, e301.

Villablanca, E. J., Renucci, A., Sapede, D., Lec, V., Soubiran, F., Sandoval, P. C., Dambly-Chaudiere, C., Ghysen, A. and Allende, M. L. (2006). Control of cell migration in the zebrafish lateral line: implication of the gene "tumour-associated calcium signal transducer," tacstd. *Dev Dyn* **235**, 1578-88.

Vitorino, P. and Meyer, T. (2008). Modular control of endothelial sheet migration. *Genes Dev* **22**, 3268-81.

Voog, J., D'Alterio, C. and Jones, D. L. (2008). Multipotent somatic stem cells contribute to the stem cell niche in the Drosophila testis. *Nature* **454**, 1132-6.

Wang, J., Mark, S., Zhang, X., Qian, D., Yoo, S. J., Radde-Gallwitz, K., Zhang, Y., Lin, X., Collazo, A., Wynshaw-Boris, A. et al. (2005). Regulation of polarized extension and planar cell polarity in the cochlea by the vertebrate PCP pathway. *Nat Genet* **37**, 980-5.

Wang, Y., Guo, N. and Nathans, J. (2006). The role of Frizzled3 and Frizzled6 in neural tube closure and in the planar polarity of inner-ear sensory hair cells. *J Neurosci* **26**, 2147-56.

Weiner, O. D. (2002). Regulation of cell polarity during eukaryotic chemotaxis: the chemotactic compass. *Curr Opin Cell Biol* **14**, 196-202.

Weinmaster, G., Roberts, V. J. and Lemke, G. (1991). A homolog of Drosophila Notch expressed during mammalian development. *Development* **113**, 199-205.

Wibowo, I., Pinto-Teixeira, F., Satou, C., Higashijima, S. and Lopez-Schier, H. (2011). Compartmentalized Notch signaling sustains epithelial mirror symmetry. *Development* **138**, 1143-52.

Williams, J. A. and Holder, N. (2000). Cell turnover in neuromasts of zebrafish larvae. *Hear Res* **143**, 171-81.
Wilson, A., Laurenti, E., Oser, G., van der Wath, R. C., Blanco-Bose, W., Jaworski, M., Offner, S., Dunant, C. F., Eshkind, L., Bockamp, E. et al. (2008). Hematopoietic stem cells reversibly switch from dormancy to self-renewal during homeostasis and repair. *Cell* **135**, 1118-29.
Winklbauer, R. (1989). Development of the lateral line system in Xenopus. *Prog Neurobiol* **32**, 181-206.
Winston, F. and Carlson, M. (1992). Yeast SNF/SWI transcriptional activators and the SPT/SIN chromatin connection. *Trends Genet* **8**, 387-91.
Wodarz, A. and Nathke, I. (2007). Cell polarity in development and cancer. *Nat Cell Biol* **9**, 1016-24.
Woods, C., Montcouquiol, M. and Kelley, M. W. (2004). Math1 regulates development of the sensory epithelium in the mammalian cochlea. *Nat Neurosci* **7**, 1310-8.
Yamada, S. and Nelson, W. J. (2007). Localized zones of Rho and Rac activities drive initiation and expansion of epithelial cell-cell adhesion. *J Cell Biol* **178**, 517-27.
Yan, Z., Cui, K., Murray, D. M., Ling, C., Xue, Y., Gerstein, A., Parsons, R., Zhao, K. and Wang, W. (2005). PBAF chromatin-remodeling complex requires a novel specificity subunit, BAF200, to regulate expression of selective interferon-responsive genes. *Genes Dev* **19**, 1662-7.
Yates, L. L., Schnatwinkel, C., Murdoch, J. N., Bogani, D., Formstone, C. J., Townsend, S., Greenfield, A., Niswander, L. A. and Dean, C. H. (2010). The PCP genes Celsr1 and Vangl2 are required for normal lung branching morphogenesis. *Hum Mol Genet* **19**, 2251-67.
Zallen, J. A. (2007). Planar polarity and tissue morphogenesis. *Cell* **129**, 1051-63.

List of Acronyms

All	Anterior Lateral Line
Apc	Adenomatous polyposis coli
Atoh	Atonal
Atp2b1a	adenosine triphosphate type 2b1a
BrdU	Bromodeoxyuridine
bHLH	basic helix-loop-helix
Brg1	Brahma
Brg1	Brahma related gene 1
Cldnb	ClaudinB
Cxcr4	c-x-c chemokine receptor type 4
Cxcr7	c-x-c chemokine receptor type 7
Dapt	*N*-[(3,5-Difluorophenyl)acetyl]-L-al anyl-2-phenyl]glycine-1,1-dimethylethyl ester
Diasp	4-(4-(diethylamino)styryl)-*N*-methylpyridinium iodide
Dpf	Days Post Fertilization
Dkk	Dickkopf
Fgf	Fybroblast growth factor
Fgfr	Fybroblast growth factor receptor
Gal4	Galactosidase 4
GFP	Green Fluorescent Protein
Hpf	Hours Post Fertilization
Hpt	Hours Post Treatment
NICD	Notch Intracelular Domain
PCP	Planar Cell Polarity
pLLp	Posterior Lateral Line Primordium
PrimII	Secondary Primordium
Sdf1a	Stromal cell derived factor 1
SWI/SNIF	Switch/Sucrose NonFermented
Tg(SqEt20)	Trangenic Enhancer Trap 20

Tg(SqEt4)	Trangenic Enhancer Trap 4
UHCP	Unipotent Hair Cell Progenitor
Vangl2	Van Gogh-like protein 2
Wnt	Wingless integration site